PRELIMINARY STEPS IN THE DEVELOPMENT OF A 3-D THERMAL-STRESS MODEL OF CONTINUOUS CASTING

BY

JEAN ANTOINE AZZI

B. S., University of Dayton, 1986

THESIS

Submitted in partial fulfillment of the requirements
for the degree of Master of Science in Mechanical Enginneering
in the Graduate College of the
University of Illinois at Urbana-Champaign, 1988

Urbana, Illinois

ACKNOWLEDGEMENTS

I would like to express my appreciation to Dr. Brian G. Thomas, my thesis advisor, for his guidance and support during the course of my graduate studies. I gratefully acknowledge Dr. Daniel Saab and Mr. Fadi Najjar for many interesting discussions and helpful suggestions. Finally, I wish to thank my family for their everlasting love and support.

Also, I would like to thank Inland Steel Company, Armco Inc., and Bethlehem Steel Corporation for their financial support.

TABLE OF CONTENTS

APPENDICES

INTRODUCTION

In recent years, continuous casting has made rapid gains among steel producing companies. This is because continuous casting offers several advantages over other methods of metal casting. Some of its advantages are: the adaptability to cast large sections in a wide range of shapes and sizes, potentially higher quality steel with more uniform physical and mechanical properties, and economic advantages due to significantly better thermal efficiency.

The continuous casting operation is simple. Basically, molten metal is poured into a water cooled bottomless mold where it begins to solidify. A high temperature gradient develops near the mold wall, where a solidified shell develops to contain the liquid metal. When the metal leaves the mold, the solidified shell must support the liquid metal that it contains in order to prevent a "break out". Also, shell growth in the mold has a great effect on the development of material microstructure, segregation, distribution, precipitates, pores and most importantly, defects [1].

Some of the defects found in continuous casting are surface cracks, shell breakouts, severe meniscus marks and surface depressions. The interaction between the mold and the strand is largely responsible for such defects. Due to the difficulty of performing experiments, mathematical models of the continuous casting process are being developed.

The wide availability and decreasing cost of computers have created an increasing interest in the use of computer simulation in the design of metallurgical

processes. Continuous casting is one area of design where mathematical modeling has been used effectively. Mathematical modeling helps in understanding the casting process and the role of important variables. Successful casting requires careful balance and control of those variables.

To help achieve the goal of developing better mathematical models, the present study was undertaken. An analysis of the mold and a study of the steels behavior in the strand while being solidified is divided into two parts. The first objective of this thesis is to describe the development and use of a 3-D model of a continuous slab-casting mold using finite element analysis. The model relies on the heat flow from the steel strand as input data in order to calculate the temperature distribution in the mold. The temperature solution is then used to calculate displacements and stresses. The thermal stresses induced in the mold change its shape. This distortion is desired because of its potential effect on the heat flow from the strand.

The second objective is the development and implementation of constitutive equations for steel under continuous casting conditions. To model the stress-strain development in the strand requires the availability of accurate constitutive equations. The steel, while being solidified, changes its volume and generates residual stresses which lead to crack formation. The development of a stress-strain relationship to describe this behavior is greatly complicated by:

- Extreme temperature range (solidus - room temperature)
- Varying load history due to changing temperature gradients, and phase changes
- Low and varying strain rate (1e-2 - 1e-7 sec^{-1})
- Small strain (less than 2%)
- Relaxation
- Creep.

Thus, the second goal of this thesis was to develop a constitutive model for steel that both incorporates the important aspects of this behavior and is simple enough to be implemented into a comprehensive finite element model.

1. THERMAL-STRESS ANALYSIS OF THE MOLD

The shape and design of the casting mold have a big impact on the steel process. Since steel solidification starts in the mold, it is important to know the thermal gradients within the mold wall. These thermal gradients control the heat transfer between the mold and the steel, thus, affecting shell growth and microstructure development. Also, these gradients generate thermal stresses in the mold itself. The thermal stresses deflect the mold and change its shape, thus, contributing to the formation of a gap between the casting mold and the solidifying strand.

Many models have been built to study the temperature distribution and the distortion of a continuous casting mold [2, 3]. Most of the previous models use two dimensional analysis because they are easier and take less time to simulate. The 2-D models are useful if the right assumptions are made but might not reflect the behavior of the real system under some conditions.

In order to get a better understanding of a continuous casting mold, a three dimensional model is developed using ANSYS, a finite element package [4]. Because of symmetry, only a quarter of the mold is used in the analysis. The mold is assumed to distort elastically under steady state conditions. The steady state temperature distribution in the mold is calculated. Using this distribution, a thermal stress analysis is performed to find the mold deflection. To confirm the results obtained from the 3-D model, a thin slice located in the middle of the quarter mold is analyzed by assuming generalized plane strain.

1.1 MODEL DESCRIPTION

Quarter mold:

A model of a quarter mold shown in Fig. 1.1 has been analyzed using ANSYS. This 112.77 cm x 38.32 cm x 70 cm mold is typical of the design used in steel slab casting machines, and blueprints are provided by Armco Steel. The mesh shown in Fig. 1.1 contains 840 elements and 1224 nodes. In order to solve the problem accurately and efficiently, it is important to use a mesh that is as coarse as possible, while retaining accuracy. The mesh was created in a way to achieve continuity among the elements of the side plate in contact with those of the wide plate. In addition, the large number of water channels was difficult to implement as boundary conditions on the model.

To develop an efficient mesh, a block with 24 elements including the cooling channels of the mold, as shown in Fig. 1.2, was analyzed first. The thermal results for the block were previously calculated using a 3-D finite element program by Storkman [5]. The comparison of the two studies implied that the accuracy of the mesh fineness was not so crucial. A detailed discussion of the results is found in the next section. Thus, the mesh used for the small block was applied to the entire mold.

The cooling water channels were modeled as convective boundary conditions on element faces, in order to avoid creating more elements. This approximate model of the thin rectangular channels was proven accurate with the "small block" model previously mentioned. The width of these water channels is 2.5 cm which is exactly the same as the actual model. Two square water channels were used to approximate the cooling channels in the narrow face mold walls. The squares are located at the

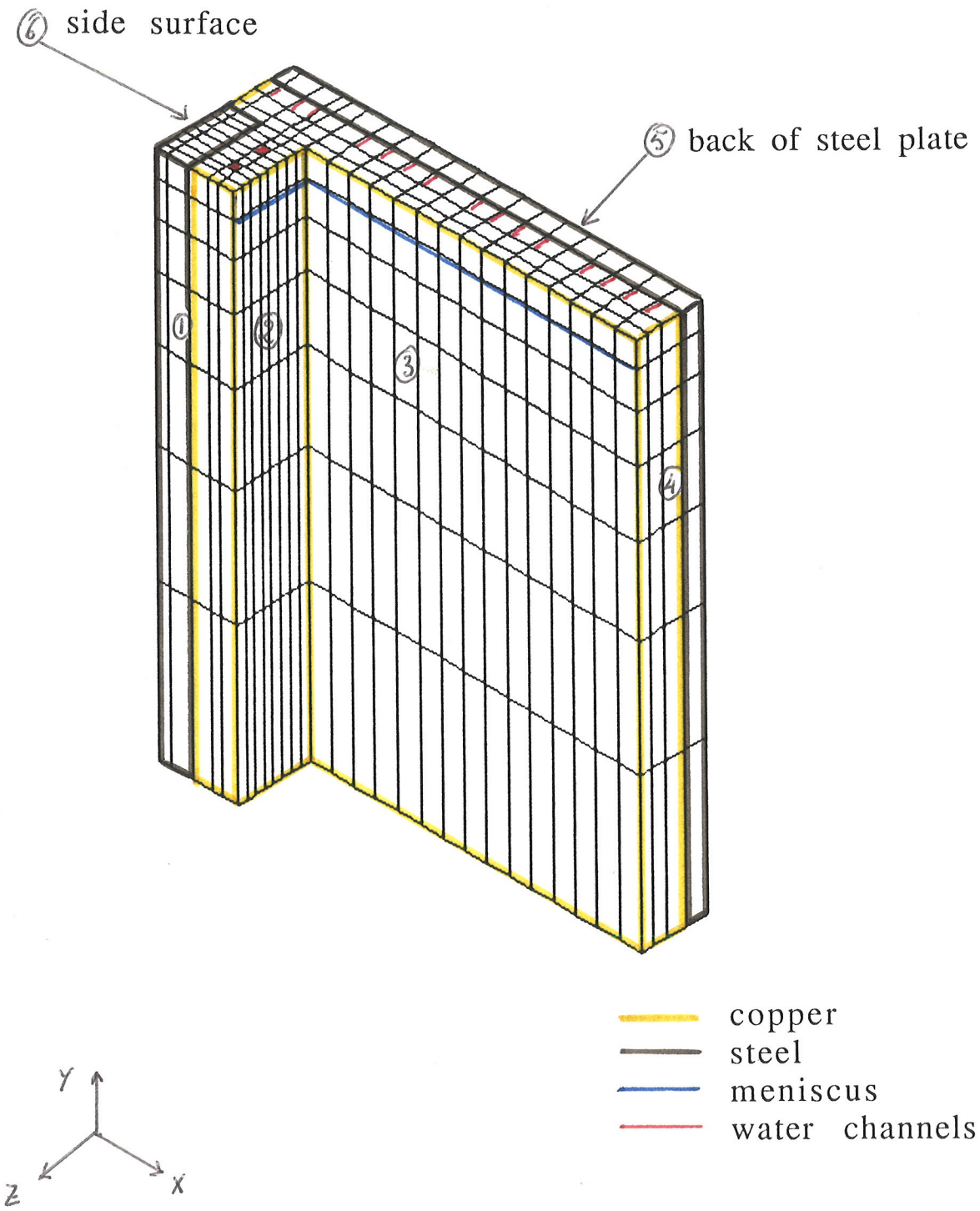

Fig. 1.1 Schematic of the quarter mold showing surface designation.

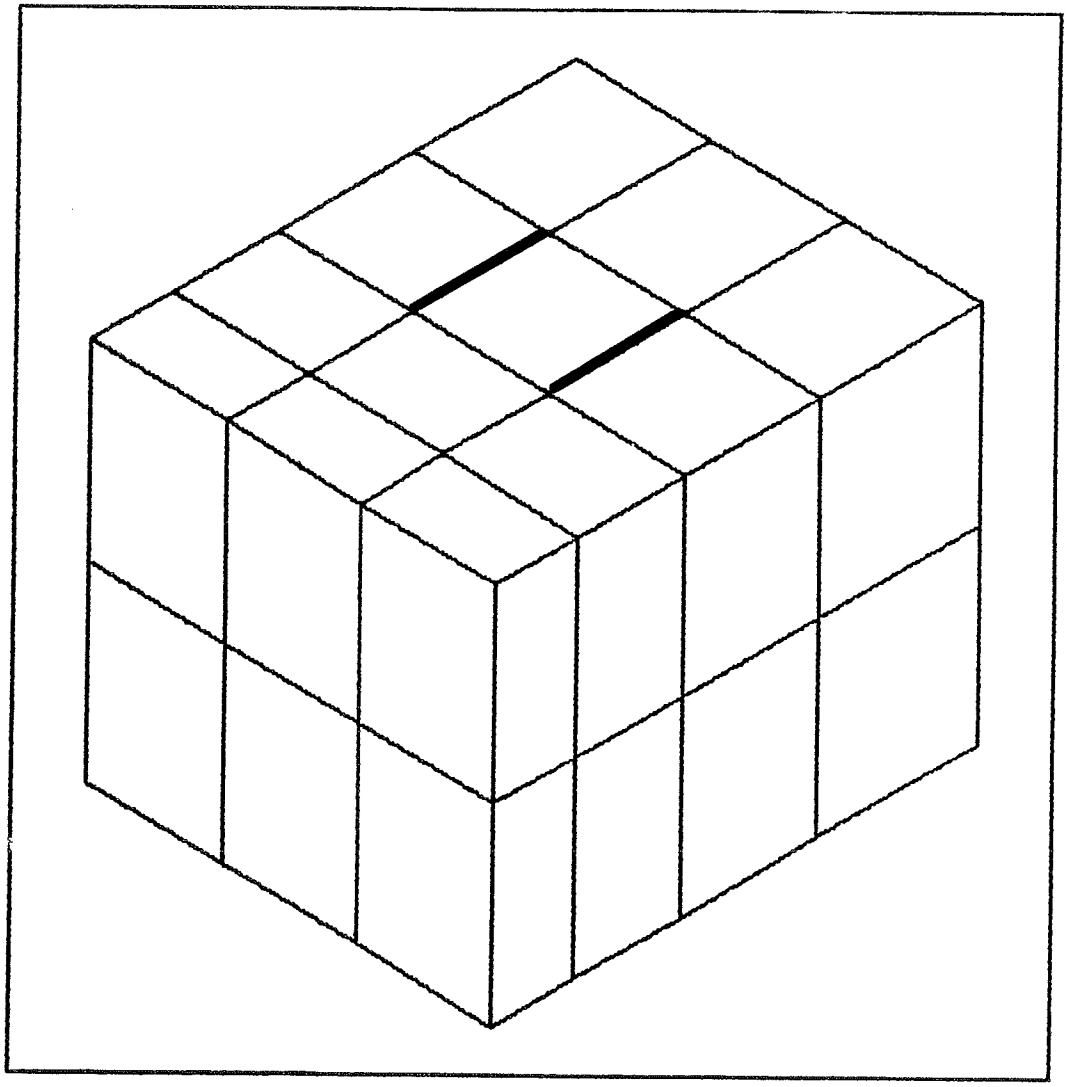

Fig. 1.2 Schematic of the small block.

same distance from the copper hot face as the actual circular channels, and also have the same internal surface area. The heat convection coefficient of these channels, h, is taken to be 2.1 W/cm^2 K with a constant water temperature, T_∞, equal to 35 °C.

The most important boundary condition is the heat flux coming from the molten steel into the copper hot face, shown as surfaces 2 and 3 in Fig. 1.1. Using a casting speed of 1 m/min, the heat flux is calculated for each of the element faces from the high heat flux curve shown in appendix A [2]. Due to lack of data, it is assumed as a first approximation that the heat flux does not vary across the mold surface (x and z direction). This heat flux starts out very high (4400 KW/m^2) at the meniscus located 100 mm from the top of the mold and decreases down the mold.

Two methods were used in applying the heat flux on the element faces. In the first method the element heat flux was calculated. Then individual node fluxes were calculated and input to the model (program in appendix B). In order to satisfy the symmetry condition, end nodes received only half the flux administered to internal nodes. The second method was to simulate heat flux through convection $Q = h A (T_S - T_\infty)$. This was accomplished using an arbitrary T_∞, taken to be six orders of magnitude greater than the highest expected surface temperature. Thus, T_S becomes negligible. Since the value of the heat flux per unit area, (Q/A), which was already known from the flux curve, could be used to calculate the appropriate value of h (program in appendix C). The second method is easier to implement since one need not to worry about calculating the area of the element face. Since the results of the two methods are similar, the results of the second method are included in this thesis.

Some other thermal boundary conditions are on surfaces 5 and 6 which are exposed to cooling water with h = 2.1 W/cm^2 K and T_∞ = 35 °C. Surfaces 1 and 4 are

adiabatic boundaries due to symmetry. The top surface loses heat to ambient air through natural convection with h = 0.025 W/cm^2 K and T_∞ = 35 °C. The bottom also convects to ambient with h = 0.015 W/cm^2 K and T_∞ = 35 °C.

With the mesh generated and boundary conditions applied, the steady state temperature distribution was calculated using a 3-D isoparametric 8-noded thermal brick element, STIF70 in ANSYS [4]. These temperatures were then loaded into an elastic stress analysis to calculate displacements using ANSYS. For the structural analysis, the 3-D linear isoparametric, STIF45 was used. The constraint system employed has a great influence on the distorted mold shape. The boundary conditions applied in this stress analysis were as follows; all nodes on surface 4 are fixed in the x direction, and all nodes on surface 1 are fixed in the z direction. These conditions were required based solely on symmetry. The mold was left essentially unconstrained from the small strains produced by thermal expansion and contraction. This is believed to be a good approximation of the constraint system actually employed in the caster. In addition, it allows the calculation of the maximum distortion possible. A copy of the stress analysis input file is found in appendix D.

Thin slice:

In order to confirm the results obtained from the 3-D model, a thin slice located at the center of the quarter mold was also analyzed using ANSYS. The dimensions of the slice are 9 cm X 70 cm X 1.75 cm. The mesh shown in Fig. 1.3 contains 495 elements and 1120 nodes.

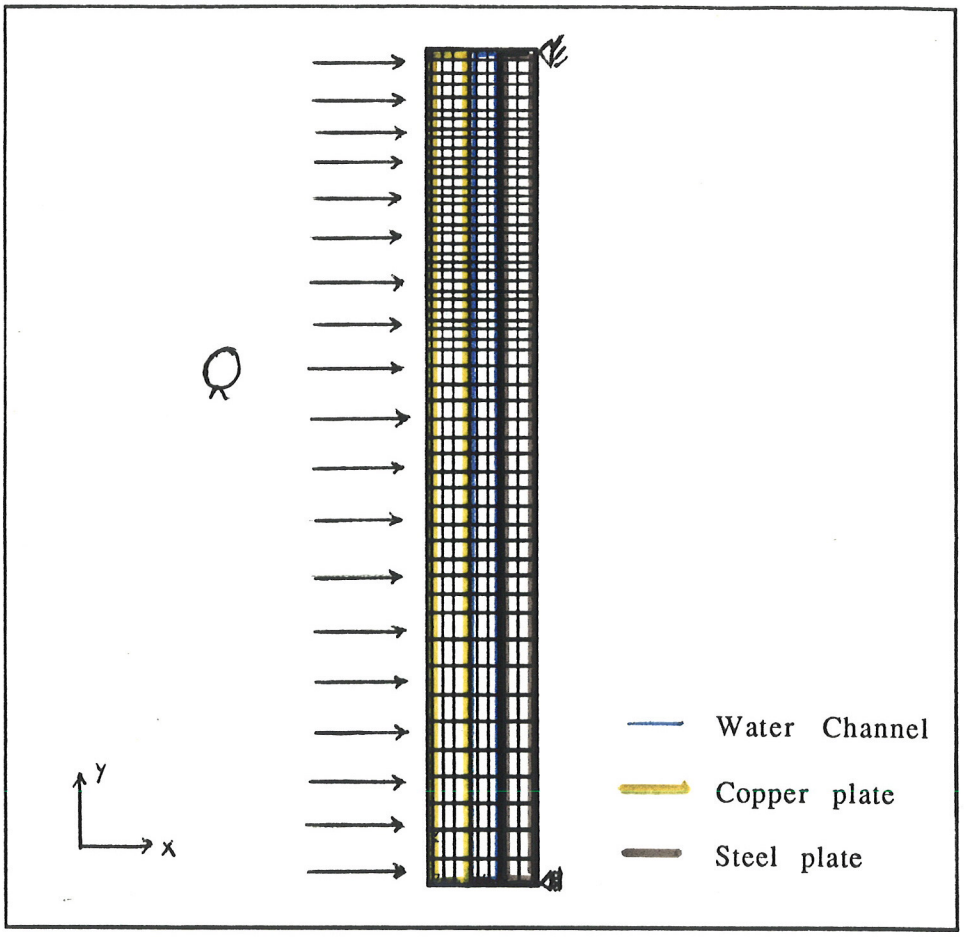

Fig. 1.3 Schematic of the thin slice.

For the thermal analysis, the same boundary conditions were applied. The top and bottom are convective with the bulk temperature, T_∞, equal to 35 °C and the heat transfer coefficient, h, equal to 0.025 W/cm^2 K and 0.015 W/cm^2 K, respectively. The right hand side surface loses heat to cooling water. The boundary condition on this surface is T_∞ = 35 °C and h = 2.1 W/cm^2 K. On the left hand side surface the heat flux from the molten steel was applied using the second method, mentioned earlier, with the same heat flux curve (see appendix A). The water channel located at 35 mm from the left surface has a width of 25 mm, and is considered to exist on the front plane only. The boundary conditions are taken to be h = 2.1 W/cm^2 K and T_∞ = 35 °C. The water temperature was assumed to be constant, as in the 3-D model.

For the stress analysis, a generalized plane strain condition was used on the slice. To prevent rigid body motion, the node in the top right corner is fixed (see Fig. 1.3). The node in the bottom right corner is restrained to a displacement in the y direction only. As in the 3-D model, the same elements were used in the analysis. STIF70 was used for the thermal analysis while STIF45 was used in the stress analysis with the generalized plane strain option. A copy of the thermal and stress analysis input files are found in appendix E and F, respectively.

1.2 RESULTS

Small block:

Before an attempt to solve the full 3-D model of the mold was undertaken, a small block of the mold was analyzed to determine the best approach to solve the problem. The objective in solving the small block first was to find out the simplifications that could be made with the geometry, and to achieve the coarsest possible mesh which could still generate accurate results, in order to save computing time. The temperature distribution in the coarse mesh block is shown in Fig. 1.4. The maximum temperature is 230 °C and the minimum is 35 °C. The results were compared to Storkman's results in a 12,810 elements and 2848 nodes mesh [5], which showed a good agreement between the two. Storkman reported a maximum temperature of 225.4 °C and a minimum temperature of 36.9 °C. The boundary conditions applied in both analysis were a heat flux of 1350 W/m^2, a convection coefficient, h, of 2.1 W/cm^2 K, and a bulk temperature, T_∞, of 35 °C. The temperature deviation from Storkman's model is mainly due to the different convection face on top of the block.

Quarter mold:

After the mesh size of the small block was verified, the 3-D model of the quarter mold was built and analyzed. The maximum temperature in the mold is 383 °C (656 K) and it is located just below the meniscus. In order to see how the temperature deviates along the hot face of the mold, a horizontal section showing temperature contours is plotted in Fig. 1.6. Fig. 1.7 and Fig. 1.8 show the temperature profile of section A-A (see Fig. 1.5) near the hot face. Notice in the temperature profile in Fig.

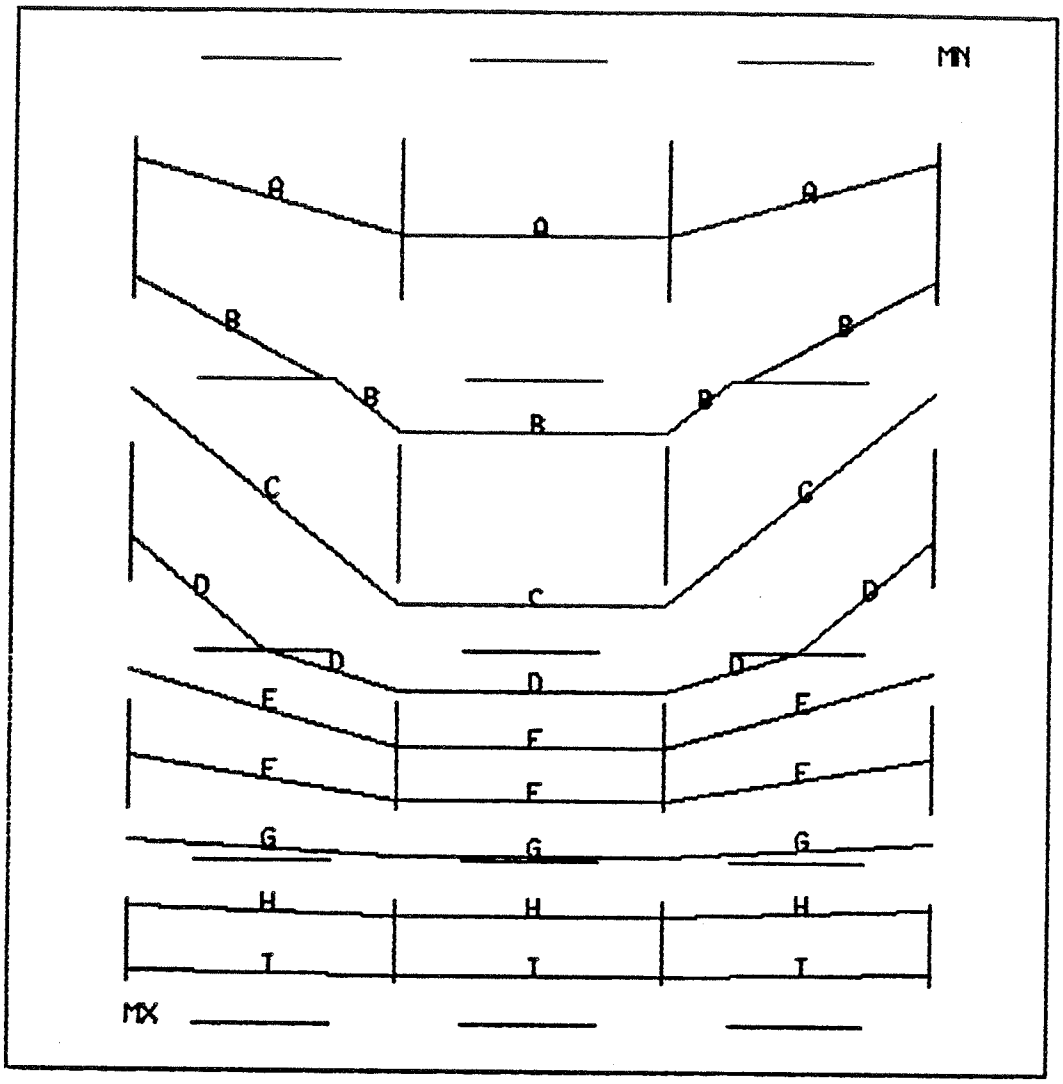

Legend:

Mx = 229 °C
Mn = 36 °C

A = 53 °C	D = 113 °C	G = 173 °C
B = 73 °C	E = 133 °C	H = 193 °C
C = 93 °C	F = 153 °C	I = 213 °C

Fig. 1.4 Temperature contours in small block.

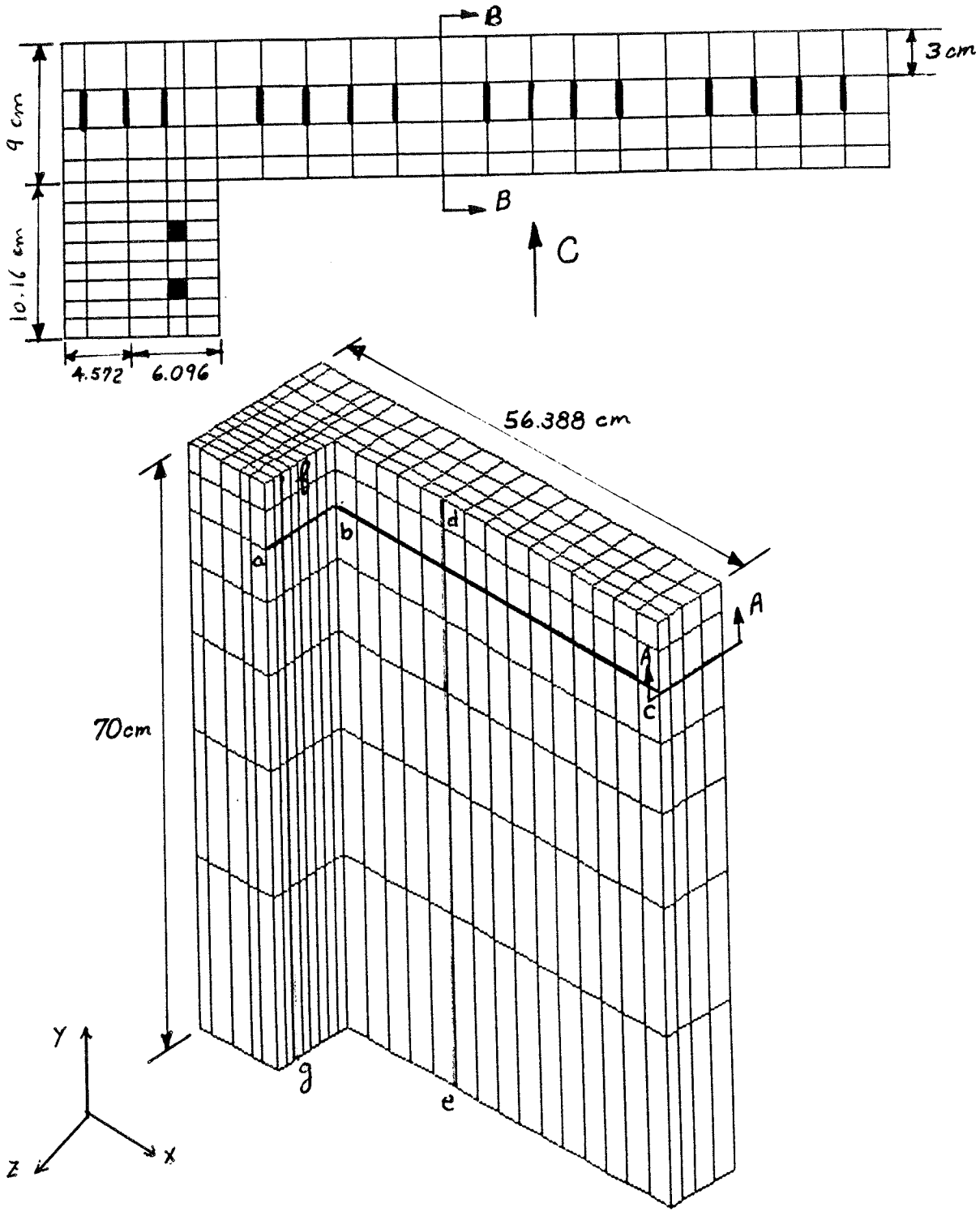

Fig. 1.5 Schematic showing sections & dimensions of quarter mold.

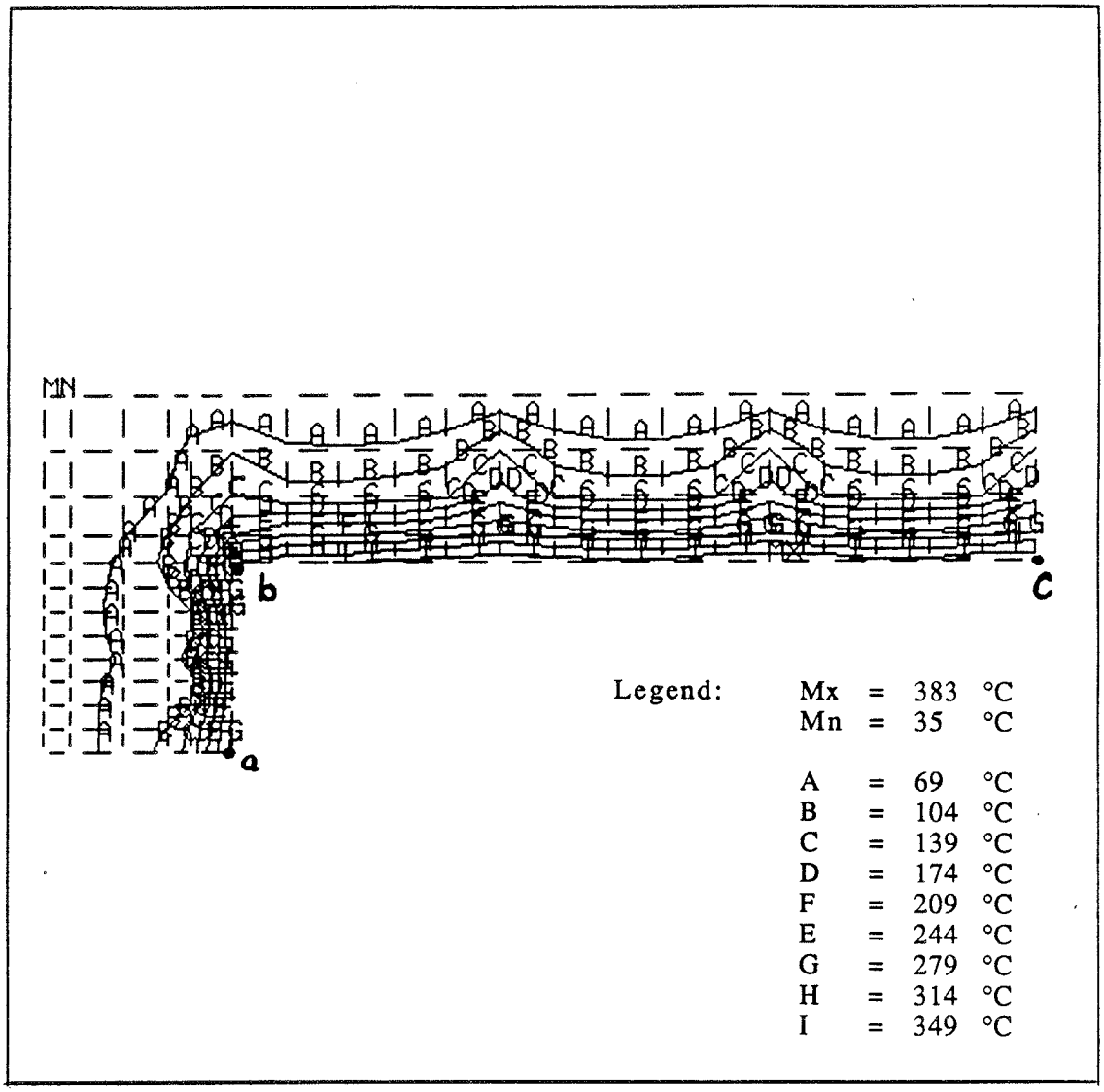

Fig. 1.6 Temperature contours at section A-A.

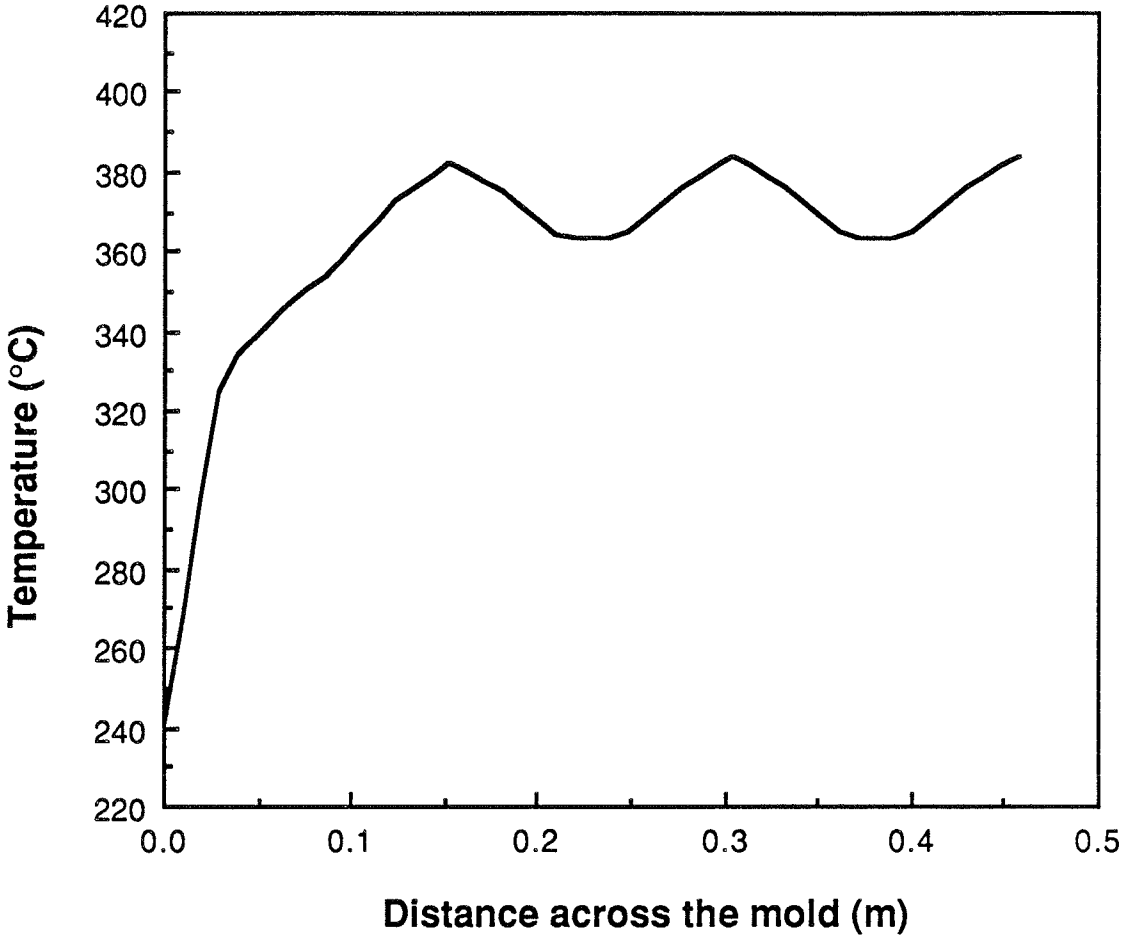

Fig. 1.7 Temperature profile between points b-c on Fig. 1.5.

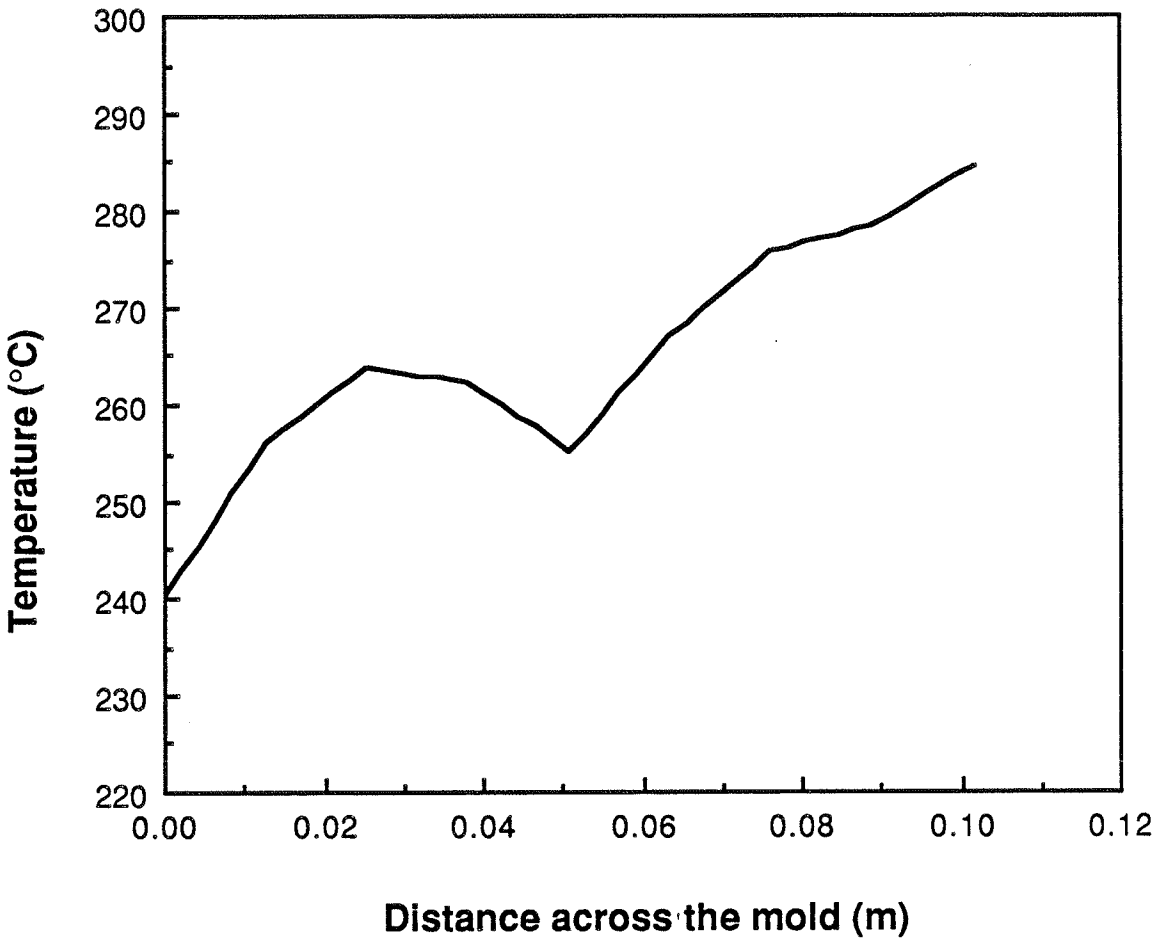

Fig. 1.8 Temperature profile between points b-a on Fig. 1.5.

1.7 that temperature is a maximum of between 360 and 383 °C (depending on proximity to the cooling channel), and it drops near the corner to 240 °C (513 K). Fig. 1.8 shows that the temperature is lower in the side plate than in the front plate. Also, the temperature contours of a vertical section of the mold are plotted in Fig. 1.9. The temperature profile shown in Fig. 1.10 is the hot face of the mold taken at section B-B. This profile is compared to some results calculated by Samarasekera et al [2]. It showed good agreement in the shape of the profile but the magnitude of the temperature was not verified because of the different cases that Samarasekera et al [2] studied. Fig. 1.11 is a temperature profile of the vertical section of the narrow plate. It was concluded that the temperatures obtained are reasonable.

The temperature output from the thermal analysis based on the second method was input to the stress analysis. The results of the thermal stress analysis were also presented. These results reveal that a maximum deflection in the z direction of 0.486 mm occurred at the center of the hot face of the front plate, and a maximum deflection in the x direction of 2.18 mm at the center of the hot face of the end plate (see Figs. 1.12 - 1.15).

Thin slice:

In order to verify the correctness of the results obtained from the quarter mold analysis, a thin slice in the quarter mold was analyzed. The second method (convection adaptation) was used in the input of the heat flux on the face. The maximum temperature obtained in the slice is 420 °C and located below the meniscus. Fig. 1.17 shows the temperature profile along the hot surfaces. The displacement profile of the hot face in the slice is shown in Fig. 1.18. The profile displays a parabolic shape with a maximum deflection in the center in the x

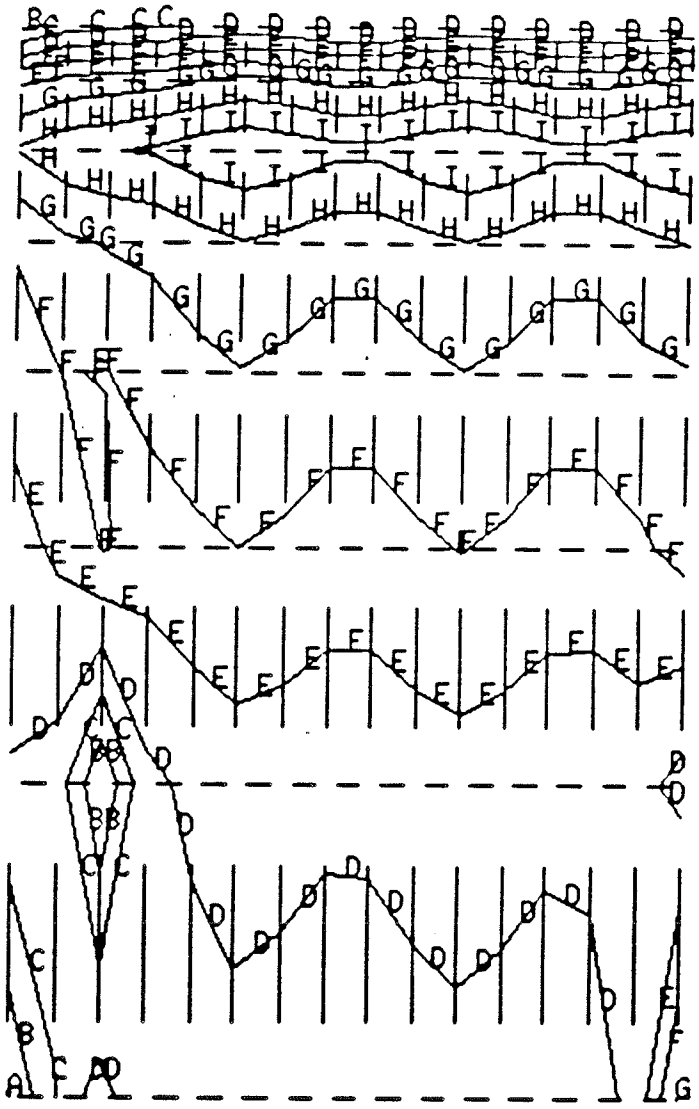

Legend:

Mx	=	377	°C
Mn	=	37	°C
A	=	67	°C
B	=	102	°C
C	=	137	°C
D	=	172	°C
F	=	207	°C
E	=	242	°C
G	=	277	°C
H	=	312	°C
I	=	347	°C

Fig. 1.9 Temperature contours for view C (refer to Fig. 1.5).

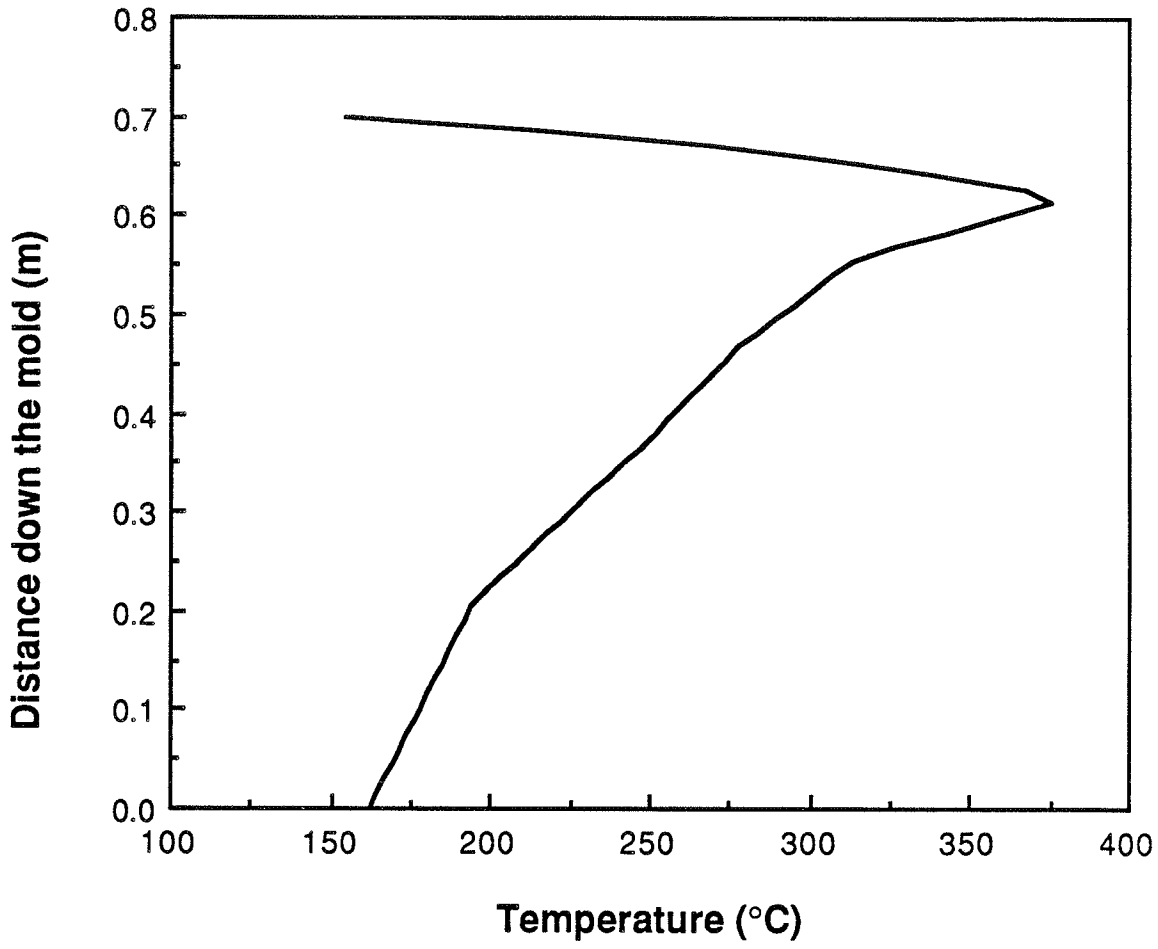

Fig. 1.10 Temperature profile between points d-e.

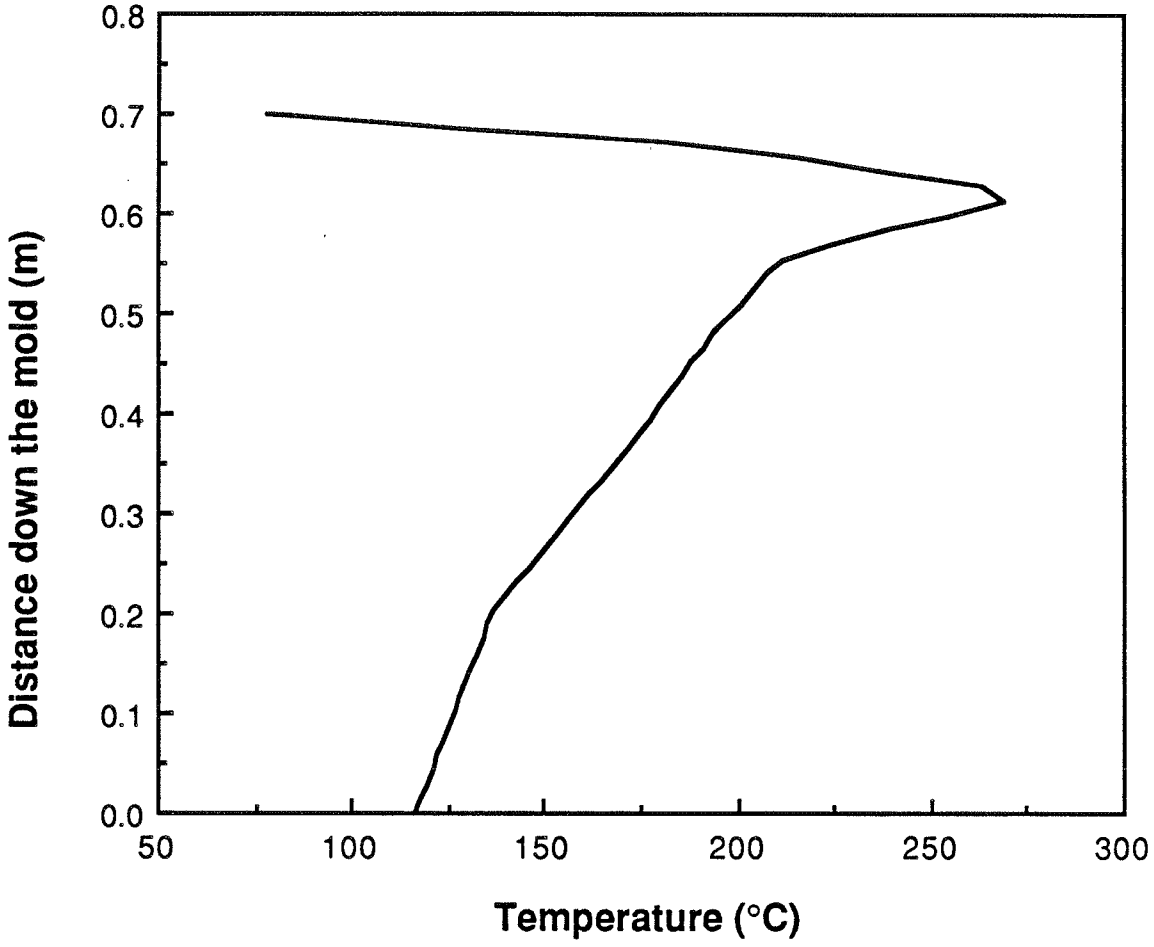

Fig. 1.11 Temperature profile between points f-g.

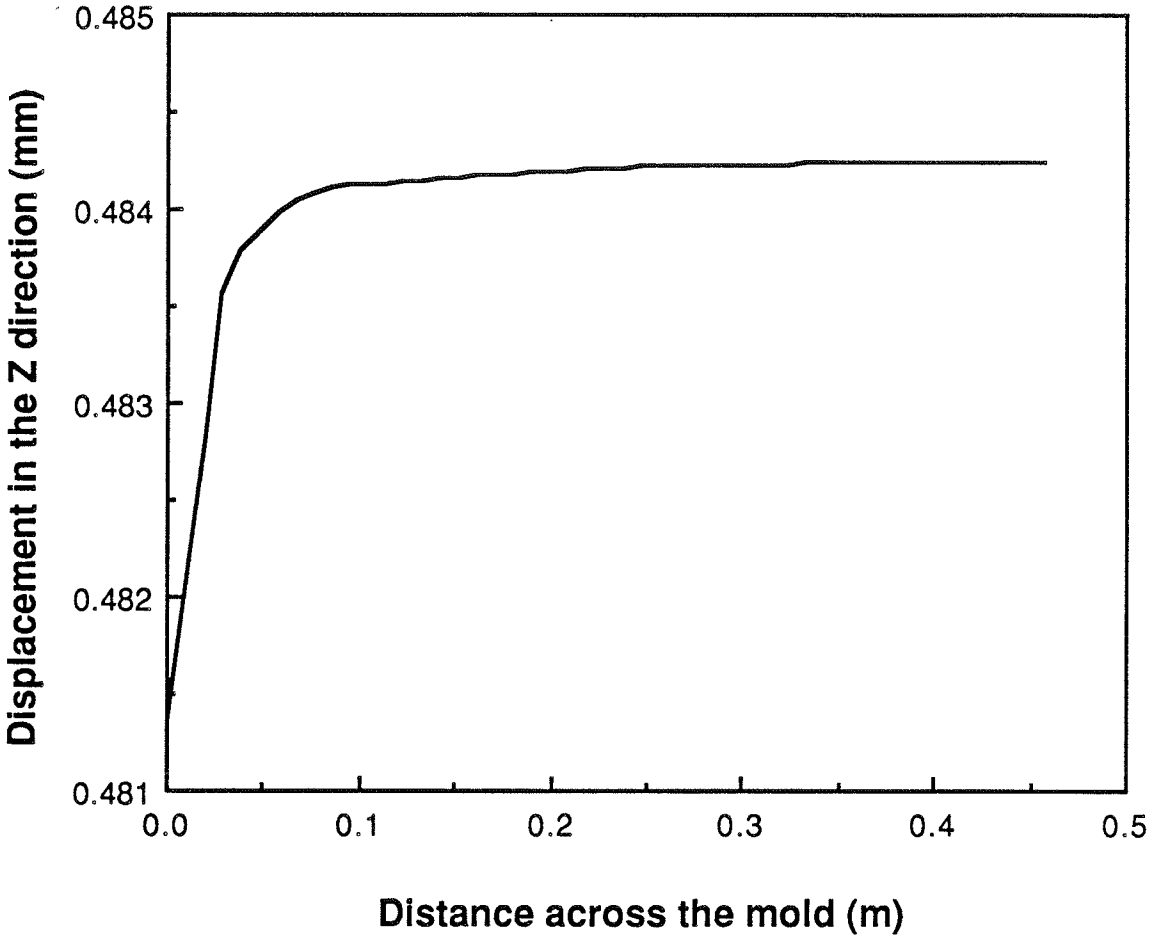

Fig. 1.12 Displacement profile between points b-c.

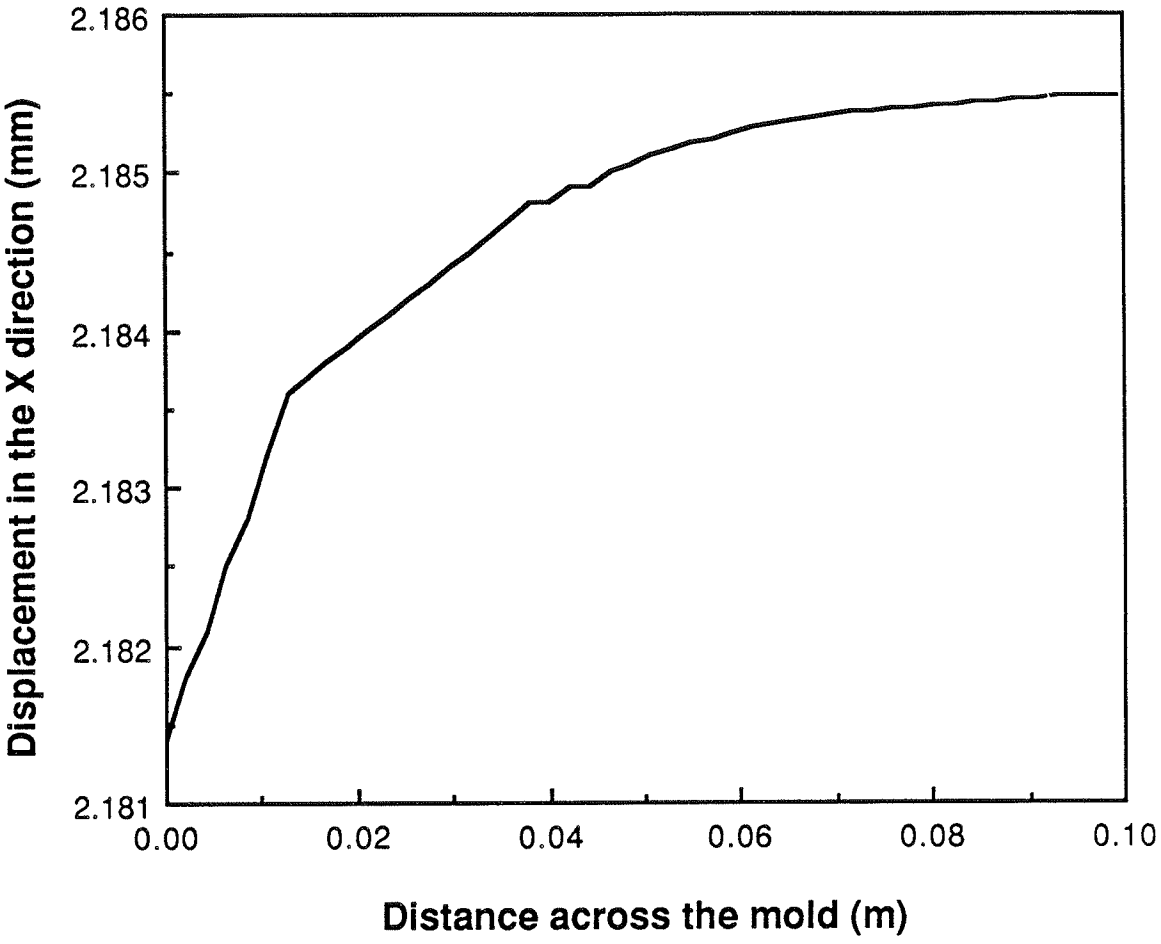

Fig. 1.13 Displacement profile between points b-a.

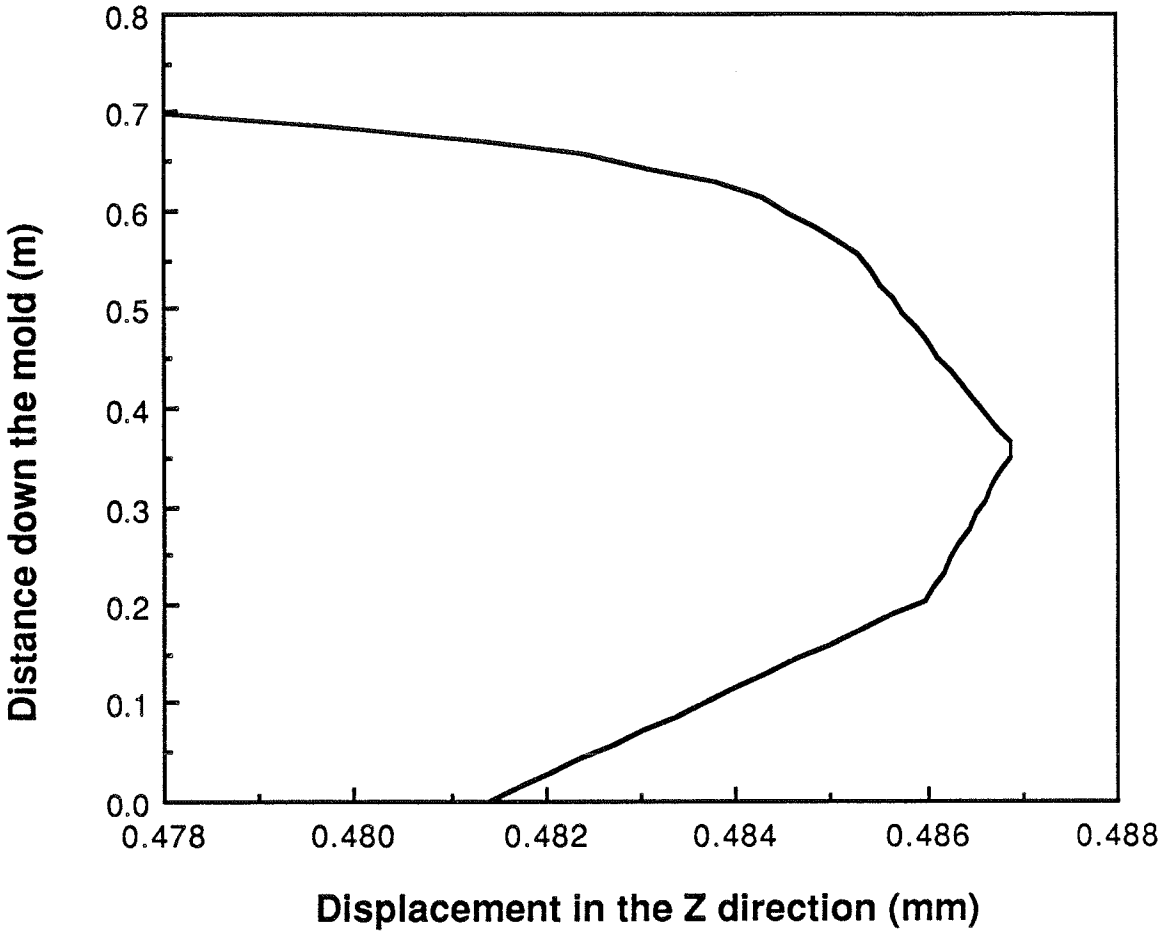

Fig. 1.14 Displacement profile between points d-e.

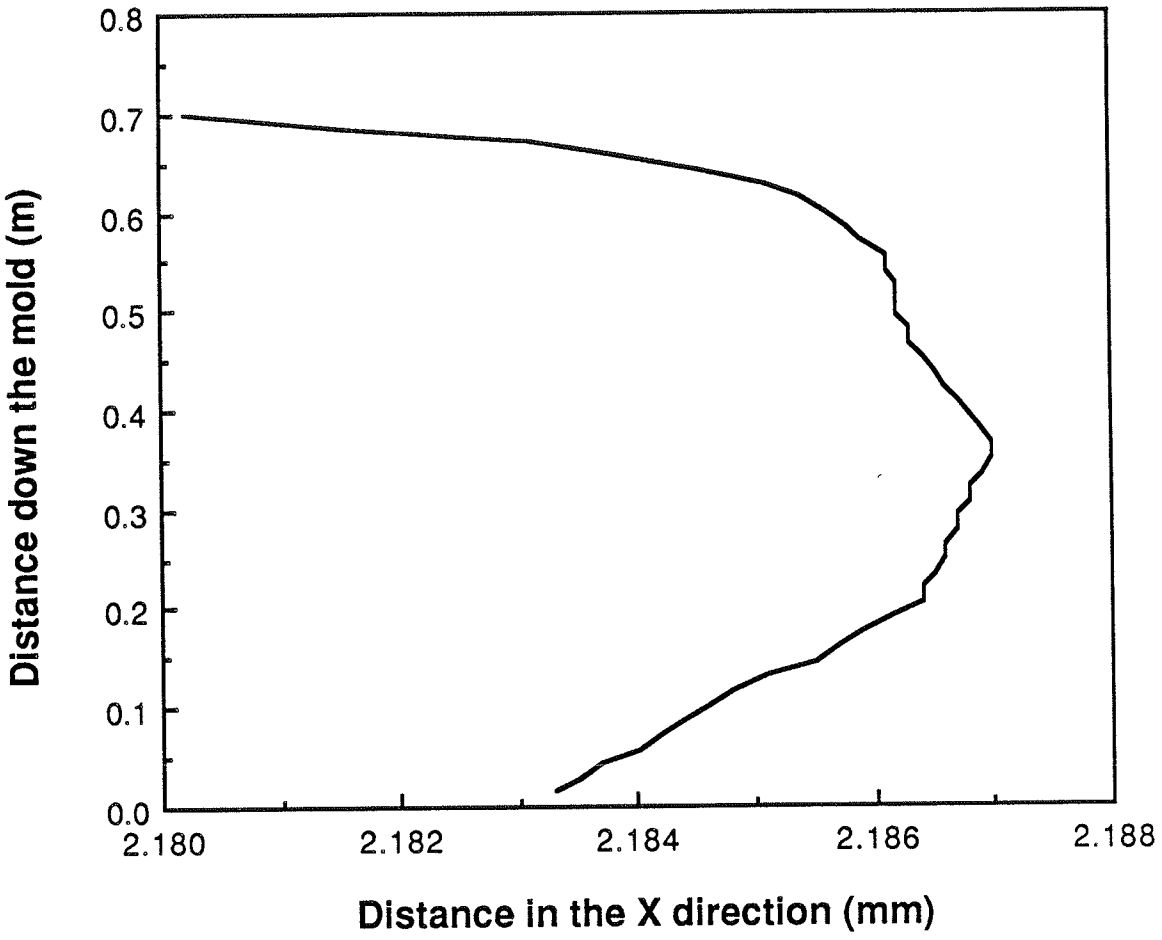

Fig. 1.15 Displacement profile between points f-g.

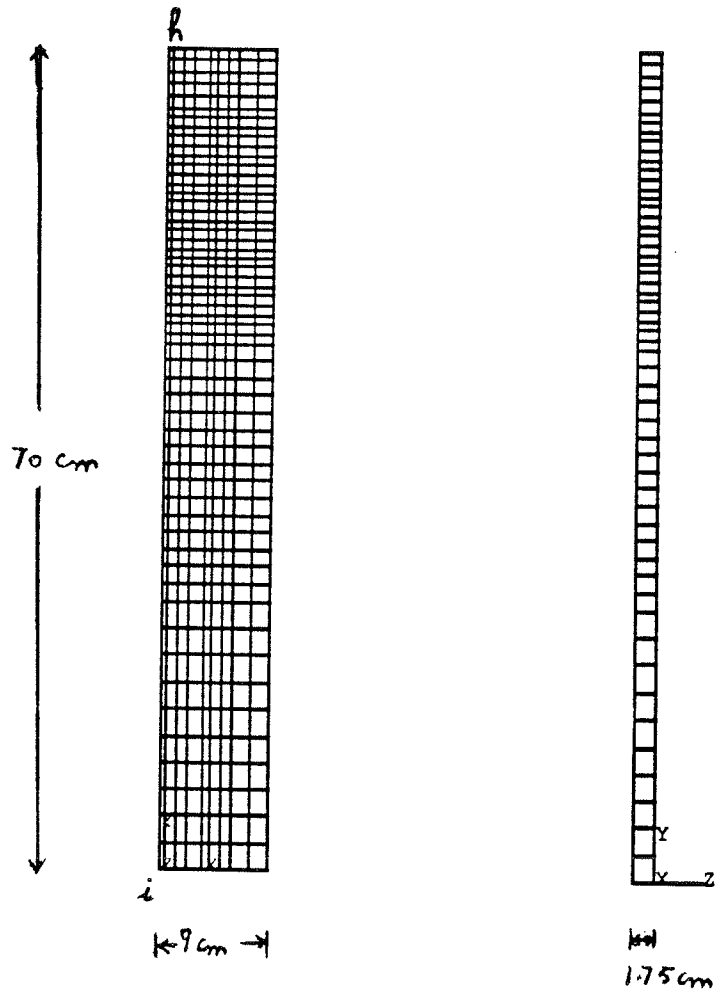

Fig. 1.16 Schematic showing sections & dimensions of the thin slice.

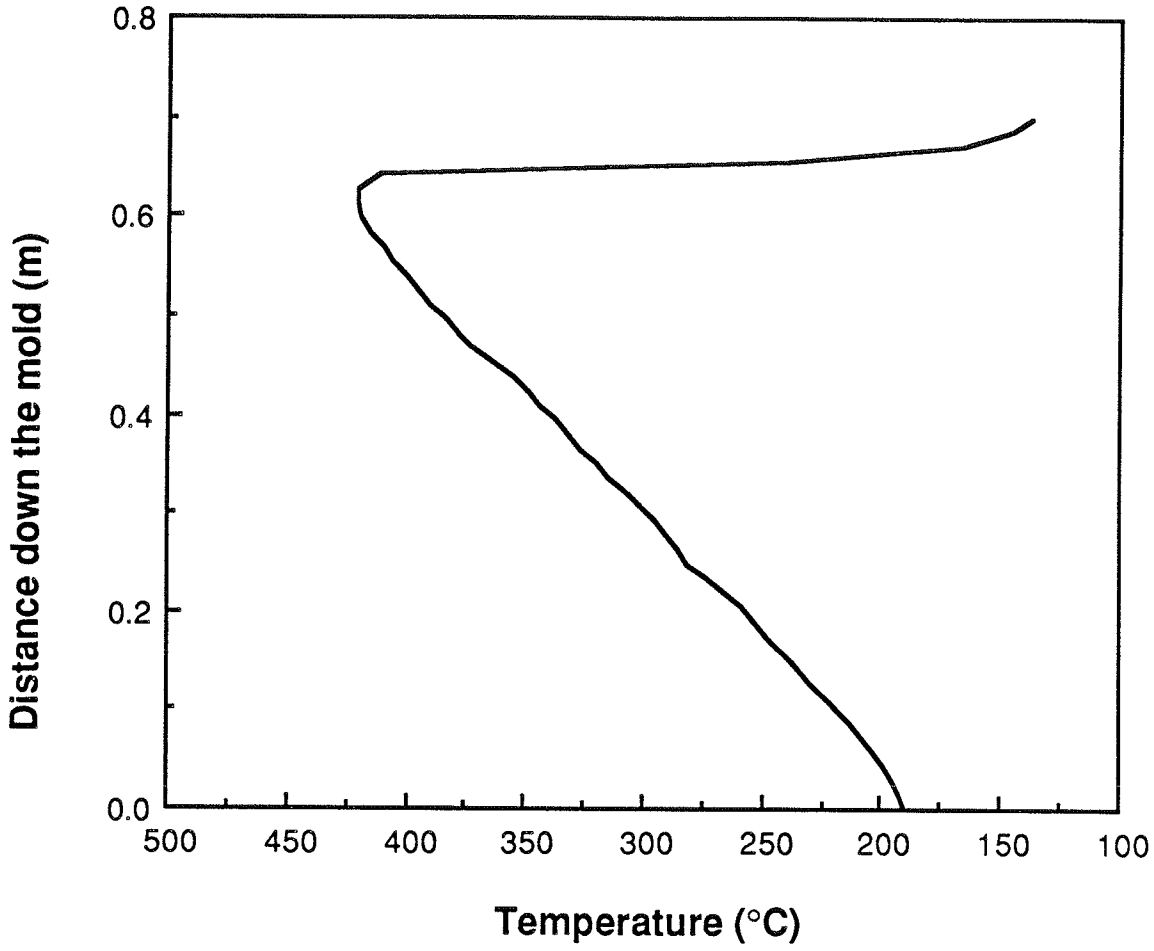

Fig. 1.17 Temperature profile between points h-i (see Fig. 1.16).

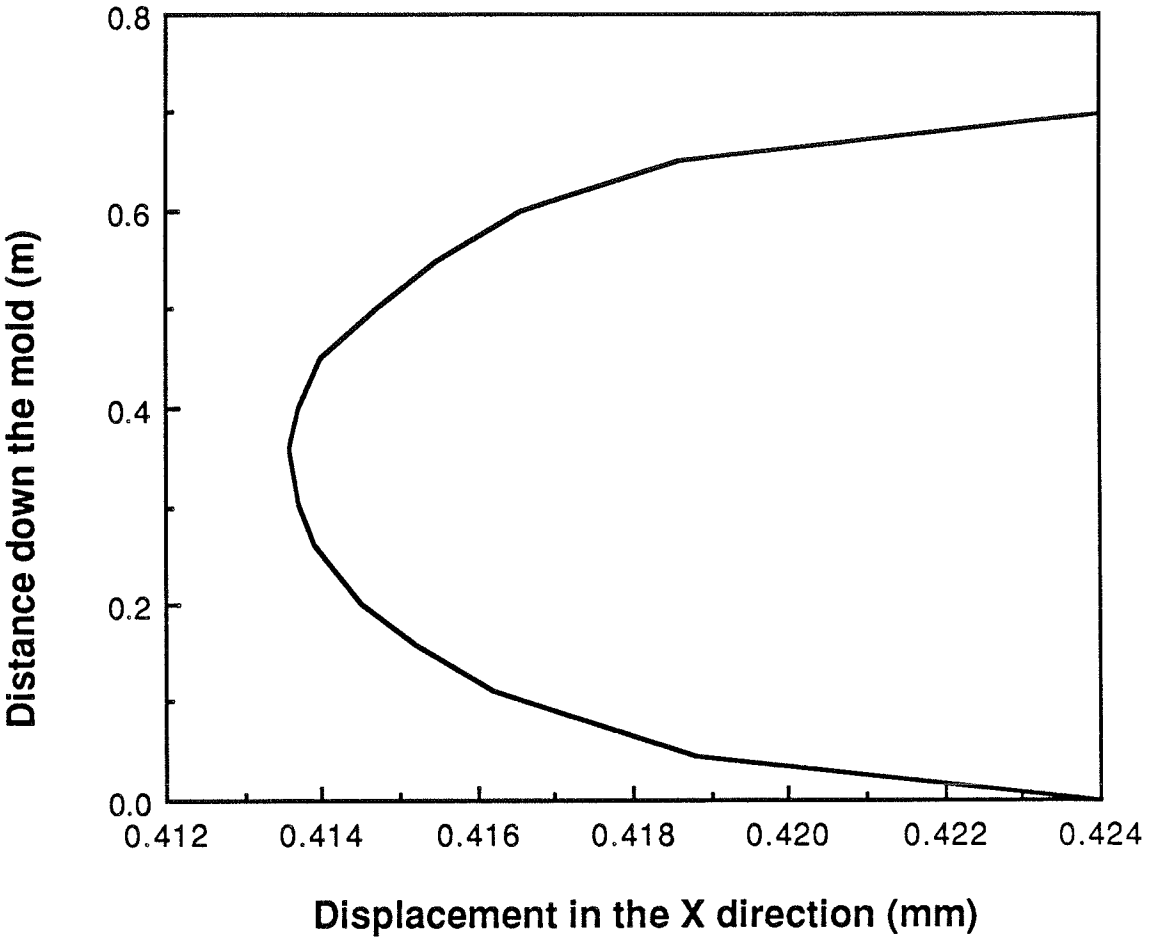

Fig. 1.18 Displacement profile between points h-i (see Fig. 1.16).

direction. The slice expands approximately linearly in the y direction. In the z direction, the slice maintains a constant displacement because of the generalized plane strain assumption.

1.3 DISCUSSION AND CONCLUSIONS

Before presenting the conclusions, it is useful to review the assumptions that underlie the present results. First of all, the heat flux to the hot face of the copper mold was assumed to vary only in the vertical direction (y direction). The consequence of this assumption is probably slightly elevated temperatures and distortions in the corner of the mold. The convection coefficients for the top and bottom of the mold were estimated using free convection from a flat plate [6]. The temperature of the water in the cooling channels was assumed constant at 35 °C with a constant heat transfer coefficient of 2.1 $W/cm^2 K$. With reasonably high flow rates this is probably a good assumption, but further investigation allowing water temperature to change is a consideration for future improvements on the model. Using an average water temperature may result in slightly lower temperature predictions at the top, and elevated temperature, at the bottom of the mold. The final assumption to be considered is that the thermal coefficient of expansion of copper was assumed constant, and no plastic flow occurs which are good assumptions except in the meniscus region.

The temperature profile results for the quarter mold seem reasonable. The maximum temperature in the mold is 383 °C, and occurs on surface 3. The horizontal location of maximum temperature coincides with areas where cooling channels are left out due to bolts. This is again a logical result. The vertical temperature profile

presented in the results section is extremely close in shape to that achieved by Samarasekera et al [2]. A numerical comparison of magnitudes is rather meaningless because many of the boundary conditions for Samarasekera's analysis are not documented. However, Samarasekera also found the maximum temperature to occur just below the meniscus, which again agrees with the predictions of our model. Furthermore, our model predicted a temperature drop around the corner of the mold of 240 °C. This trend can be attributed to the extra thermal mass that is provided by the corner.

The temperature profile for the thin slice is similar to that of the quarter mold. A slightly higher temperature of 420 °C was achieved in the slice. This higher temperature is attributed to the refinement of the mesh. More heat flux is input locally to the hot face when the finer mesh is used.

The displacement profile is parabolic in the slice and agrees with the 3-D results. The slice bulges outward toward the heat flux source. The maximum displacement occurs half-way down the mold due to bending.

From the analysis of the quarter mold and the thin slice, it was concluded that the mold expands in all directions due to general heating from the heat flux from the strand. The expansion shifts the wide face of the mold inward (toward the hot steel) a distance on the order of 0.5 mm and the narrow face about 2 mm. In addition, the surfaces of the mold in contact with the strand bends inward toward the heat source. This bulging is parabolic in shape because the mold bends due to the effect of a hot inner layer expanding but constrained by a colder outer layer (the steel backing plate) in a manner similar to a bi-metallic strip. The maximum deflection are then found at the top and bottom of the mold.

This is contrary to what happens in billet molds, which are much thinner. This allows a general temperature rise throughout the billet mold, and causes it to expand away from the heat source at the meniscus. The maximum occurs at a location higher up the mold and is in a direction outward away from the heat flow. This behavior is exactly opposite to the results obtained for slab molds.Samarasekera found a maximum displacement of -0.1 to -0.25 mm [7] in a billet mold. The magnitude of the deflection is naturally smaller than the slab mold results due to the smaller dimensions of the billet mold.

The most significant finding of this study is that the maximum difference in the distorted shape along the mold between the meniscus and mold exist is only 0.005 mm (0.487 - 0.482) or (2.187 - 2.183). A steel shell solidifying at the meniscus will shrink roughly 0.4 mm, which makes thermal distortion of the mold itself negligible in comparison. Thus, there is no need to include this mold distortion in a more comprehensive model of the strand.

2. CONSTITUTIVE EQUATION MODEL

Predicting the stress-strain behavior of steel while it is being processed at high temperatures in a continuous caster is important but very difficult. This leads us to study the constitutive equations describing the steels behavior.

A substantial amount of literature is devoted to the study of constitutive equations for the temperature and rate dependent plastic deformation behavior of metallic materials [8-15]. All the constitutive equations presented in previous studies lack in the ability to achieve both a simple, and yet accurate formulation.

Our objective is to find constitutive equations that describe the mechanical behavior of plain low-Carbon steel at temperatures between room temperature and the solidus, and for strain rates ranging from 1e-7 to 1e-2. The equations will be used to predict stresses in a 3-D model of the strand of a continuous caster so must be easily implemented into finite element models. Also, the equations must fit experimental stress-strain results. The stresses are induced from both thermal gradients and deformations in the steel. At the high temperatures and low strain rates involved in continuous casting, plastic behavior and creep in steel are very important. Therefore, to correctly simulate the behavior of steel, the equation needed for our study must contain the effects of varying temperature, strain rate, and deformation history. In addition, the equations must predict behavior under various changing loading conditions, including strain rate variations, stress relaxation and creep.

An approach is developed in the present project to evaluate a constitutive equation which is rate dependent and spans the temperature range of steel in continuous casting. Different choices for the constitutive equations are integrated

numerically under conditions of constant temperature and strain rate to generate stress-strain curves. Each curve is then compared with experimental data. One of the forms is then chosen because it fits the data most closely. A nonlinear optimizing program is developed to minimize the error between the curve and the data. The nonlinear program is then used to define the single set of equation parameters that fits the data best at different temperatures and strain rates. Details regarding the procedure for this analysis are described in the next section.

2.1 BACKGROUND

2.1.1 Nomenclature

Variables	Definition	Units
σ	Stress	MPa
ε_e	Elastic strain	m/m
ε_p	Plastic strain	m/m
ε	Total strain	m/m
E	Young's modulus	GPa
T	Temperature	K
$\dot{\sigma}$	Stress rate	MPa/s
$\dot{\varepsilon}$	Total strain rate	s^{-1}
$\dot{\varepsilon}_e$	Elastic strain rate	s^{-1}
$\dot{\varepsilon}_p$	Plastic strain rate	s^{-1}
s	Structure	
Q	Activation energy	J
R	Boltzman's constant	J/K
A	Material parameter	$(1/MPa)^n$
b, c, n	Constants	

2.1.2 Basic equations

Many finite-element programs, such as ANSYS, decompose the inelastic strain rate into a rate independent plastic part and a rate dependent creep part [5]. Using each part separately, it is difficult for a user to input appropriate constants that will produce the correct combined effect. Also, it is difficult to determine the accuracy of the model without extensive experimentation and simulation of test specimens under conditions similar to those experienced in the desired casting. To overcome this problem, a search for a "unified" constitutive equation that describes both effects, in a simple manner, is undertaken.

1) Rate independent equations:

The constitutive equations for one dimensional elastic and isotropic material are

$$\sigma = E\,\varepsilon_e \qquad (1)$$

$$\varepsilon = \varepsilon_e + \varepsilon_p \qquad (2)$$

where E the Young's modulus is a function of temperature [16], E = f (T). σ is the stress, ε_e is the elastic strain and ε_p is the plastic strain.

2) Rate dependent equations:

Equation (1) written in rate form is

$$\dot{\sigma} = E\,\dot{\varepsilon}_e \qquad (3)$$

At a given temperature, the total strain rate may be decomposed into elastic and

plastic parts

$$\dot{\varepsilon} = \dot{\varepsilon}_e + \dot{\varepsilon}_p \tag{4}$$

where, from (3) the elastic strain rate can be written as

$$\dot{\varepsilon}_e = \dot{\sigma}/E. \tag{5}$$

The plastic part is determined to be a function of stress, temperature and structure

$$\dot{\varepsilon}_p = f(\sigma, T, s) \tag{6}$$

where s, the structure, represents any number of internal "state" variables which characterize the resistance to plastic flow offered by the internal microstructure of the material [8]. In our model, we have chosen to represent the structure by ε_p, the plastic strain. This variable allows for the easiest comparison with existing experimental data, while retaining a sufficient potential to approximate the evolution of structure during casting. The model is classified as a viscoplastic model. Since $\dot{\varepsilon}_p$ is time dependent, the plastic part is considered to include both time-independent plastic strain and time-dependent creep strain.

2.1.3 Different forms of $\dot{\varepsilon}_p$

Many different forms of $\dot{\varepsilon}_p$ have been suggested for viscoplastic constitutive models. It should be noted that the form that best satisfy our needs is a form that takes into consideration the various strain rates and temperature effects, and the combination of elastic-plastic strain and creep strain. To determine a form that fits

the data closely, four different forms of $\dot{\varepsilon}_p$ are examined. Each form is given number to be easily identified.

The first form is relatively simple and has been used by many researchers to describe stress-strain behavior of steel at elevated temperatures. The equation is $\dot{\varepsilon}_p = A \exp(-Q/RT)\ \sigma^n$. This form is referred to as form 1.

Wray used an equation suggested by Sellars and Tegart [13] to fit his data. The equation relates plastic strain rates to stress and temperature of the form $\dot{\varepsilon}_p = A \exp(-Q/RT)\ [\sinh(b\sigma)]^n$ [12]. A, b, n and Q are found using experimental data to fit $\dot{\varepsilon}_p$. The data gathered from tensile tests on a Gleebel machine covers a range of temperatures, strain rates and percent Carbon [21 - 22]. The tensile test is done by fixing one end of the specimen while the other end is moved at different speed and under different temperatures. This form is referred to as form 2.

Anand proposed a constitutive equation of the form $\dot{\varepsilon}_p = A \exp(-Q/RT)\ (\sigma/s)^{1/m}$ [8], where s, the internal variable, is also defined through an evolution equation of the form $\dot{s} = \dot{s}(\sigma, T, s)$. This form is referred to as form 3.

In this thesis, a new form is suggested. This form is more general than form 1. The plastic strain rate equation is of the form $\dot{\varepsilon}_p = A \exp(-Q/RT)\ |\sigma - m\varepsilon_p^c|^{n-1}\ (\sigma - m\varepsilon_p^c)$. This form can be often reduced to $\dot{\varepsilon}_p = A \exp(-Q/RT)\ (\sigma - m\varepsilon_p^c)^n$. The reason for writing the form in different way is to take count of the negative value inside the parentheses when the form is evaluated in stress relaxation experiments. This form is referred to as form 4.

The variables in the equations mentioned above (A, Q, R, n, m, c and b) are

material parameters. R and Q denote Boltzman's constant and the activation energy, respectively. The other parameters have meanings that will be clarified in later sections.

2.1.4 Comparison to other forms

The rate independent forms (stress-strain curves) used in many finite element packages, such as ANSYS, have the advantage of simplicity. However, this form can be temperature dependent but have no variation due to time. This approach is helpful in situations where strain rate variations and time dependent behavior are not required. In our situation strain rate variations, relaxation and creep have great effects on the solution of the problem. Therefore, the rate dependent approach can not be neglected and must be applied.

Form 1 is used by other investigators to describe stress strain behavior of steel at elevated temperatures. The equation is clearly a function of only stress and temperature, $\dot{\varepsilon}_p = f(\sigma, T)$ and does not include a structure dependency. At constant temperature, A exp(-Q/RT) becomes a constant, so this form can be written as

$$\sigma = (\dot{\varepsilon}_p / K)^{1/n} \qquad (7)$$

where $K = A \exp(-Q/RT)$

Assuming that at a strain greater than 0.5%, the plastic strain rate is equal to the total strain rate, we can calculate the asymptotic value of stress achieved at high strain to be:

$$\sigma = (\dot{\varepsilon}/K)^{1/n}. \qquad (8)$$

To determine how soon the stress approaches this asymptote, different n and K values must be plotted for the same stress. It is concluded that as n gets large the stress approaches the asymptote at lower strains.

A first look at form 2 suggests that this form is considerably different. However, this form is written in terms of the stress σ,

$$\sigma = (1/b)\ \text{arcsinh}(\dot{\varepsilon}/K)^{1/n} \qquad (9)$$

it can be seen to be similar in behavior to form 1. Both forms 1 and 2 reach a constant asymptote but at different rates.

The proposed equations in form 3 seem to fit Wray's data very well, but they are significantly more complicated due to the additional presence of the evolution equation for structure, $\dot{s}$. A program implementing this form must solve for both $\dot{\varepsilon}_p$ and $\dot{s}$ simultaneously because the two equations are dependent. Also, a total of eleven parameters A, Q, m, α^*, h_0, s, n, a, B, Q_r and b must be determined for each material. This requires an extensive experimental testing program. In addition, a change in the temperature and strain rate requires a change in s_0.

The effort required to implement such a complicated formulation for the constitutive relation to simulate a 3-D model of the casting process would be formidable. The corresponding accuracy gains found in large strain simulations, such as rolling, where these complex models have been implemented, are not likely.

Therefore, a simpler formulation is sought that would be just as accurate for simple loading conditions, but require less calculation and should be determined from existing experimental data (mainly tensile tests).

Form 4 is a slightly more general form of 1. It has the same features as 1, but instead of reaching a constant asymptote it reaches a curvilinear asymptote which is a more realistic approximation of metal behavior during the critical first few percent strain that are of interest in casting. To see the behavior of form B, it is written as:

$$\sigma = (\dot{\varepsilon}/K)^{1/n} + m\varepsilon_p{}^c \qquad (10)$$

where σ_y is a function of strain and $(\dot{\varepsilon}/K)^{1/n}$ is a constant. Thus, form 4 is considered as a function of stress, temperature and structure, where the structure is the plastic strain.

2.2 NUMERICAL MODEL

Classical "closed-form" integration methods give solutions for only a restricted class of differential equations. Unfortunately, the equations (3) - (6) are first order nonlinear differential equations which could not be solved in general using analytical methods. Thus, a numerical method was developed to evaluate the three constitutive equation forms described in the previous section. In order to determine the best numerical method for solving the equations, a review of the time stepping techniques is necessary. Two different methods of integration are considered [17].

The first integration type is the one step or "explicit" method. In this method,

only the information available at point (x_m, y_m) is needed to find y_{m+1}. Also, iteration is not required at any point. In addition, the evaluation of any derivative of f(x,y) is not required which makes this method attractive to use. Forward Euler formula uses the one step method. Euler's method is one of the oldest and best known numerical methods for integrating differential equations. However, it is unstable, since small errors become magnified as the value of x increases. Thus, Euler's method can be improved in a number of different ways. One way is to iterate at each time step. This method is called the multistep method.

The multistep method is the second type of integration. It requires iteration at every point on the curve. The iteration is done until the function approaches a sufficiently accurate value. Methods of this type are called predictor-corrector. As implied by the name, an initial value of the function is predicted. Then, the value is corrected by iterating. A small step requires less iteration. However, more points on the curve must be calculated. On the other hand, a large step creates fewer points with many iteration per point. Hence, choosing a step size that avoids going through many iterations is more efficient and feasible economically.

Equations (3) - (6) are programmed using the multistep method. The modulus of elasticity , E, is included as a temperature dependent function [16]. In addition, the total strain rate is taken to be constant.

The algorithm used is presented in Fig. 2.1 to show the steps followed in the integration of the constitutive equations. Note that convergence within a step is based on the plastic strain rate, $\dot{\varepsilon}_p$. A copy of the program using this algorithm is found in appendix G.

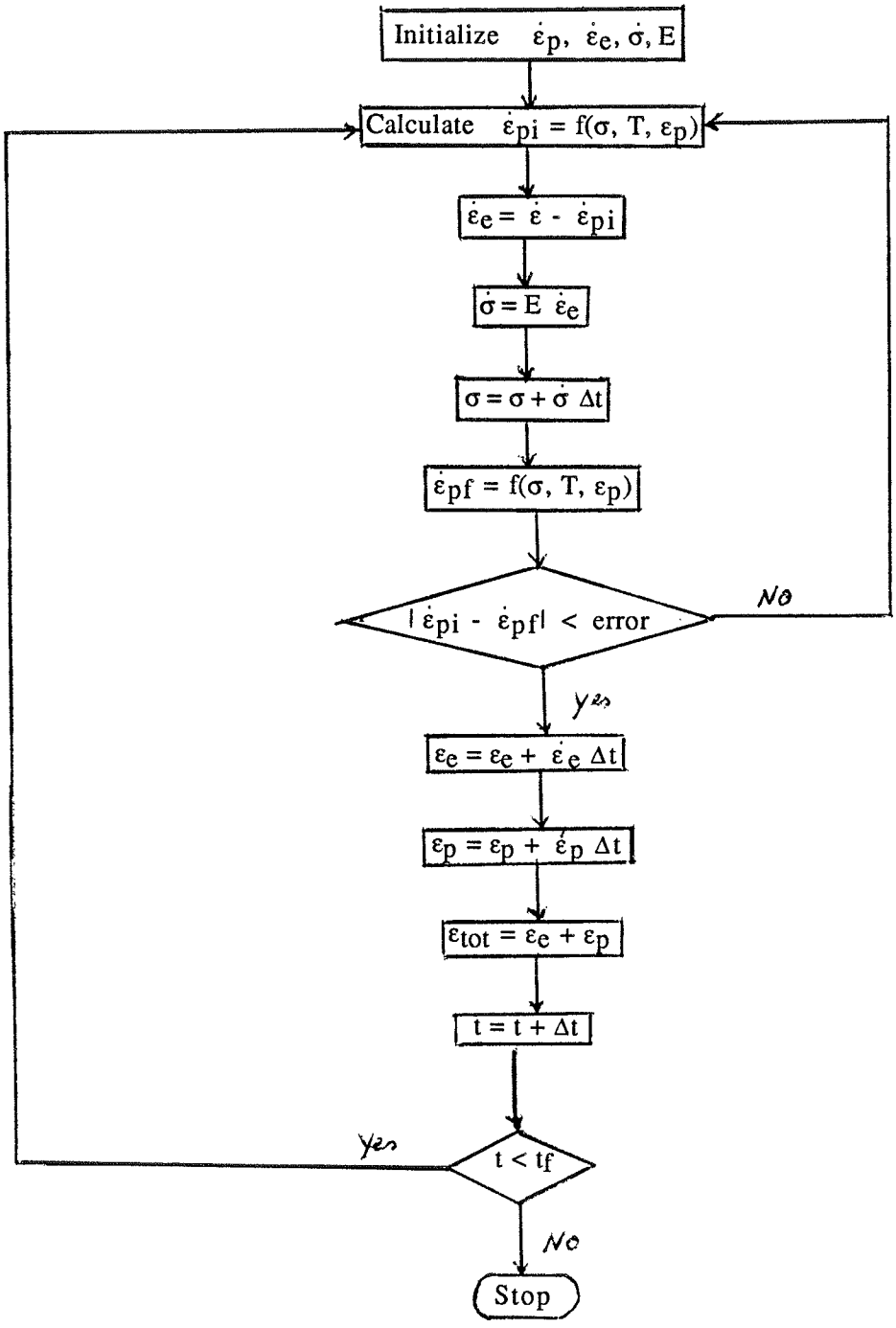

Fig. 2.1 Flowchart of the program used in solving for $\dot{\varepsilon}_p$.

2.3 RESULTS

Three forms of $\dot{\varepsilon}_p$ described in the previous section (forms 1, 2 and 4) were integrated using the algorithm mentioned in the previous section. The results are plotted and compared to the data obtained from P.J. Wray [22] in Fig. 2.2. The variables b, c, n, m and K are chosen to fit the data as close as possible for a temperature of 1100 ^{o}C and a strain rate of 2.3e-2. Note that at very small strains, the stress values in forms 1 and 2 reach constants and approach the asymptotes calculated in equations (8) and (9). The two forms differ in the strains at which the asymptotes are reached. Changing the parameters in forms 1 and 2 has little effect on the shape of these curves because of the previously discussed mathematical limitations of these forms.

As shown in Fig. 2.2, form 4 simulates the data closer than the other two forms. This behavior is expected because form 4 is capable of following a strain-dependent asymptote given in equation (10). Since form 4 can be controlled to simulate the data, the next step is to find out how to choose the five parameters that fit the data best at different temperatures and strain rates.

A nonlinear program, Simplex (appendix H), based on the method suggested by Nelder and Mead [18] is used to find the best values of the parameters to fit experimental data points. The method is explained in detail in Himmeblau [19]. The method is called "flexible polyhedron", which searches for the minimum of a certain function by changing the function parameters. In our case, the function is the error between experimental data and the integrated function of the stress versus strain. Since it is most effective at making only minor adjustments to the

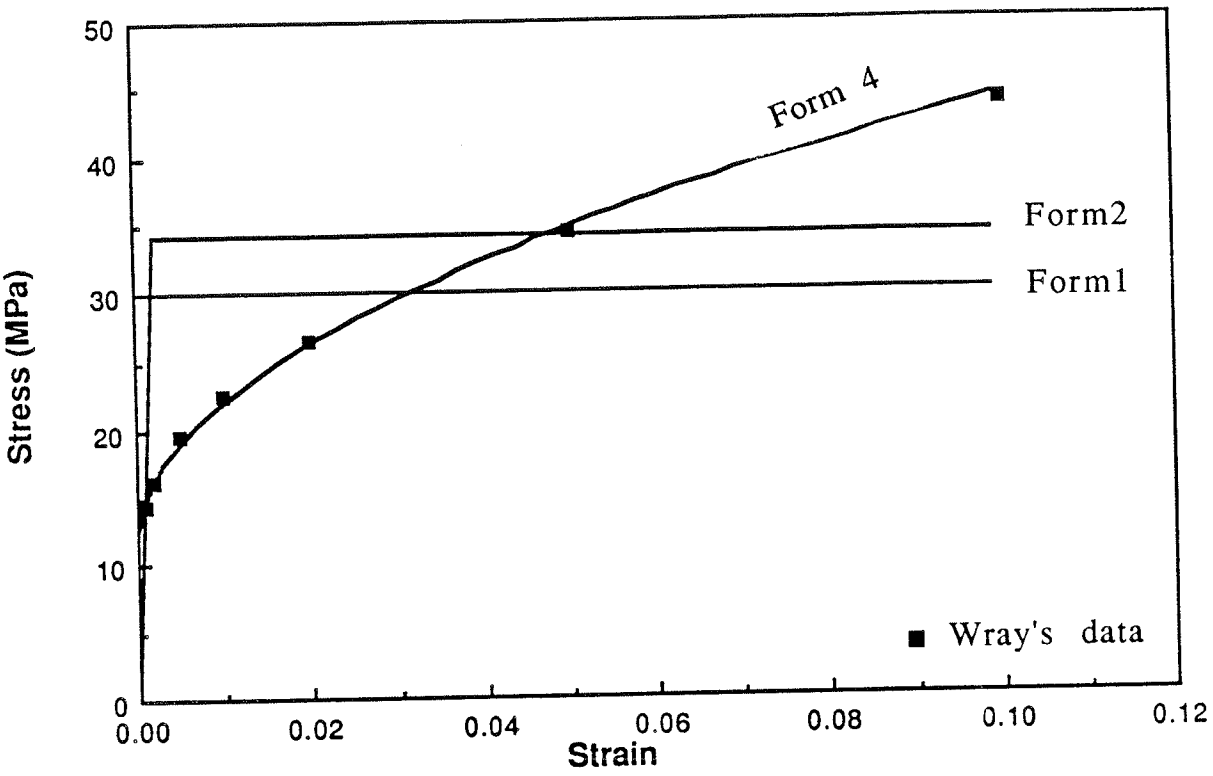

Fig. 2.2 Calculated stress-strain curves of different $\dot{\varepsilon}_p$ and stress-strain data for Fe 0.051 weight percent Carbon at a temperature of 1100 °C and a strain rate of 2.3e-2.

parameters, it is important to supply a very good initial guess of the parameter values. This is obtained by developing an understanding of the importance of each parameters on the shape of curve, just described. To show the effect of each parameter, form 4 can be written in different way,

$$\sigma = (\dot{\varepsilon}_p/K)^{1/n} + m\varepsilon_p{}^c \qquad (11)$$

where $K = A \exp(-Q/RT)$

The term $(\dot{\varepsilon}_p/K)^{1/n}$ in equation (11) controls the start of the curvature (points A and B), m controls the slope of the curve in the plastic part of the curve, c controls the curvature in the plastic part, and n controls the "stiffness", as shown in Fig. 2.3.

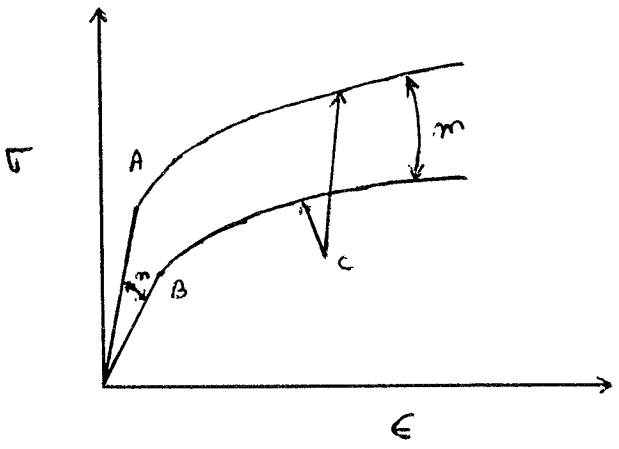

Fig. 2.3 The effect of each parameter on a stress-strain curve.

Once the parameters are estimated, Simplex is then used to minimize the error to obtain the best fit. A total of 25 experimental tensile test curves were discritized into 5 stress-strain points each. The result of a simplex run is a set of parameters that describe the best fit to a given set of data. An example of the fit obtained to an individual stress-strain curve, is shown in Fig. 2.2. However, a single set of

parameters is needed which accurately describe flow behavior over the entire range of temperatures and strain rates.

The temperature range between 100 °C and 1300 °C was divided into 3 regions. This natural division corresponds to the three phases of steel in this temperature range (two ferrite and one austenite). The temperature range from 900 °C to 1300 °C is austenite. The temperature range from 100 °C to 900 °C is ferrite. This temperature range is further divided into two regions due to an interesting strain rate effect. Region 100 °C to 500 °C has minimal strain rate effect, while 500 °C to 900°C has significant strain rate effect. The experimental data used are gathered from three different papers. For the temperature range between 100 °C and 500 °C, the data are taken from Manjoine [20]. For the temperature range between 500 °C and 900 °C, the data are taken from Wray [21]. Finally, for the temperature range between 900 °C and 1300 °C, the data are from Wray [22]. A single set of parameters is found for each range of temperature defined above and strain rates between 1e-7 and 1e-2 using simplex. The parameters are found in Table 2.1.

The ability of the model to generate stress-strain curves as a function of temperature or strain rate are plotted and compared to experimental data. Figs. 2.4 - 2.6 are plots of the stress-strain curves using the first set of parameters compared to experimental data taken from Manjoine [20]. For a constant strain rate of 2e-2, stress-strain curves of various temperature are shown in Fig. 2.4. Fig. 2.5 and Fig. 2.6 show the curves of various strain rate at a temperature equal to 200 °C and 400 °C, respectively. Figs. 2.7 - 2.8 are plots of the stress-strain curves using the second set of parameters compared to experimental data taken from Wray [21]. Fig. 2.7 shows stress-strain curves of various temperatures at a constant strain rate equal to 2.3e-2. At a temperature of 700 °C, stress-strain curves of various strain rates are plotted as

Table 2.1 Experimental data and parameters.

Temperature ranges (^{o} C)	100 - 500	500 - 900	900 - 1300
Phase	α	α	γ
Tensile data sources	Manjoine (1944)	Wray (1984)	Wray (1982)
Chemical Compositions	Mild low Carbon	0.007 C 0.011 Mn 0.24 Si 0.002 S	0.051 C 0.82 Mn 0.28 Si 0.018 S
Parameters	A = 1.0E-3 m = 1256.5 - 0.614 T (K) c = 0.286 n =1	A = 1.01E+5 Q/R= 35247 m = 418.1 - 0.285 T (K) c = 0.52 n = 6.01	A = 6.33E+4 Q/R = 40333 m = 428.15 - 0.241 T (K) c = 0.57 n= 5.42

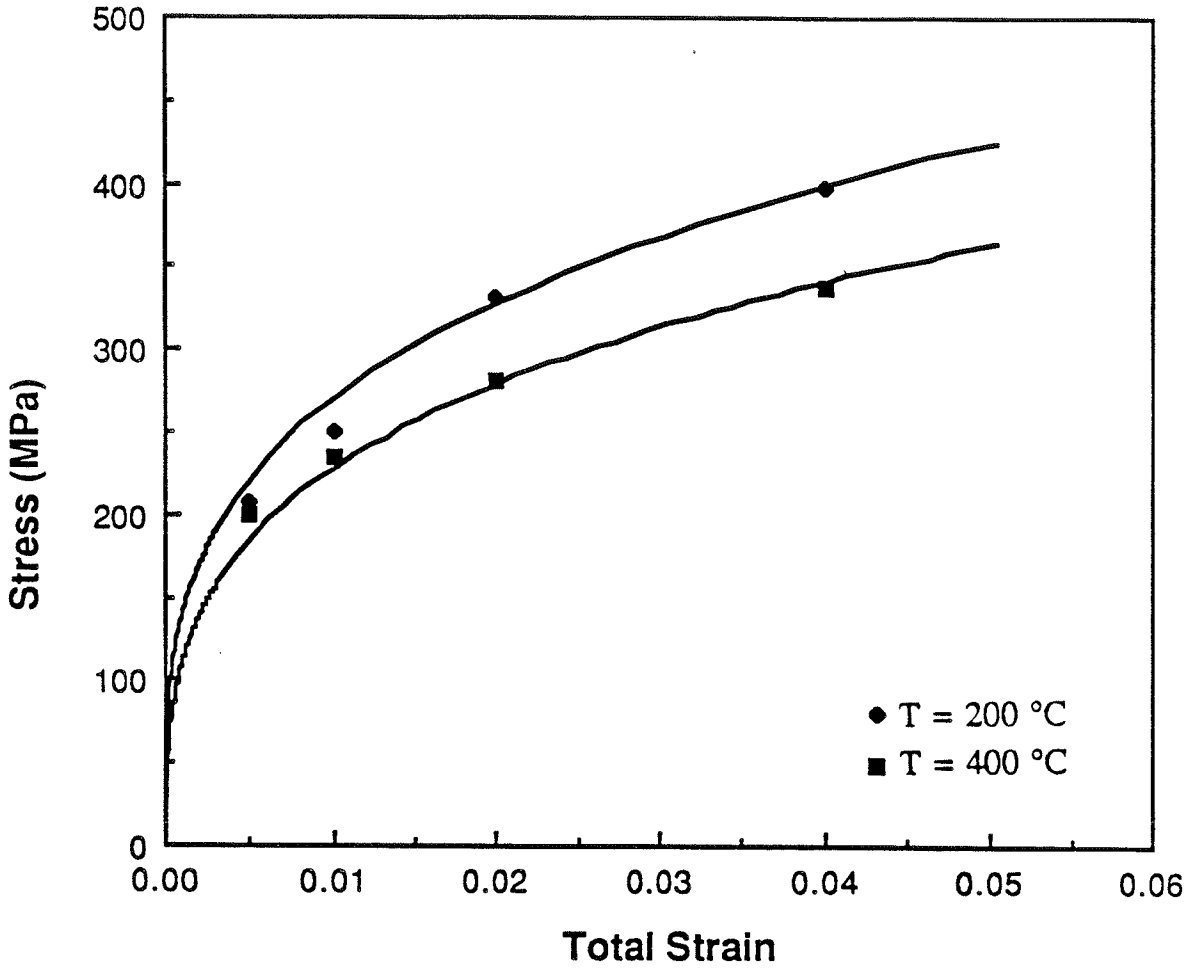

Fig. 2.4 Calculated stress-strain curves and the corresponding data at a constant strain rate of 2e-2 and at different temperatures.

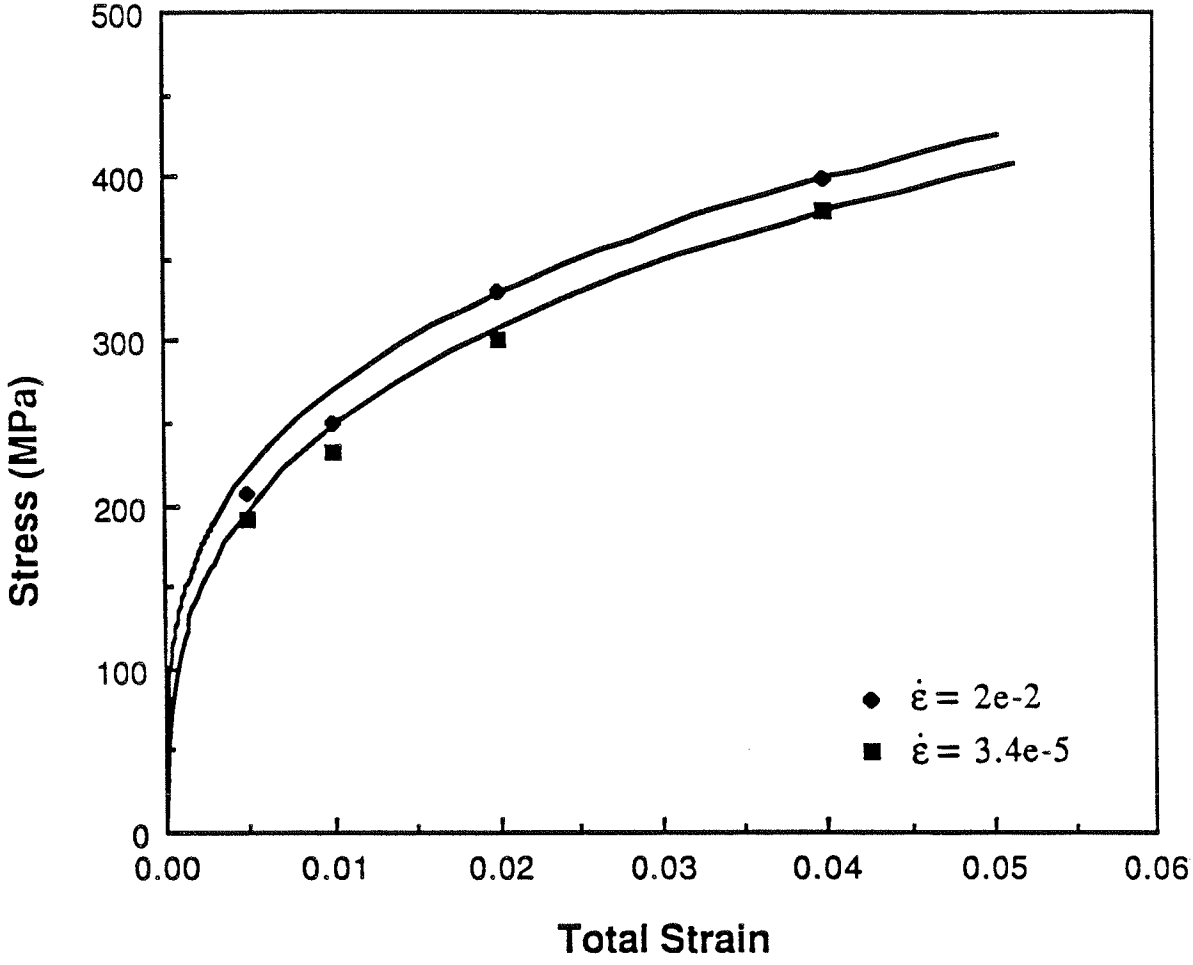

Fig. 2.5 Calculated stress-strain curves and the corresponding data at a constant temperature of 200 °C and at different strain rates.

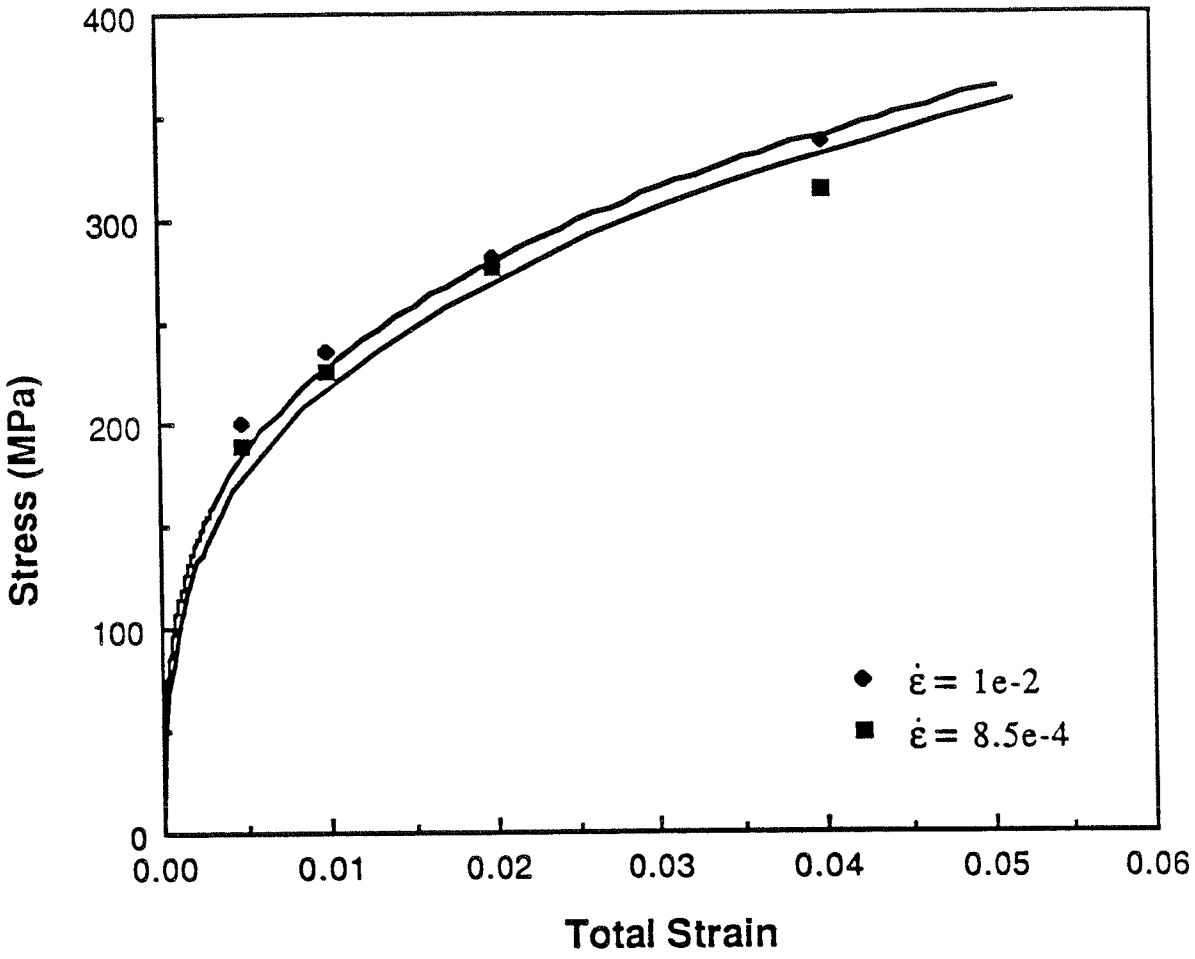

Fig. 2.6 Calculated stress-strain curves and the corresponding data at a constant temperature of 400 °C and at different strain rates.

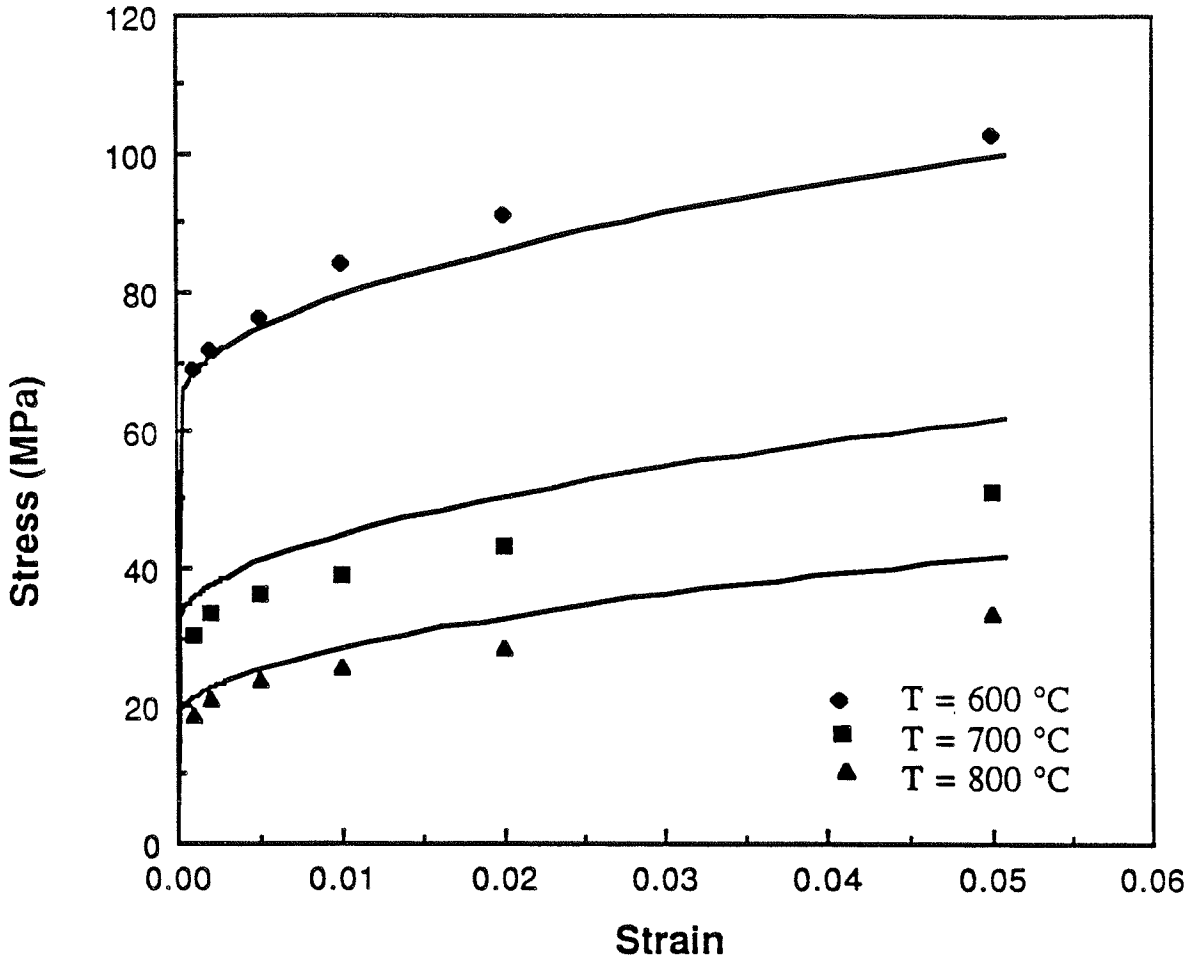

Fig. 2.7 Calculated stress-strain curves and the corresponding data at a constant strain rate of 2.3e-2 and at different temperatures.

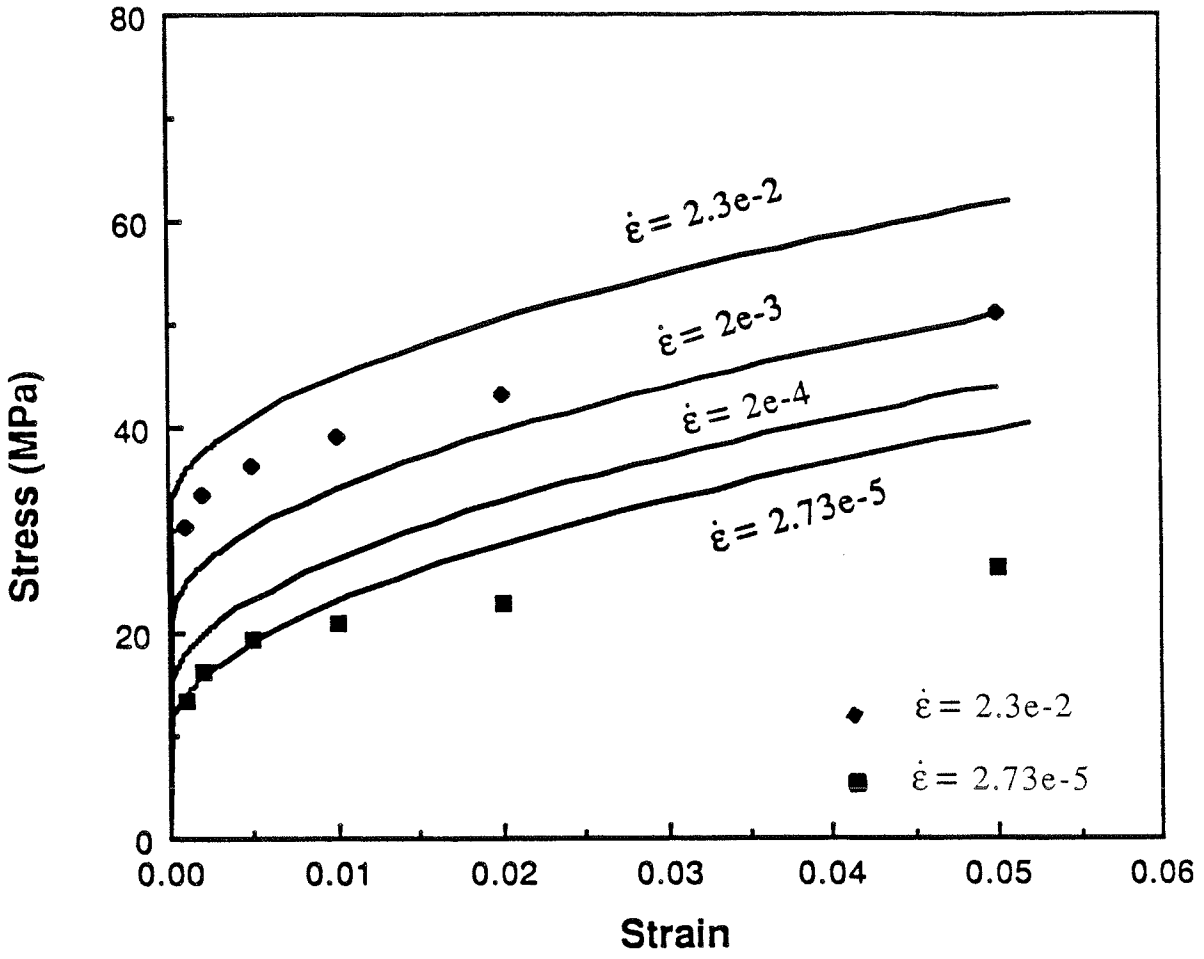

Fig. 2.8 Calculated stress-strain curves and the corresponding data at a constant temperature of 700 °C and at different strain rates.

shown in Fig. 2.8. Figs. 2.9 - 2.11 are plots of stress-strain curves using the third set parameters compared to experimental data taken from Wray [22]. For a constant strain rate of 2.3e-2, stress-strain curves of various temperature are shown in Fig. 2.9. Fig. 2.10 and Fig. 2.11 show the curves of various strain rates at temperatures equal to 950 °C and 1100 °C, respectively. Fig. 2.12 shows a plot of stress-strain typical for casting at a strain rate of 1e-4 and at different temperatures.

Since the strain rate and temperature change continuously in a steel casting, it is important that the constitutive model account for changes in strain rate and temperature during deformation. To evaluate the model's ability to do this, two further tests were run. The first test is a decrement of strain rates with a fixed temperature between 2.3e-2 and 2.9e-3. The second test is an increment between strain rates of 2.9e-3 and 2.3e-2 for a fixed temperature. Both tests are made at 2% strain and the results are shown in Figs. 2.13 - 2.14.

Another important behavior of steel at high temperature is stress relaxation. The behavior is defined as applying a constant strain while stress relaxes its value with respect to time due to the exchange of elastic strain with plastic creep. Fig. 2.15 is a plot of the results of the constitutive model developed in this work applied to stress relaxation at 600 °C. The experimental data are taken from Milczarek [23]. The steel used by Milczarek is Armco iron of composition: 0.028 C; 0.21 Mn; 0.004 Si; 0.013 S. The initial strain rate is 0.011 sec-1. The specimen is pre-strained at 0.1.

Moreover, the steel behavior under creep is considered. Fig. 2.16 shows the results of the constitutive model at a constant stress of 250 MPa and a temperature of 450 °C.

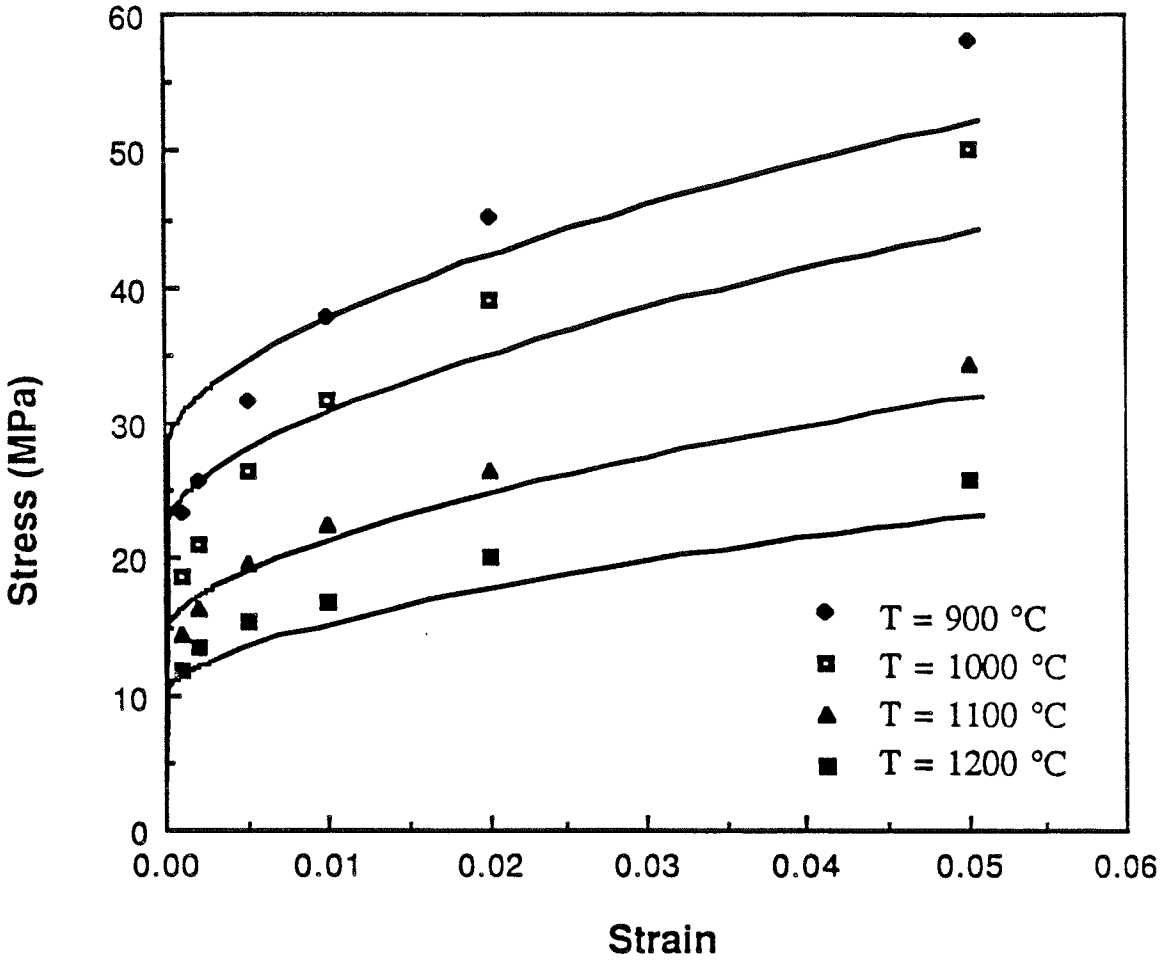

Fig. 2.9 Calculated stress-strain curves and the corresponding data at a constant strain rate of 2.3e-2 and at different temperatures.

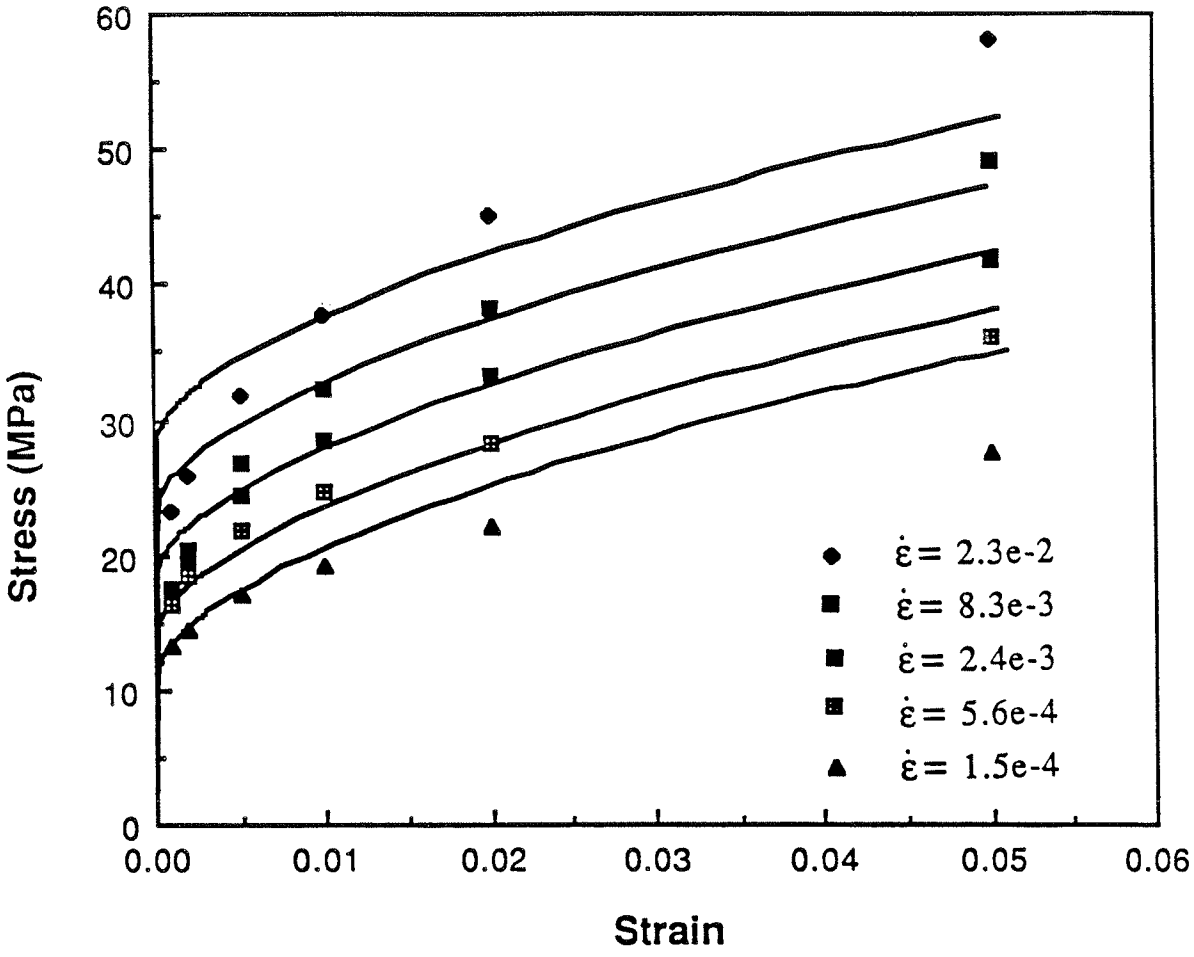

Fig. 2.10 Calculated stress-strain curves and the corresponding data at a constant temperature of 950 °C and at different strain rates.

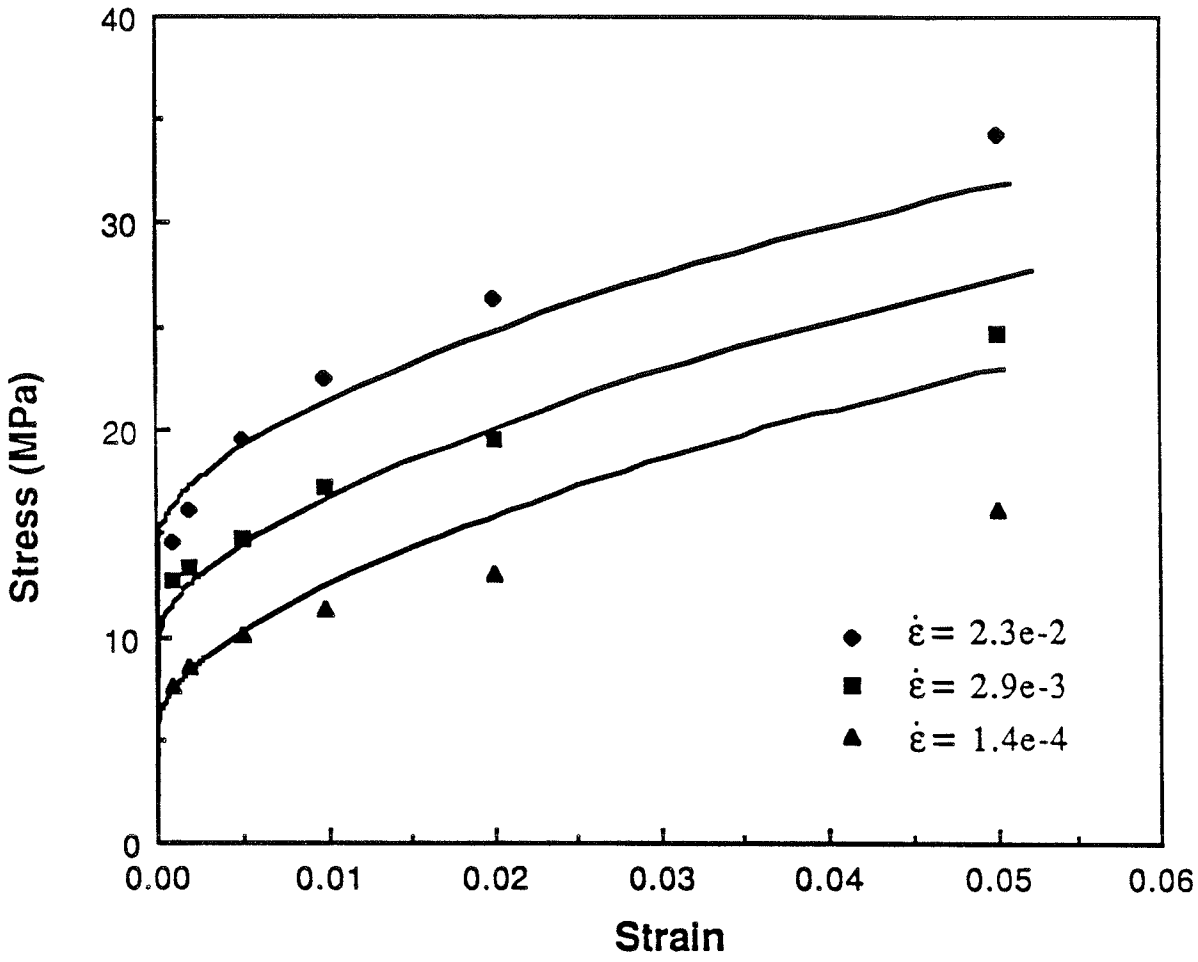

Fig. 2.11 Calculated stress-strain curves and the corresponding data at a constant temperature of 1100 °C and at different strain rates.

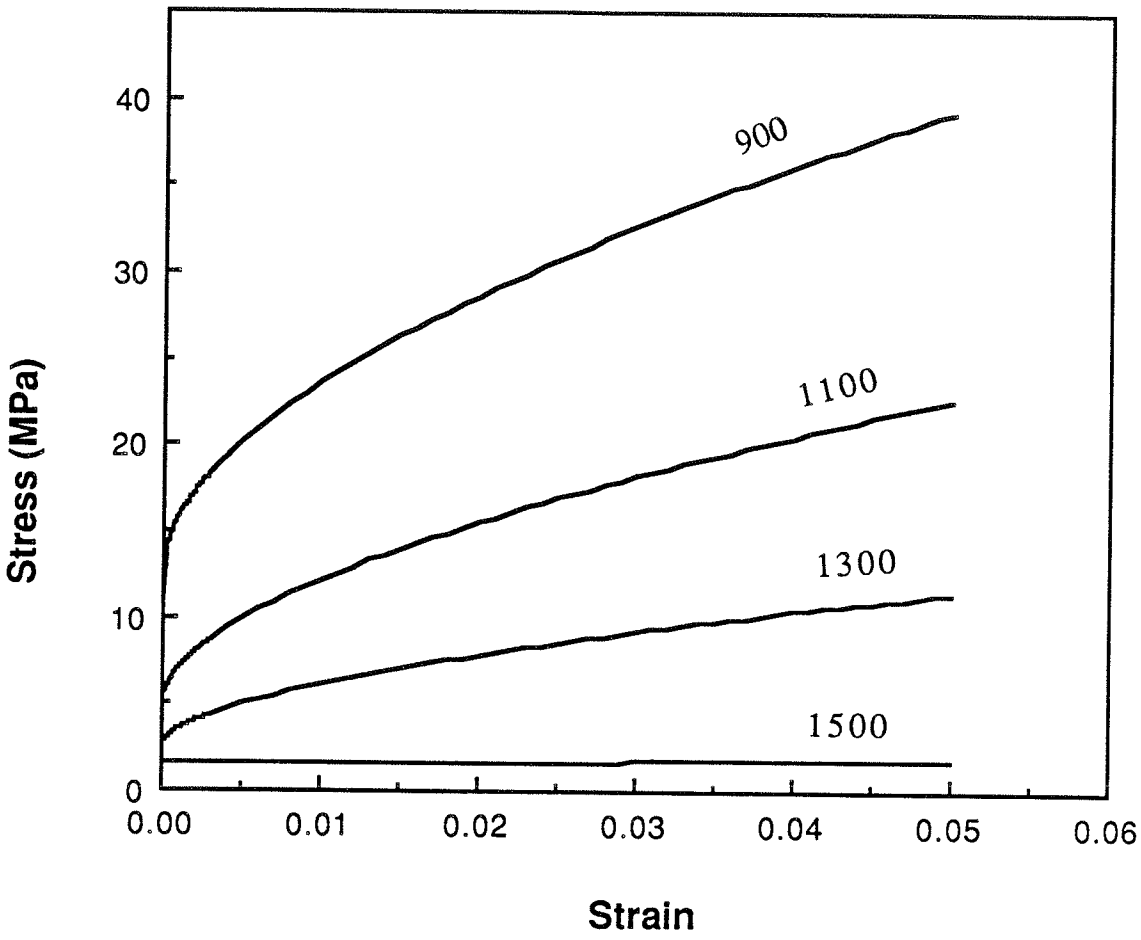

Fig. 2.12 Calculated stress-strain curves at a constant strain rate of 1e-4 and at different temperatures.

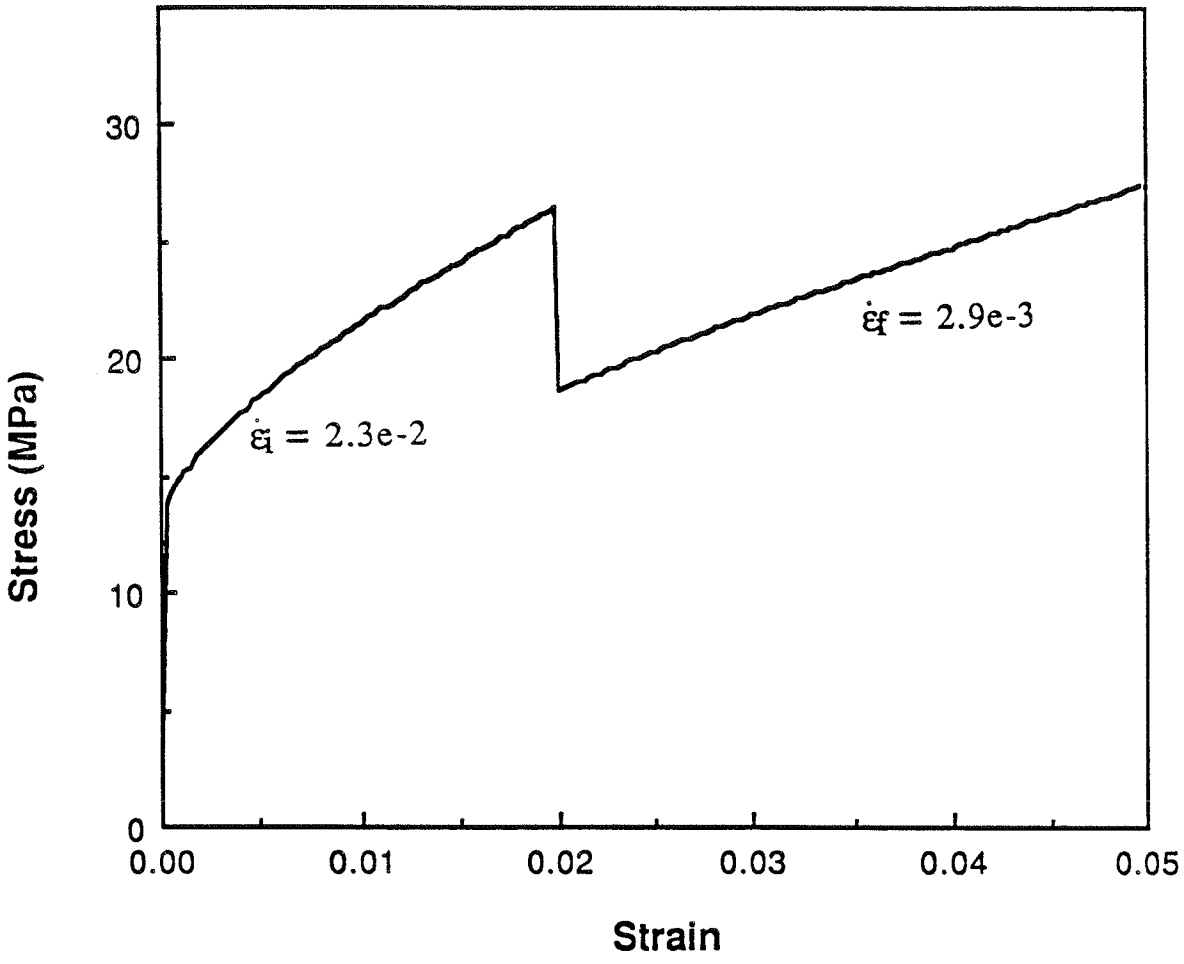

Fig. 2.13 Calculated stress-strain curve at a constant temperature of 1100 °C for decrement strain rates. $\dot{\varepsilon}_i$ = 2.3e-2 and $\dot{\varepsilon}_f$ = 2.9e-3.

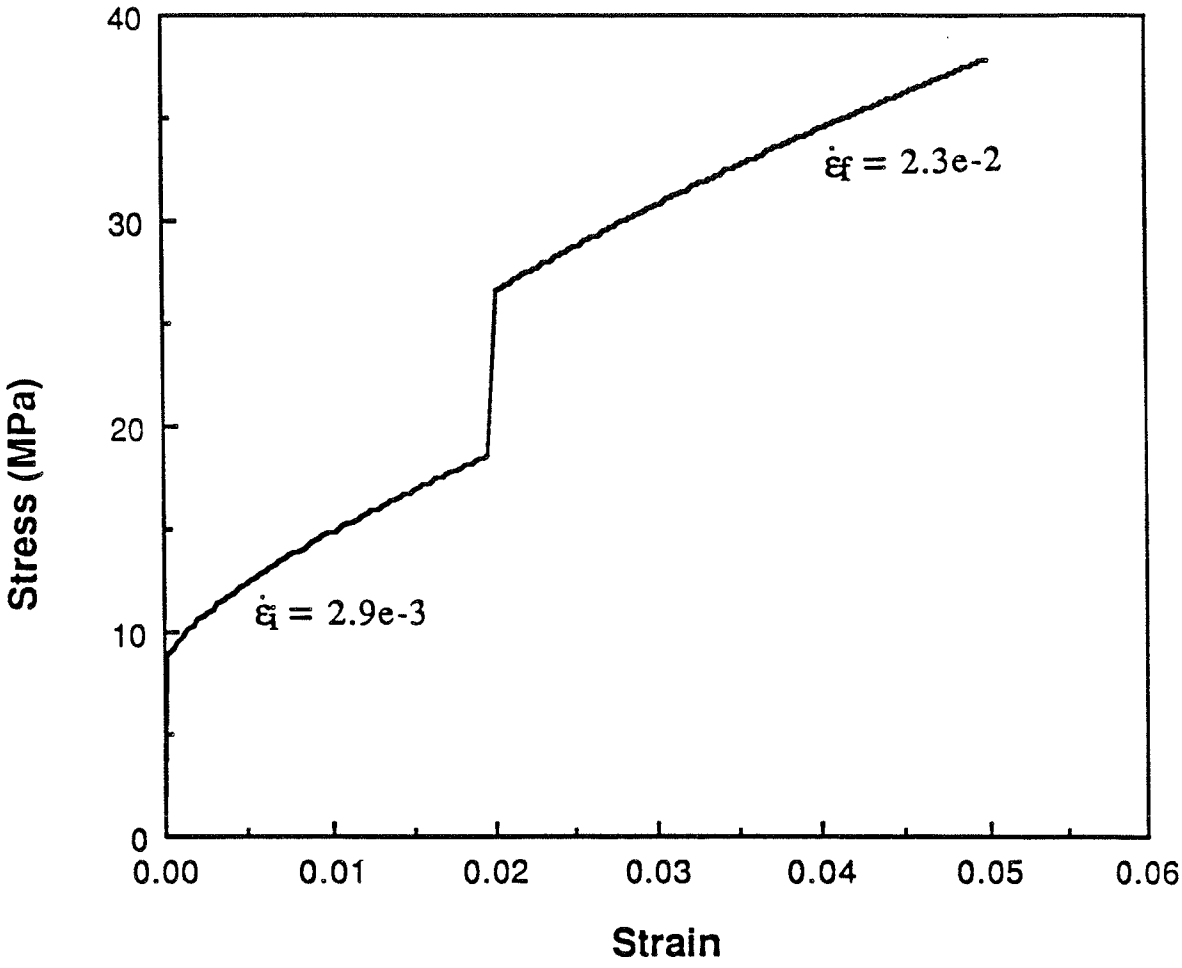

Fig. 2.14 Calculated stress-strain curve at a constant temperature of 1100 °C for increment strain rates. $\dot{\varepsilon}_i$ = 2.9e-3 and $\dot{\varepsilon}_f$ = 2.3e-2.

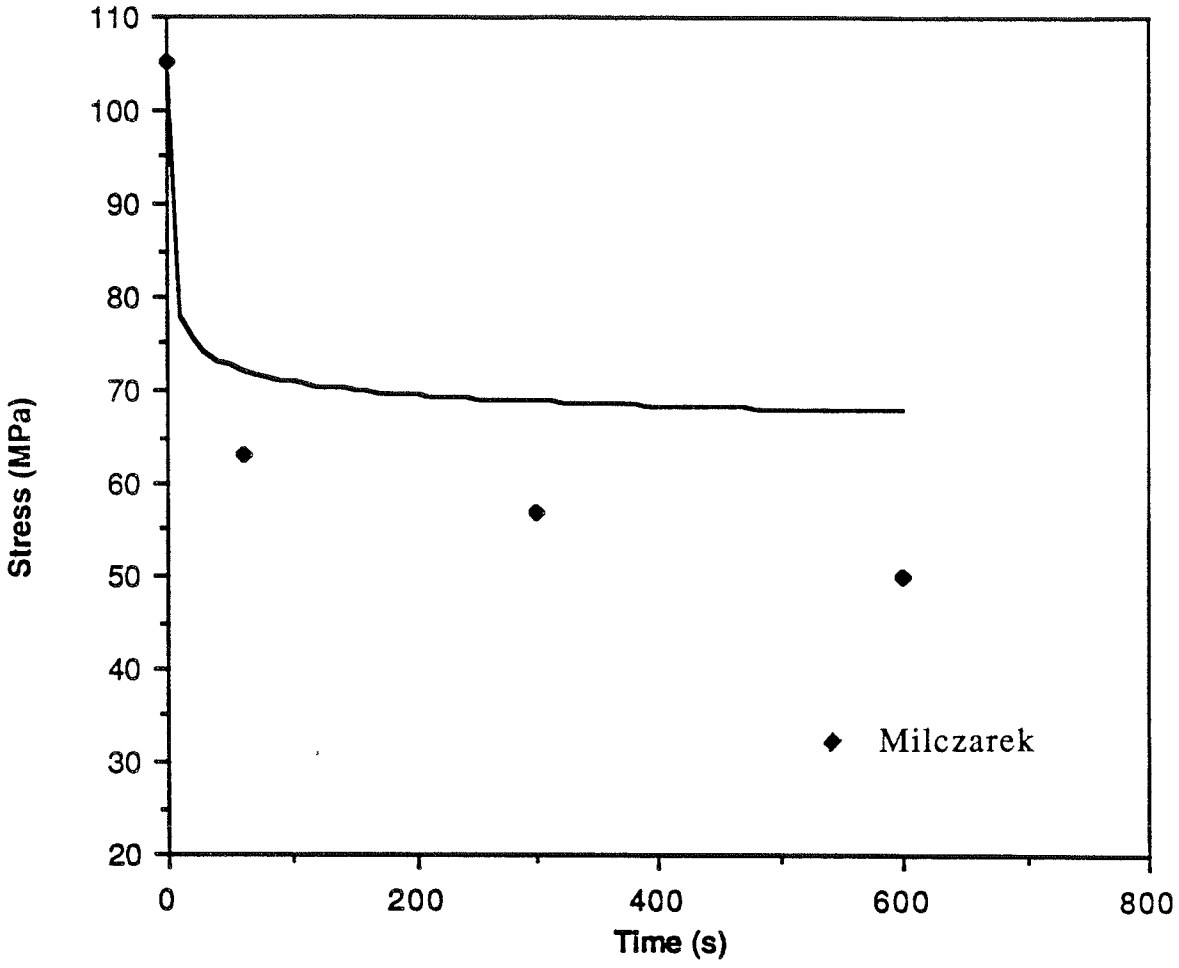

Fig. 2.15 Stress relaxation as a function of time at a temperature of 600 °C. Pre-strain $\varepsilon = 0.10$.

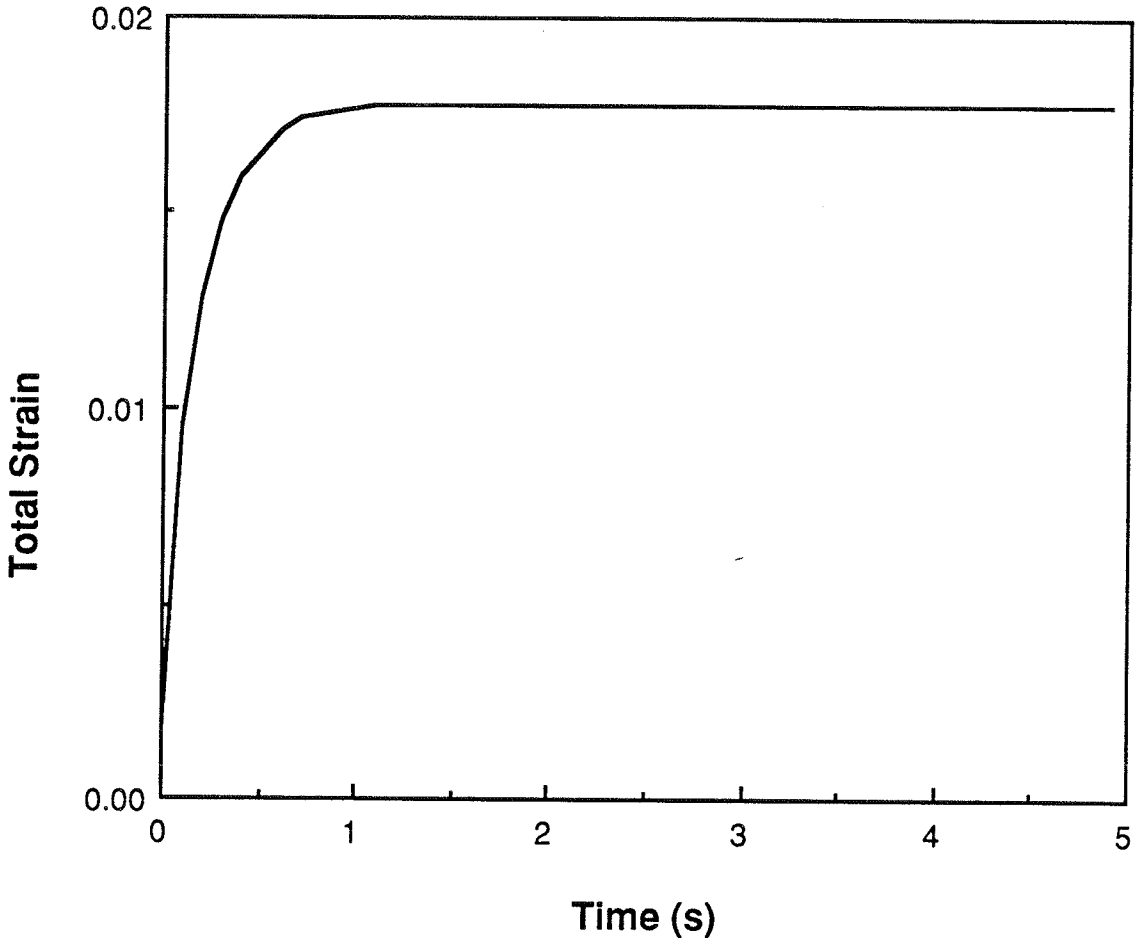

Fig. 2.16 Creep curve at a temperature of 450 °C and constant stress of 250 MPa.

2.4 DISCUSSION

This study has revealed results in two major disciplines. First, a better understanding is gained about the effect of time stepping on the numerical stability of the model which is important to finite element simulations using similar time stepping methods. Second, constitutive equations are studied and a simple equation has been developed to fit the data.

2.4.1 Effect of time step on stability

The integration procedure used in solving the constitutive equations relies on the time step size. The equations are very stiff in the elastic region, which means that a small time step is required to maintain stability. Also, the speed of the program is controlled by step size and number of iterations at each step. In addition, the stability of the integration depends on the strain rate. In this study the time step chosen is equal to 1e-3. Using this value the program required only one iteration per time step. For relatively small strain rate (1e-5 - 1c-7), a smaller time step is required. However, smaller step size increases computation time; thus, increases cost. In order to enhance the speed, the time step should be dynamically controlled. As a guideline, the time step size can be controlled by minimizing the local truncation error resulting from the integration. In our case, the dynamic time stepping is not a feasible approach due to two reasons: first, a criterion to change the time step can not be defined properly; second, as the stress-strain curve flattens out, the dynamic time stepping procedure produces unstable behavior. In order to speed up the integration process at low strain rates, the plastic strain function, $\dot{\varepsilon}_p = f(\sigma, T, \varepsilon_p)$, is written as $\sigma = f(\dot{\varepsilon}_p, T, \varepsilon_p)$; thus, avoiding the time stepping instability. Fig. 2.17 shows

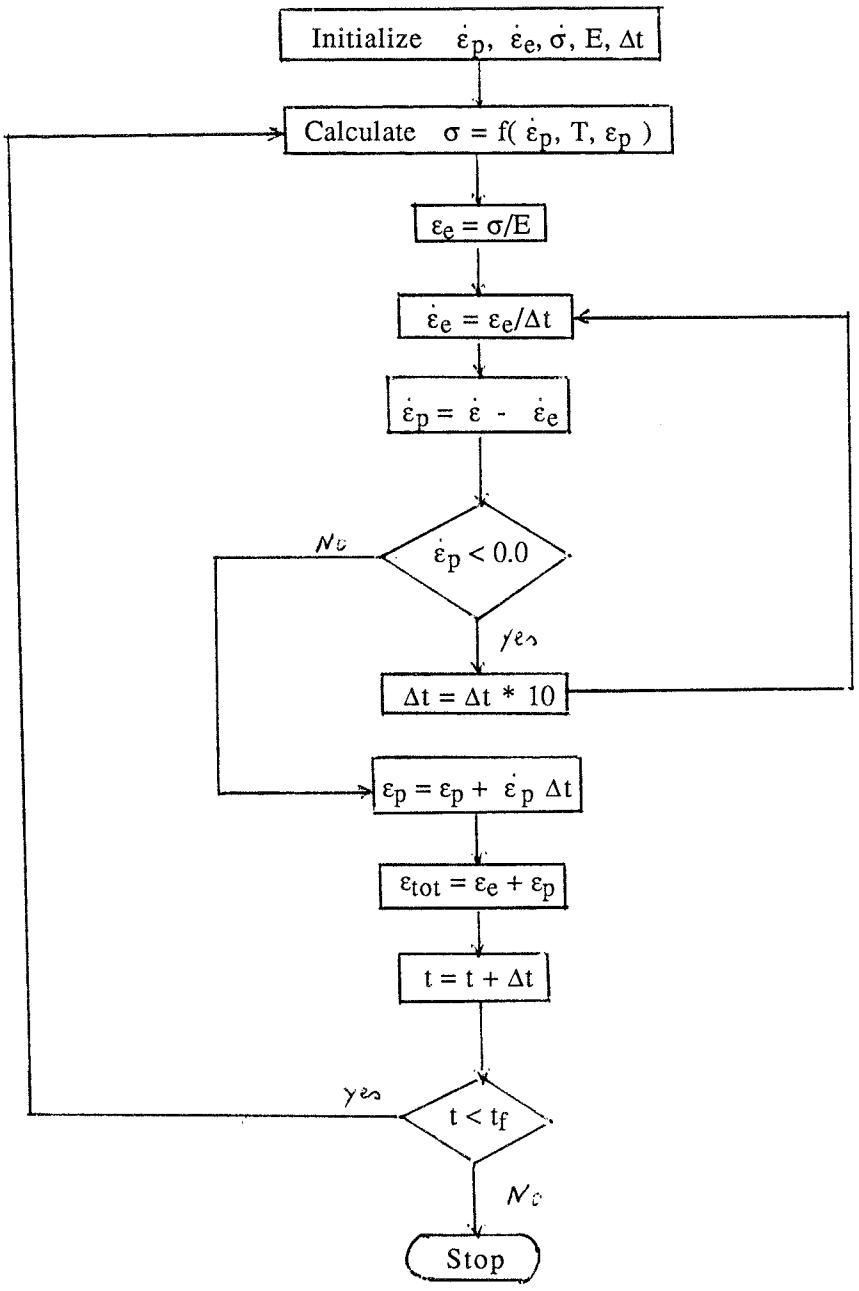

Fig. 2.17 Flowchart of the program used in solving for σ.

the algorithm using the stress function.

2.4.2 Simple equation to fit data

The constitutive equation developed to fit experimental data is relatively simple. Fitting the data requires calculating only five parameters. Each parameter has an important role in the curve fitting. Knowing the role of every parameter helps in choosing the magnitude of the input parameter prior to optimization. Simplex is then used to minimize error between the single set of chosen parameters and all of the 25 different data sets for a given steel including 9 different temperatures at 7 different strain rates. The fit is equally good over the entire temperature range. However, the calculated curves fit the data best at low strains (less than 2%) and low strain rates. Since the plastic strain is the only structure parameter, it is difficult to vary the slope of plastic region of the stress-strain curves as a function of different strain rates. This leads to some discrepancy at higher strain rates and higher strains. However, in casting operations (including continuous casting), the maximum strain is estimated generally not to exceed a value of 2%. Since the developed equation is to be used in simulating low strain, low strain rate casting operations, the calculated curves are considered to be sufficiently accurate.

The model also has been applied to several loading conditions outside of the constant strain rate tensile tests to which it was fitted. These include step change in strain rate, stress relaxation, and creep. The calculated material response to a step change in strain rate is very close to that predicted by Anand [6]. The integrated curve appears to be following the general trend of the stress relaxation data. It must be emphasized that the data used for comparison with the stress relaxation data are for a different steel grade. The reason for choosing data for 2.8% C steel is the lack of experimental data for plain low-Carbon steel.

On the other hand, the constitutive model under creep conditions reproduced the general trends of creep behavior, but it did not predict the experimental results found in Nishihara et al [24].

Finally, it should be mentioned that more data are needed to refine the prediction of the stress-strain behavior under variable strain rates, particularly at very high temperatures and low strains. The only way to find an accurate constitutive equation is through the use of experimentally measured data.

2.5 CONCLUSIONS

A simple form of the plastic strain rate equation has been developed that captures the temperature and strain rate dependencies of steel during casting conditions. It is based on literature data for constant strain rate tensile tests on low carbon steel. Also, a general procedure for optimizing the fit between the constitutive form and experimental data has been developed. The constitutive equation fits experimental tensile test data with an acceptable accuracy over the range of temperatures and strain rates of interest. Using only plastic strain to define the structure parameter it is impossible to obtain a comprehensive, perfect fit to the experimental data. Also, the constitutive equation accommodates for strain rate variations which are encountered in continuous casting operations. Finally, model predictions have been compared with experimental measurements of stress relaxation. The correct general trends were reproduced.

REFERENCES

[1] W. Kurz and D. J. Fisher, Fundamentals of Solidification, Trans Tech Publications, Aedermannsdorf, Switzerland, p. 9, 1986.

[2] I. V. Samarasekera and J. K. Brimacombe, Continuous Casting, Vol. 2, ISS-AIME, p. 33-58, 1984.

[3] J. E. Kelly, K. P. Michalek, B. G. Thomas and J. A. Dantzig, Initial Development of Thermal and Stress Fields in Continuously Cast Steel Billets, Metallurgical Transactions, to appear.

[4] G. J. DeSalvo and R. W. Gorman, ANSYS, Swanson Analysis Systems, Inc., Rev. 4.3, 1987.

[5] W. Storkman, The Development and Use of a Three Dimensional Finite Element Heat Transfer Model, Report for ME 345 Finite Element Analysis, University of Illinois, 1986.

[6] F. P. Incropera and D. P. Dewitt, Fundamentals of Heat Transfer, Wiley, p.325-331, 1981.

[7] I. V. Samarasekera and J. K. Brimacombe, Thermal and Mechanical Behaviour of Continuous -Casting Billet Moulds, Continuous Casting, Vol. 2, ISS-AIME, p. 59-72, 1984.

[8] L. Anand, Constitutive Equations for the Rate-Dependent Deformation of Metals at Elevated Temperatures, Trans. of the ASME, Journal of Eng. Mat. and Tech., Vol.104, p. 12-17, Jan. 1982.

[9] J. R. Rice, Continuum Mechanics and Thermodynamics of Plasticity in Relation to Microscale Deformation Mechanisms, Constitutive Equations in Plasticity, ed., Argon, A.S., The MIT Press, Cambridge, p. 23-79, 1975.

[10] S. Sakui and T. Sakai, Deformation Behaviours of a 0.16% Carbon Steel in the Austenite Range, The science University of Tokyo, 1976.

[11] C. R. Barret and W. D. Nix, A Model for Steady State Creep Based on the Motion of Jogged Screw Dislocations, Dms Report, Stanford University, Sept. 1964.

[12] P. J. Wray, Mechanical, Onset of Recrystallization During the Tensile Deformation of Austenitic Iron at intermediate Strain Rates, Met. Trans., Vol. 6A, p. 1202, 1975.

[13] C. M. Sellars and W. J. Tegart, Mem. Sci. Rev. Met., 63, p. 731, 1966.

[14] S. K. Samanta, The Dynamic Compression Testing Of steels at Elevated Temperatures, Proc. 11th Int. MTDR Conf., Birmingham, Sept 1970, Macmillan, London, Vol. B, p. 827-853, 1971.

[15] S. K. Samanta, Some Experiments in Dynamic Plasticity at Elevated Temperatures, CIRP Ann., 19, p. 755-765, 1971.

[16] B. G. Thomas, I. V. Samarasekera and J. K. Brimacombe, Mathematical Model of the Thermal Processing of Steel Ingots: Part 2. Stress Model, Met. Trans., 1987.

[17] D. D. McCracken and W. S. Dorn, Numerical Methods And Fortran Programming, John Wiley and Sons, Inc., p. 311-341, 1965.

[18] J. A. Nelder and R. Mead, Computer J., 7: 308, 1964.

[19] D. M. Himmeblau, Applied Nonlinear Programming, McGraw-Hill Book Comp., p. 148-157 and p. 452-454, 1972.

[20] M. J. Manjoine, Influence of rate of strain and temperature as yield stresses of mild steel, Journal of Applied Mechanics, p. 211-218, 1944

[21] P. J. Wray, High Temperature plastic Flow Behavior of Mixtures of Austenite, Cementite, Ferrite and Pearlite in Plain-Carbon Steels, Metallurgical Transactions, Vol. 15A, p. 2041-2058, 1984.

[22] P. J. Wray, Effect of Carbon Content on the Plastic Flow of Plain Carbon Steels at Elevated Temperatures, Met. Trans., Vol. 13A, p.125-134, 1982.

[23] E. Milszarek, The dependence of the flow stress of Armco Iron on strain history, Journal of Mechanical Working, 1983

[24] T. Nishihara, S. Taira, K. Tanaka, and M. Ohnami, Creep of Low Carbon Steel Under Varying Temperatures, The First Japan Congress On Testing Materials - Metallic Materials, p. 48-51, 1958.

APPENDIX A

HEAT FLUX CURVE

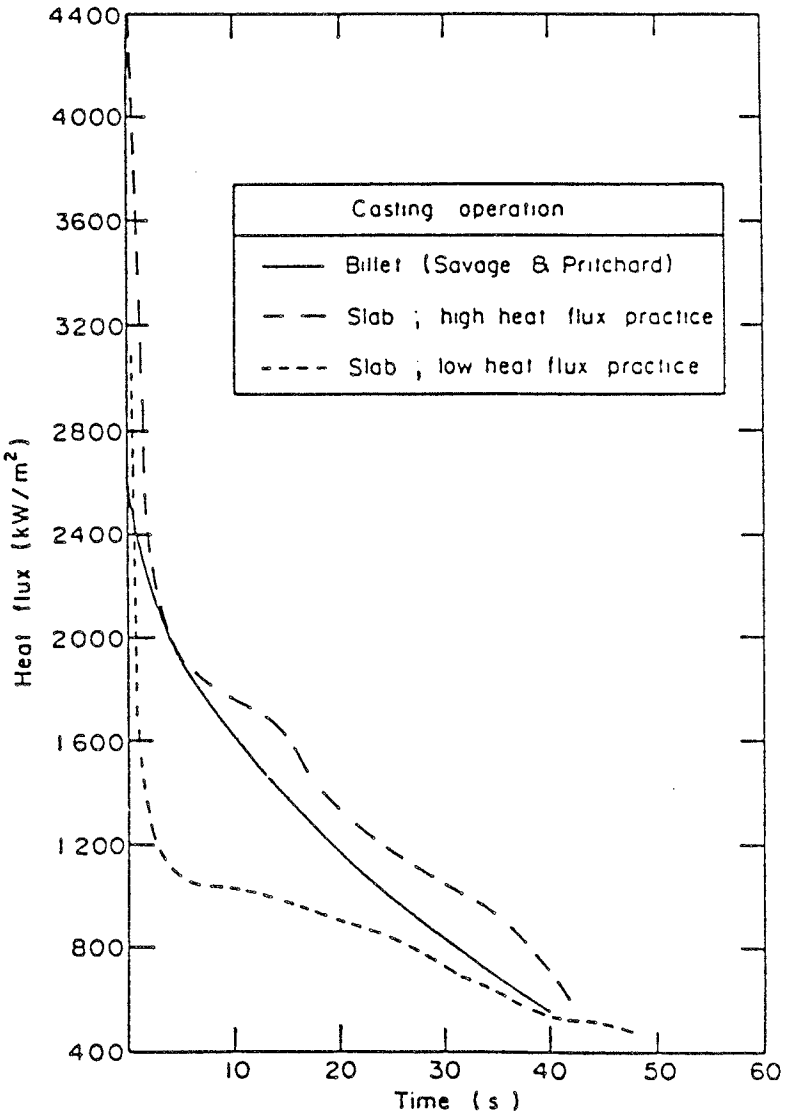

APPENDIX B

QUARTER MOLD THERMAL ANALYSIS (1st METHOD)

```
/int,no
/PREP7
/TITLE,CASTER
C***                                    "CASTER"
C***
C*** THIS COMPUTER PROGRAM IS AN INPUT FILE TO "ANSYS" REV. 4.3.
C*** THIS FILE CREATES THE MESH OF THE 3-D QUATER MOLD
C*** AND DOES THE THERMAL ANALYIS USING THE FIRST METHOD.
C*** THE OUTPUT FILES ARE STORED AS CASTER#.
C***
KAN,-1                                  * thermal analysis
ET,1,70                                 * element type
KXX,1,52                                * K for steel in W/(m.K)
KXX,2,390                               * K for copper in W/(m.K)
C***
C*** MESH GENERATION
C***
K,1,0,0,0                               * key points in meters
K,2,0,0,3E-2
K,3,0,0,9E-2
K,4,54.864E-2,0,9E-2
K,5,54.864E-2,0,3E-2
K,6,54.864E-2,0,0
K,7,0,0,19.16E-2
K,8,3.048E-2,0,19.16E-2
K,9,5.644E-2,0,19.16E-2
K,10,6.944E-2,0,19.16E-2
K,11,9.144E-2,0,19.16E-2
K,12,9.144E-2,0,9E-2
K,13,6.944E-2,0,9E-2
K,14,5.644E-2,0,9E-2
K,15,3.048E-2,0,9E-2
```

K,16,-1.524E-2,0,19.16E-2
K,17,-1.524E-2,0,9E-2
K,18,-1.524E-2,0,3E-2
K,19,-1.524E-2,0,0
K,20,9.144E-2,0,3e-2
K,21,9.144E-2,0,0
K,22,6.944E-2,0,0
K,23,5.644E-2,0,0
K,24,3.048E-2,0,0
K,25,3.048E-2,0,3E-2
K,26,5.644E-2,0,3E-2
K,27,6.944E-2,0,3e-2
K,28,0,70E-2,0
L,1,2,1
L,20,5,15
L,5,6,1
L,6,21,15
L,2,3,3,.6060606
L,3,4,18
L,4,5,3,1.65
L,8,15,8
L,7,8,1
L,8,9,1
L,9,10,1
L,10,11,1
L,11,12,8
L,12,13,1
L,13,14,1
L,14,15,1
L,15,3,1
L,3,17,1
L,17,16,8
L,16,7,1
L,17,18,3,1.65
L,18,19,1
L,19,1,1

```
L,15,25,3,1.65
L,14,26,3,1.65
L,13,27,3,1.65
L,12,20,3,1.65
L,20,21,1
L,27,22,1
L,26,23,1
L,25,24,1
L,1,24,1
L,24,23,1
L,23,22,1
L,22,21,1
L,2,25,1
L,25,26,1
L,26,27,1
L,27,20,1
L,1,28,7,.16666
A,21,20,5,6
A,20,12,4,5
A,1,2,18,19
A,2,3,17,18
A,3,7,16,17
A,3,7,8,15
A,8,9,14,15
A,9,10,13,14
A,10,11,12,13
A,2,3,15,25
A,14,15,25,26
A,13,14,26,27
A,12,13,27,20
A,20,21,22,27
A,22,23,26,27
A,23,24,25,26
A,1,2,25,24
VDRAG,1,,,,,,40
MAT,1
```

```
VMESH,1
VDRAG,2,,,,,,40
MAT,2
VMESH,2
VDRAG,3,,,,,,40
MAT,1
VMESH,3
VDRAG,4,,,,,,40
MAT,2
VMESH,4
VDRAG,5,,,,,,40
MAT,1
VMESH,5
VDRAG,6,,,,,,40
MAT,1
VMESH,6
VDRAG,7,8,9,10,11,12,40
MAT,2
VMESH,7,12,1
VDRAG,13,,,,,,40
MAT,2
VMESH,13
VDRAG,14,15,16,17,,,40
MAT,1
VMESH,14,17,1
C***
C*** BOUNDARY CONDITIONS
C***
NRSEL,X,-1E-2,1E-2              * water channel 1
NRSEL,Y,-10E-2,80E-2
NRSEL,Z,2.5E-2,6E-2
CVSF,ALL,,,21000,308
CVBC,1
NALL
NRSEL,X,27E-3,33E-3             * water channel 2
NRSEL,Y,-10E-2,80E-2
```

```
NRSEL,Z,2.5E-2,6E-2
CVSF,ALL,,,21000,308
CVBC,1
NALL
NRSEL,X,50E-3,62E-3          * water channel 3
NRSEL,Y,-10E-2,80E-2
NRSEL,Z,2.5E-2,6E-2
CVSF,ALL,,,21000,308
CVBC,1
NALL
NRSEL,X,115E-3,125E-3        * water channel 4
NRSEL,Y,-10E-2,80E-2
NRSEL,Z,2.5E-2,6E-2
CVSF,ALL,,,21000,308
CVBC,1
NALL
NRSEL,X,145E-3,155E-3        * water channel 5
NRSEL,Y,-10E-2,80E-2
NRSEL,Z,2.5E-2,6E-2
CVSF,ALL,,,21000,308
CVBC,1
NALL
NRSEL,X,175E-3,190E-3        * water channel 6
NRSEL,Y,-10E-2,80E-2
NRSEL,Z,2.5E-2,6E-2
CVSF,ALL,,,21000,308
CVBC,1
NALL
NRSEL,X,200E-3,220E-3        * water channel 7
NRSEL,Y,-10E-2,80E-2
NRSEL,Z,2.5E-2,6E-2
CVSF,ALL,,,21000,308
CVBC,1
NALL
NRSEL,X,265E-3,280E-3        * water channel 8
NRSEL,Y,-10E-2,80E-2
```

```
NRSEL,Z,2.5E-2,6E-2
CVSF,ALL,,,21000,308
CVBC,1
NALL
NRSEL,X,295E-3,310E-3          * water channel 9
NRSEL,Y,-10E-2,80E-2
NRSEL,Z,2.5E-2,6E-2
CVSF,ALL,,,21000,308
CVBC,1
NALL
NRSEL,X,325E-3,345E-3          * water channel 10
NRSEL,Y,-10E-2,80E-2
NRSEL,Z,2.5E-2,6E-2
CVSF,ALL,,,21000,308
CVBC,1
NALL
NRSEL,X,355E-3,375E-3          * water channel 11
NRSEL,Y,-10E-2,80E-2
NRSEL,Z,2.5E-2,6E-2
CVSF,ALL,,,21000,308
CVBC,1
NALL
NRSEL,X,415E-3,435E-3          * water channel 12
NRSEL,Y,-10E-2,80E-2
NRSEL,Z,2.5E-2,6E-2
CVSF,ALL,,,21000,308
CVBC,1
NALL
NRSEL,X,445E-3,465E-3          * water channel 13
NRSEL,Y,-10E-2,80E-2
NRSEL,Z,2.5E-2,6E-2
CVSF,ALL,,,21000,308
CVBC,1
NALL
NRSEL,X,475E-3,495E-3          * water channel 14
NRSEL,Y,-10E-2,80E-2
```

```
NRSEL,Z,2.5E-2,6E-2
CVSF,ALL,,,21000,308
CVBC,1
NALL
NRSEL,X,505E-3,525E-3          * water channel 15
NRSEL,Y,-10E-2,80E-2
NRSEL,Z,2.5E-2,6E-2
CVSF,ALL,,,21000,308
CVBC,1
NALL
NRSEL,X,50E-3,74E-3             * top horz. face of pipe 1
NRSEL,Y,-10E-2,80E-2
NRSEL,Z,110E-3,120E-3
CVSF,ALL,,,21000,308
CVBC,1
NALL
NRSEL,X,50E-3,74E-3            * bott. horz. face of pipe 1
NRSEL,Y,-10E-2,80E-2
NRSEL,Z,120E-3,135E-3
CVSF,ALL,,,21000,308
CVBC,1
NALL
NRSEL,X,50E-3,74E-3            * top horz. face of pipe 2
NRSEL,Y,-10E-2,80E-2
NRSEL,Z,147E-3,160E-3
CVSF,ALL,,,21000,308
CVBC,1
NALL
NRSEL,X,50E-3,74E-3            * bott. horz. face of pipe 2
NRSEL,Y,-10E-2,80E-2
NRSEL,Z,160E-3,170E-3
CVSF,ALL,,,21000,308
CVBC,1
NALL
NRSEL,X,50E-3,63E-3            * left vert. face of pipe 1
NRSEL,Y,-10E-2,80E-2
```

```
NRSEL,Z,110E-3,135E-3
CVSF,ALL,,,21000,308
CVBC,1
NALL
NRSEL,X,50E-3,63E-3          * left vert. face of pipe 2
NRSEL,Y,-10E-2,80E-2
NRSEL,Z,147E-3,170E-3
CVSF,ALL,,,21000,308
CVBC,1
NALL
NRSEL,X,63E-3,74E-3          * right vert. face of pipe 1
NRSEL,Y,-10E-2,80E-2
NRSEL,Z,110E-3,135E-3
CVSF,ALL,,,21000,308
CVBC,1
NALL
NRSEL,X,63E-3,74E-3          * right vert. face of pipe 2
NRSEL,Y,-10E-2,80E-2
NRSEL,Z,147E-3,170E-3
CVSF,ALL,,,21000,308
CVBC,1
NALL
NRSEL,X,-20E-3,560E-3        * bottom face of mold
NRSEL,Y,-10E-3,25E-3
NRSEL,Z,-10E-3,200E-3
CVSF,ALL,,,150,298
CVBC,1
NALL
NRSEL,X,-20E-3,560E-3        * top face of mold
NRSEL,Y,69.5E-2,71.5E-2
NRSEL,Z,-10E-3,200E-3
CVSF,ALL,,,250,298
CVBC,1
NALL
NRSEL,X,-20E-3,560E-3        * outer horz. top mold face
NRSEL,Y,-10E-2,80E-2
```

```
NRSEL,Z,-10E-2,1.5E-2
CVSF,ALL,,,21000,308
CVBC,1
NALL
NRSEL,X,-20E-3,-7E-3          * outer vert. left mold face
NRSEL,Y,-10E-2,80E-2
NRSEL,Z,-10E-3,200E-3
CVSF,ALL,,,21000,308
CVBC,1
NALL
NRSEL,X,85E-3,100E-3          * inner vert. mold face(flux)
NRSEL,Y,65E-2,68E-2           * level 1 (meniscus)
NRSEL,Z,87E-3,200E-3
HFLOW,ALL,HEAT,964.3
HFBC,1
NALL
NRSEL,X,85E-3,100E-3          * inner vert. mold face(flux)
NRSEL,Y,57E-2,63E-2           * level 2
NRSEL,Z,87E-3,200E-3
HFLOW,ALL,HEAT,1781.5
HFBC,1
NALL
NRSEL,X,85E-3,100E-3          * inner vert. mold face(flux)
NRSEL,Y,53E-2,57E-2           * level 3
NRSEL,Z,87E-3,200E-3
HFLOW,ALL,HEAT,1768.4
HFBC,1
NALL
NRSEL,X,85E-3,100E-3          * inner vert. mold face(flux)
NRSEL,Y,46E-2,48E-2           * level 4
NRSEL,Z,87E-3,200E-3
HFLOW,ALL,HEAT,2073.3
HFBC,1
NALL
NRSEL,X,85E-3,100E-3          * inner vert. mold face(flux)
NRSEL,Y,35E-2,37E-2           * level 5
```

```
NRSEL,Z,87E-3,200E-3
HFLOW,ALL,HEAT,2388.7
HFBC,1
NALL
NRSEL,X,85E-3,100E-3          * inner vert. mold face(flux)
NRSEL,Y,19E-2,21E-2           * level 6
NRSEL,Z,87E-3,200E-3
HFLOW,ALL,HEAT,2472.3
HFBC,1
NALL
NRSEL,X,85E-3,100E-3          * inner vert. mold face(flux)
NRSEL,Y,-1E-2,1E-2            * level 7 (bottom)
NRSEL,Z,87E-3,200E-3
HFLOW,ALL,HEAT,1205.7
HFBC,1
NALL
NRSEL,X,95E-3,560E-3          * inner horz. mold face(flux)
NRSEL,Y,65E-2,68E-2           * level 1 (meniscus)
NRSEL,Z,87E-3,95E-3
HFLOW,ALL,HEAT,2313.8
HFBC,1
NALL
NRSEL,X,95E-3,560E-3          * inner horz. mold face(flux)
NRSEL,Y,57E-2,63E-2           * level 2
NRSEL,Z,87E-3,95E-3
HFLOW,ALL,HEAT,4275.4
HFBC,1
NALL
NRSEL,X,95E-3,560E-3          * inner horz. mold face(flux)
NRSEL,Y,53E-2,57E-2           * level 3
NRSEL,Z,87E-3,95E-3
HFLOW,ALL,HEAT,4243
HFBC,1
NALL
NRSEL,X,95E-3,560E-3          * inner horz. mold face(flux)
NRSEL,Y,46E-2,49E-2           * level 4
```

```
NRSEL,Z,87E-3,95E-3
HFLOW,ALL,HEAT,4976.2
HFBC,1
NALL
NRSEL,X,95E-3,560E-3          * inner horz. mold face(flux)
NRSEL,Y,35E-2,37E-2           * level 5
NRSEL,Z,87E-3,95E-3
HFLOW,ALL,HEAT,5732.6
HFBC,1
NALL
NRSEL,X,95E-3,560E-3          * inner horz. mold face(flux)
NRSEL,Y,19E-2,22E-2           * level 6
NRSEL,Z,87E-3,95E-3
HFLOW,ALL,HEAT,5933
HFBC,1
NALL
NRSEL,X,95E-3,560E-3          * inner horz. mold face(flux)
NRSEL,Y,-1E-2,1E-2            * level 7 (bottom)
NRSEL,Z,87E-3,95E-3
HFLOW,ALL,HEAT,2893.6
HFBC,1
NALL
HFLOW,353,HEAT,1157           * Start Heat Flow Front nodes (meniscus)
HFLOW,352,HEAT,2138
HFLOW,351,HEAT,2121.5
HFLOW,350,HEAT,2488
HFLOW,349,HEAT,2866
HFLOW,348,HEAT,2966.5
HFLOW,360,HEAT,1447
HFLOW,1345,HEAT,482           * Start of Side Nodes (meniscus)
HFLOW,1344,HEAT,891
HFLOW,1343,HEAT,884
HFLOW,1342,HEAT,1037
HFLOW,1341,HEAT,1194
HFLOW,1340,HEAT,1236
HFLOW,1331,HEAT,603
```

```
MERGE,ALL
AFWRIT
FINISH
/EXE
/INPUT,27
FINISH
/eof
/POST1
STORE,DISPL
SET,1,1
/NOSHOW
/VIEW,1,1,1,1
EPLOT
/TYPE,1,1
/FOCUS,1,274.32E-3,1E-3,95.58E-3
/VIEW,1,0,1,0
/clabel,1,1
PLNSTR,TEMP
/RESET
/TYPE,1,1
/FOCUS,1,274.32E-3,35E-2,95.58E-3
/VIEW,1,0,1,0
/CLABEL,1,1
PLNSTR,TEMP
/RESET
/TYPE,1,1
/FOCUS,1,274.32E-3,69E-2,95.58E-3
/VIEW,1,0,1,0
/CLABEL,1,1
PLNSTR,TEMP
/RESET
```

APPENDIX C

QUARTER MOLD THERMAL ANALYSIS (2nd METHOD)

```
/int,no
/PREP7
/TITLE,NEWCASTER
C***                                    "NEWCASTER"
C***
C*** THIS COMPUTER PROGRAM IS AN INPUT FILE TO "ANSYS" REV. 4.3.
C*** THIS FILE CREATES THE MESH OF THE 3-D QUARTER MOLD
C*** AND DOES THE THERMAL ANALYSIS USING THE SECOND METHOD.
C*** THE OUTPUT FILES ARE STORED AS NEWCAST#.
C***
KAN,-1                                  * thermal analysis
ET,1,70                                 * element type
KXX,1,52                                * K for steel in W/(m.K)
KXX,2,390                               * K for copper in W/(m.K)
C***
C*** MESH GENERATION
C***
K,1,0,0,0                               * key points in meters
K,2,0,0,3E-2
K,3,0,0,9E-2
K,4,54.864E-2,0,9E-2
K,5,54.864E-2,0,3E-2
K,6,54.864E-2,0,0
K,7,0,0,19.16E-2
K,8,3.048E-2,0,19.16E-2
K,9,5.644E-2,0,19.16E-2
K,10,6.944E-2,0,19.16E-2
K,11,9.144E-2,0,19.16E-2
K,12,9.144E-2,0,9E-2
K,13,6.944E-2,0,9E-2
K,14,5.644E-2,0,9E-2
```

K,15,3.048E-2,0,9E-2
K,16,-1.524E-2,0,19.16E-2
K,17,-1.524E-2,0,9E-2
K,18,-1.524E-2,0,3E-2
K,19,-1.524E-2,0,0
K,20,9.144E-2,0,3e-2
K,21,9.144E-2,0,0
K,22,6.944E-2,0,0
K,23,5.644E-2,0,0
K,24,3.048E-2,0,0
K,25,3.048E-2,0,3E-2
K,26,5.644E-2,0,3E-2
K,27,6.944E-2,0,3e-2
K,28,0,70E-2,0
L,1,2,1
L,20,5,15
L,5,6,1
L,6,21,15
L,2,3,3,.6060606
L,3,4,18
L,4,5,3,1.65
L,8,15,8
L,7,8,1
L,8,9,1
L,9,10,1
L,10,11,1
L,11,12,8
L,12,13,1
L,13,14,1
L,14,15,1
L,15,3,1
L,3,17,1
L,17,16,8
L,16,7,1
L,17,18,3,1.65
L,18,19,1

```
L,19,1,1
L,15,25,3,1.65
L,14,26,3,1.65
L,13,27,3,1.65
L,12,20,3,1.65
L,20,21,1
L,27,22,1
L,26,23,1
L,25,24,1
L,1,24,1
L,24,23,1
L,23,22,1
L,22,21,1
L,2,25,1
L,25,26,1
L,26,27,1
L,27,20,1
L,1,28,7,.16666
A,21,20,5,6
A,20,12,4,5
A,1,2,18,19
A,2,3,17,18
A,3,7,16,17
A,3,7,8,15
A,8,9,14,15
A,9,10,13,14
A,10,11,12,13
A,2,3,15,25
A,14,15,25,26
A,13,14,26,27
A,12,13,27,20
A,20,21,22,27
A,22,23,26,27
A,23,24,25,26
A,1,2,25,24
VDRAG,1,,,,,,40
```

```
MAT,1
VMESH,1
VDRAG,2,,,,,,40
MAT,2
VMESH,2
VDRAG,3,,,,,,40
MAT,1
VMESH,3
VDRAG,4,,,,,,40
MAT,2
VMESH,4
VDRAG,5,,,,,,40
MAT,1
VMESH,5
VDRAG,6,,,,,,40
MAT,1
VMESH,6
VDRAG,7,8,9,10,11,12,40
MAT,2
VMESH,7,12,1
VDRAG,13,,,,,,40
MAT,2
VMESH,13
VDRAG,14,15,16,17,,,40
MAT,1
VMESH,14,17,1
C***
C*** BOUNDARY CONDITIONS
C***
NRSEL,X,-1E-2,1E-2              * water channel 1
NRSEL,Y,-10E-2,80E-2
NRSEL,Z,2.5E-2,6E-2             * T in K
CVSF,ALL,,,21000,308            * h in W/(mm2 . K)
CVBC,1
NALL
NRSEL,X,27E-3,33E-3             * water channel 2
```

```
NRSEL,Y,-10E-2,80E-2
NRSEL,Z,2.5E-2,6E-2
CVSF,ALL,,,21000,308
CVBC,1
NALL
NRSEL,X,50E-3,62E-3          * water channel 3
NRSEL,Y,-10E-2,80E-2
NRSEL,Z,2.5E-2,6E-2
CVSF,ALL,,,21000,308
CVBC,1
NALL
NRSEL,X,115E-3,125E-3        * water channel 4
NRSEL,Y,-10E-2,80E-2
NRSEL,Z,2.5E-2,6E-2
CVSF,ALL,,,21000,308
CVBC,1
NALL
NRSEL,X,145E-3,155E-3        * water channel 5
NRSEL,Y,-10E-2,80E-2
NRSEL,Z,2.5E-2,6E-2
CVSF,ALL,,,21000,308
CVBC,1
NALL
NRSEL,X,175E-3,190E-3        * water channel 6
NRSEL,Y,-10E-2,80E-2
NRSEL,Z,2.5E-2,6E-2
CVSF,ALL,,,21000,308
CVBC,1
NALL
NRSEL,X,200E-3,220E-3        * water channel 7
NRSEL,Y,-10E-2,80E-2
NRSEL,Z,2.5E-2,6E-2
CVSF,ALL,,,21000,308
CVBC,1
NALL
NRSEL,X,265E-3,280E-3        * water channel 8
```

```
NRSEL,Y,-10E-2,80E-2
NRSEL,Z,2.5E-2,6E-2
CVSF,ALL,,,21000,308
CVBC,1
NALL
NRSEL,X,295E-3,310E-3          * water channel 9
NRSEL,Y,-10E-2,80E-2
NRSEL,Z,2.5E-2,6E-2
CVSF,ALL,,,21000,308
CVBC,1
NALL
NRSEL,X,325E-3,345E-3          * water channel 10
NRSEL,Y,-10E-2,80E-2
NRSEL,Z,2.5E-2,6E-2
CVSF,ALL,,,21000,308
CVBC,1
NALL
NRSEL,X,355E-3,375E-3          * water channel 11
NRSEL,Y,-10E-2,80E-2
NRSEL,Z,2.5E-2,6E-2
CVSF,ALL,,,21000,308
CVBC,1
NALL
NRSEL,X,415E-3,435E-3          * water channel 12
NRSEL,Y,-10E-2,80E-2
NRSEL,Z,2.5E-2,6E-2
CVSF,ALL,,,21000,308
CVBC,1
NALL
NRSEL,X,445E-3,465E-3          * water channel 13
NRSEL,Y,-10E-2,80E-2
NRSEL,Z,2.5E-2,6E-2
CVSF,ALL,,,21000,308
CVBC,1
NALL
NRSEL,X,475E-3,495E-3          * water channel 14
```

```
NRSEL,Y,-10E-2,80E-2
NRSEL,Z,2.5E-2,6E-2
CVSF,ALL,,,21000,308
CVBC,1
NALL
NRSEL,X,505E-3,525E-3          * water channel 15
NRSEL,Y,-10E-2,80E-2
NRSEL,Z,2.5E-2,6E-2
CVSF,ALL,,,21000,308
CVBC,1
NALL
NRSEL,X,50E-3,74E-3            * top horz. face of pipe 1
NRSEL,Y,-10E-2,80E-2
NRSEL,Z,110E-3,120E-3
CVSF,ALL,,,21000,308
CVBC,1
NALL
NRSEL,X,50E-3,74E-3            * bott. horz. face of pipe 1
NRSEL,Y,-10E-2,80E-2
NRSEL,Z,120E-3,135E-3
CVSF,ALL,,,21000,308
CVBC,1
NALL
NRSEL,X,50E-3,74E-3            * top horz. face of pipe 2
NRSEL,Y,-10E-2,80E-2
NRSEL,Z,147E-3,160E-3
CVSF,ALL,,,21000,308
CVBC,1
NALL
NRSEL,X,50E-3,74E-3            * bott. horz. face of pipe 2
NRSEL,Y,-10E-2,80E-2
NRSEL,Z,160E-3,170E-3
CVSF,ALL,,,21000,308
CVBC,1
NALL
NRSEL,X,50E-3,63E-3            * left vert. face of pipe 1
```

```
NRSEL,Y,-10E-2,80E-2
NRSEL,Z,110E-3,135E-3
CVSF,ALL,,,21000,308
CVBC,1
NALL
NRSEL,X,50E-3,63E-3          * left vert. face of pipe 2
NRSEL,Y,-10E-2,80E-2
NRSEL,Z,147E-3,170E-3
CVSF,ALL,,,21000,308
CVBC,1
NALL
NRSEL,X,63E-3,74E-3          * right vert. face of pipe 1
NRSEL,Y,-10E-2,80E-2
NRSEL,Z,110E-3,135E-3
CVSF,ALL,,,21000,308
CVBC,1
NALL
NRSEL,X,63E-3,74E-3          * right vert. face of pipe 2
NRSEL,Y,-10E-2,80E-2
NRSEL,Z,147E-3,170E-3
CVSF,ALL,,,21000,308
CVBC,1
NALL
NRSEL,X,-20E-3,560E-3        * bottom face of mold
NRSEL,Y,-10E-3,25E-3
NRSEL,Z,-10E-3,200E-3
CVSF,ALL,,,150,298
CVBC,1
NALL
NRSEL,X,-20E-3,560E-3        * top face of mold
NRSEL,Y,69.5E-2,71.5E-2
NRSEL,Z,-10E-3,200E-3
CVSF,ALL,,,250,298
CVBC,1
NALL
NRSEL,X,-20E-3,560E-3        * outer horz. top mold face
```

```
NRSEL,Y,-10E-2,80E-2
NRSEL,Z,-10E-2,1.5E-2
CVSF,ALL,,,21000,308
CVBC,1
NALL
NRSEL,X,-20E-3,-7E-3          * outer vert. left mold face
NRSEL,Y,-10E-2,80E-2
NRSEL,Z,-10E-3,200E-3
CVSF,ALL,,,21000,308
CVBC,1
NALL
NRSEL,X,85E-3,100E-3          * inner vert. mold face(flux)
NRSEL,Y,64E-2,71E-2           *   level 0 (above meniscus)
NRSEL,Z,87E-3,200E-3
CVSF,ALL,,,1.787E-3,600E+6
CVBC,1
NALL
NRSEL,X,85E-3,100E-3          * inner vert. mold face(flux)
NRSEL,Y,58E-2,68E-2           *   level 1 (below meniscus)
NRSEL,Z,87E-3,200E-3
CVSF,ALL,,,5.546E-3,600E+6
CVBC,1
NALL
NRSEL,X,85E-3,100E-3          * inner vert. mold face(flux)
NRSEL,Y,51E-2,64E-2           * level 2
NRSEL,Z,87E-3,200E-3
CVSF,ALL,,,3.266E-3,600E+6
CVBC,1
NALL
NRSEL,X,85E-3,100E-3          * inner vert. mold face(flux)
NRSEL,Y,41E-2,58E-2           * level 3
NRSEL,Z,87E-3,200E-3
CVSF,ALL,,,2.922E-3,600E+6
CVBC,1
NALL
NRSEL,X,85E-3,100E-3          * inner vert. mold face(flux)
```

```
NRSEL,Y,27E-2,51E-2          * level 4
NRSEL,Z,87E-3,200E-3
CVSF,ALL,,,2.58E-3,600E+6
CVBC,1
NALL
NRSEL,X,85E-3,100E-3         * inner vert. mold face(flux)
NRSEL,Y,10E-2,41E-2          * level 5
NRSEL,Z,87E-3,200E-3
CVSF,ALL,,,2.13E-3,600E+6
CVBC,1
NALL
NRSEL,X,85E-3,100E-3         * inner vert. mold face(flux)
NRSEL,Y,-10E-2,27E-2         * level 6
NRSEL,Z,87E-3,200E-3
CVSF,ALL,,,1.52E-3,600E+6
CVBC,1
NALL
NRSEL,X,85E-3,560E-3         * inner horz. mold face(flux)
NRSEL,Y,64E-2,71E-2          * level 0 (above meniscus)
NRSEL,Z,87E-3,95E-3
CVSF,ALL,,,1.787E-3,600E+6
CVBC,1
NALL
NRSEL,X,85E-3,560E-3         * inner horz. mold face(flux)
NRSEL,Y,58E-2,68E-2          * level 1 (below meniscus)
NRSEL,Z,87E-3,95E-3
CVSF,ALL,,,5.546E-3,600E+6
CVBC,1
NALL
NRSEL,X,85E-3,560E-3         * inner horz. mold face(flux)
NRSEL,Y,51E-2,64E-2          * level 2
NRSEL,Z,87E-3,95E-3
CVSF,ALL,,,3.266E-3,600E+6
CVBC,1
NALL
NRSEL,X,85E-3,560E-3         * inner horz. mold face(flux)
```

```
NRSEL,Y,41E-2,58E-2              * level 3
NRSEL,Z,87E-3,95E-3
CVSF,ALL,,,2.922E-3,600E+6
CVBC,1
NALL
NRSEL,X,85E-3,560E-3             * inner horz. mold face(flux)
NRSEL,Y,27E-2,51E-2              * level 4
NRSEL,Z,87E-3,95E-3
CVSF,ALL,,,2.58E-3,600E+6
CVBC,1
NALL
NRSEL,X,85E-3,560E-3             * inner horz. mold face(flux)
NRSEL,Y,10E-2,41E-2              * level 5
NRSEL,Z,87E-3,95E-3
CVSF,ALL,,,2.13E-3,600E+6
CVBC,1
NALL
NRSEL,X,85E-3,560E-3             * inner horz. mold face(flux)
NRSEL,Y,-10E-2,27E-2             * level 6
NRSEL,Z,87E-3,95E-3
CVSF,ALL,,,1.52E-3,600E+6
CVBC,1
NALL
MERGE,ALL
AFWRIT
FINISH
/EXE
/INPUT,27
FINISH
/eof
/POST1
STORE,DISPL
SET,1,1
/NOSHOW
/VIEW,1,1,1,1
EPLOT
```

/TYPE,1,1
/FOCUS,1,274.32E-3,1E-3,95.58E-3
/VIEW,1,0,1,0
/clabel,1,1
PLNSTR,TEMP
/RESET
/TYPE,1,1
/FOCUS,1,274.32E-3,35E-2,95.58E-3
/VIEW,1,0,1,0
/CLABEL,1,1
PLNSTR,TEMP
/RESET
/TYPE,1,1
/FOCUS,1,274.32E-3,69E-2,95.58E-3
/VIEW,1,0,1,0
/CLABEL,1,1
PLNSTR,TEMP
/RESET

APPENDIX D

QUARTER MOLD STRESS ANALYSIS

```
/PREP7
/TITLE,THERMAL STRESS
C***
C***                                "THSTRALL"
C***
C*** THIS COMPUTER PROGRAM IS AN INPUT FILE TO "ANSYS" REV. 4.3.
C*** THIS FILE RESUMES THE MESH AND THE THERMAL ANALYSIS FROM
C*** EITHER THE ANALYIS USING FILE CASTER OR NEWCASTER. THIS FILE
C*** DOES THE STRESS ANALYSIS.
C*** THE OUTPUT FILES ARE STORED AS THSTRAL#.
RESUME
KAN,0                               * stress analysis
ET,1,45                             * element type
TREF,308                            * reference temperature
C***
C*** MATERIAL
C***
DENS,1,0                            * zero mass, no dynamic analysis
DENS,2,0
ALPX,1,15.5E-6                      * alpha for steel in 1/K
EX,1,210E9                          * Young's modulus of steel in Pa
NUXY,1,.3                           * thermal expansion coeff. of steel
ALPX,2,15.2E-6                      * alpha for copper in 1/K
EX,2,1.1E8                          * Young's modulus of copper in Pa
NUXY,2,.36                          * thermal expansion coeff. of copper
C***
C*** BOUNDARY CONDITIONS
C***
NRSEL,X,530E-3,550E-3               * fixing the right hand side of the mold
NRSEL,Y,-1E-2,80E-2
NRSEL,Z,-10E-3,100E-3
```

```
D,ALL,UX,0
NALL
NRSEL,X,-20E-3,110E-3          * fixing the front left side of the mold
NRSEL,Y,-1E-2,80E-2
NRSEL,Z,190E-3,195E-3
D,ALL,UZ,0
NALL
NRSEL,X,-2E-2,-1E-2            * fixing the left upper corner of the mold
NRSEL,Y,68E-2,71E-2
NRSEL,Z,-1E-2,1E-2
D,ALL,UY,0
NALL
EALL
NRSEL,X,-20-3,92E-3            * start wave in side of mold
WSORT,Z,-1,0
NALL
NRSEL,X,92E-3,560E-3           * start wave in back plate
WSORT,X,0,0
NALL
WFRONT,1
/CHECK
AFWRITE
FINISH
/EXEC
/INPUT,27
FINISH
/eof
```

APPENDIX E

THIN SLICE THERMAL ANALYSIS

```
/INT,NO
/Prep7
/TITLE,CASTSL
C***
C***                                    "CASTSL"
C***
C*** THIS COMPUTER PROGRAM IS AN INPUT FILE TO "ANSYS" REV. 4.3.
C*** THIS FILE CREATES THE MESH OF THE THIN SLICE IN THE MOLD
C*** AND DOES THE THERMAL ANALYSIS USING THE SECOND METHOD.
C*** THE OUPUT FILES ARE STORED AS CAST#.
C***
KAN,-1                                  * thermal analysis
ET,1,70                                 * element type
KXX,1,52                                * K for steel in W/(m.K)
KXX,2,390                               * K for copper in W/(m.K)
C***
C*** MESH GENERATION
C***
K,1,0,0,0
K,2,3.5E-2,0,0
K,3,6E-2,0,0
K,4,9E-2,0,0
K,5,9E-2,23E-2,0
K,6,6E-2,23E-2,0
K,7,3.5E-2,23E-2,0
K,8,0,23E-2,0
K,9,0,45E-2,0
K,10,3.5E-2,45E-2,0
K,11,6E-2,45E-2,0
K,12,9E-2,45E-2,0
K,13,9E-2,65E-2,0
K,14,6E-2,65E-2,0
```

K,15,3.5E-2,65E-2,0
K,16,0,65E-2,0
K,17,0,70E-2,0
K,18,3.5E-2,70E-2,0
K,19,6E-2,70E-2,0
K,20,9E-2,70E-2,0
K,21,0,0,-1.75E-2
L,1,2,4,1.7
L,8,7,4,1.7
L,9,10,4,1.7
L,16,15,4,1.7
L,17,18,4,1.7
L,2,3,3,1
L,7,6,3,1
L,10,11,3,1
L,15,14,3,1
L,18,19,3,1
L,3,4,2,1
L,6,5,2,1
L,11,12,2,1
L,14,13,2,1
L,19,20,2,1
L,1,8,10,1
L,2,7,10,1
L,3,6,10,1
L,4,5,10,1
L,8,9,15,1
L,7,10,15,1
L,6,11,15,1
L,5,12,15,1
L,9,16,25,1
L,10,15,25,1
L,11,14,25,1
L,12,13,25,1
L,16,17,5,1
L,15,18,5,1

```
L,14,19,5,1
L,13,20,5,1
L,1,21,1
A,1,2,7,8
A,2,3,6,7
A,3,4,5,6
A,8,7,10,9
A,7,6,11,10
A,6,5,12,11
A,9,10,15,16
A,10,11,14,15
A,11,12,13,14
A,16,15,18,17
A,15,14,19,18
A,14,13,20,19
VDRAG,1,,,,,,32
MAT,2
VMESH,1
VDRAG,2,,,,,,32
MAT,2
VMESH,2
VDRAG,3,,,,,,32
MAT,1
VMESH,3
VDRAG,4,,,,,,32
MAT,2
VMESH,4
VDRAG,5,,,,,,32
MAT,2
VMESH,5
VDRAG,6,,,,,,32
MAT,1
VMESH,6
VDRAG,7,,,,,,32
MAT,2
VMESH,7
```

```
VDRAG,8,,,,,,32
MAT,2
VMESH,8
VDRAG,9,,,,,,32
MAT,1
VMESH,9
VDRAG,10,,,,,,32
MAT,2
VMESH,10
VDRAG,11,,,,,,32
MAT,2
VMESH,11
VDRAG,12,,,,,,32
MAT,1
VMESH,12
C***
C*** BOUNDARY CONDITIONS
C***
NRSEL,Y,69.5E-2,71E-2          * top face of mold
CVSF,ALL,,,250,298
CVBC,1
NALL
NRSEL,Y,-1E-2,1E-2             * bottom face of mold
CVSF,ALL,,,150,298
CVBC,1
NALL
NRSEL,X,3.4E-2,6.1E-2          * water channel
NRSEL,Z,-1E-2,1E-2
CVSF,ALL,,,21000,308
CVBC,1
NALL
NRSEL,X,8.9E-2,9.1E-2          * outer face
CVSF,ALL,,,21000,308
CVBC,1
NALL
NRSEL,X,-1E-2,.5E-2
```

```
NRSEL,Y,-.0115,.0345          * Flux at the face bottom
CVSF,ALL,,,1.2688e-3,600E6
CVBC,1
NALL
NRSEL,X,-1E-2,.5E-2
NRSEL,Y,.0115,.0575
CVSF,ALL,,,1.351e-3,600E6
CVBC,1
NALL
NRSEL,X,-1E-2,.5E-2
NRSEL,Y,.0345,.0805
CVSF,ALL,,,1.434e-3,600E6
CVBC,1
NALL
NRSEL,X,-1E-2,.5E-2
NRSEL,Y,.0575,.1035
CVSF,ALL,,,1.517e-3,600E6
CVBC,1
NALL
NRSEL,X,-1E-2,.5E-2
NRSEL,Y,.0805,.1265
CVSF,ALL,,,1.6e-3,600E6
CVBC,1
NALL
NRSEL,X,-1E-2,.5E-2
NRSEL,Y,.1035,.1495
CVSF,ALL,,,1.683e-3,600E6
CVBC,1
NALL
NRSEL,X,-1E-2,.5E-2
NRSEL,Y,.1265,.1725
CVSF,ALL,,,1.765e-3,600E6
CVBC,1
NALL
NRSEL,X,-1E-2,.5E-2
NRSEL,Y,.1495,.1955
```

CVSF,ALL,,,1.848e-3,600E6
CVBC,1
NALL
NRSEL,X,-1E-2,.5E-2
NRSEL,Y,.1725,.2185
CVSF,ALL,,,1.93e-3,600E6
CVBC,1
NALL
NRSEL,X,-1E-2,.5E-2
NRSEL,Y,.1955,.24
CVSF,ALL,,,2.014e-3,600E6
CVBC,1
NALL
NRSEL,X,-1E-2,.5E-2
NRSEL,Y,.22,.252
CVSF,ALL,,,2.074e-3,600E6
CVBC,1
NALL
NRSEL,X,-1E-2,.5E-2
NRSEL,Y,.23,.26667
CVSF,ALL,,,2.134e-3,600E6
CVBC,1
NALL
NRSEL,X,-1E-2,.5E-2
NRSEL,Y,.252,.28134
CVSF,ALL,,,2.1875e-3,600E6
CVBC,1
NALL
NRSEL,X,-1E-2,.5E-2
NRSEL,Y,.26667,.296
CVSF,ALL,,,2.176e-3,600E6
CVBC,1
NALL
NRSEL,X,-1E-2,.5E-2
NRSEL,Y,.28,.31
CVSF,ALL,,,2.235e-3,600E6

CVBC,1
NALL
NRSEL,X,-1E-2,.5E-2
NRSEL,Y,.296,.325
CVSF,ALL,,,2.34e-3,600E6
CVBC,1
NALL
NRSEL,X,-1E-2,.5E-2
NRSEL,Y,.31,.34
CVSF,ALL,,,2.397e-3,600E6
CVBC,1
NALL
NRSEL,X,-1E-2,.5E-2
NRSEL,Y,.325,.35
CVSF,ALL,,,2.45e-3,600E6
CVBC,1
NALL
NRSEL,X,-1E-2,.5E-2
NRSEL,Y,.34,.369
CVSF,ALL,,,2.487e-3,600E6
CVBC,1
NALL
NRSEL,X,-1E-2,.5E-2
NRSEL,Y,.35,.38
CVSF,ALL,,,2.556e-3,600E6
CVBC,1
NALL
NRSEL,X,-1E-2,.5E-2
NRSEL,Y,.369,.394
CVSF,ALL,,,2.595e-3,600E6
CVBC,1
NALL
NRSEL,X,-1E-2,.5E-2
NRSEL,Y,.38,.41
CVSF,ALL,,,2.645e-3,600E6
CVBC,1

```
NALL
NRSEL,X,-1E-2,.5E-2
NRSEL,Y,.394,.428
CVSF,ALL,,,2.7e-3,600E6
CVBC,1
NALL
NRSEL,X,-1E-2,.5E-2
NRSEL,Y,.41,.442
CVSF,ALL,,,2.768e-3,600E6
CVBC,1
NALL
NRSEL,X,-1E-2,.5E-2
NRSEL,Y,.428,.455
CVSF,ALL,,,2.82e-3,600E6
CVBC,1
NALL
NRSEL,X,-1E-2,.5E-2
NRSEL,Y,.442,.474
CVSF,ALL,,,2.876e-3,600E6
CVBC,1
NALL
NRSEL,X,-1E-2,.5E-2
NRSEL,Y,.458,.49
CVSF,ALL,,,2.934e-3,600E6
CVBC,1
NALL
NRSEL,X,-1E-2,.5E-2
NRSEL,Y,.474,.506
CVSF,ALL,,,2.99e-3,600E6
CVBC,1
NALL
NRSEL,X,-1E-2,.5E-2
NRSEL,Y,.49,.522
CVSF,ALL,,,3.05e-3,600E6
CVBC,1
NALL
```

```
NRSEL,X,-1E-2,.5E-2
NRSEL,Y,.506,.538
CVSF,ALL,,,3.106e-3,600E6
CVBC,1
NALL
NRSEL,X,-1E-2,.5E-2
NRSEL,Y,.522,.554
CVSF,ALL,,,3.16e-3,600E6
CVBC,1
NALL
NRSEL,X,-1E-2,.5E-2
NRSEL,Y,.538,.57
CVSF,ALL,,,3.22e-3,600E6
CVBC,1
NALL
NRSEL,X,-1E-2,.5E-2
NRSEL,Y,.554,.586
CVSF,ALL,,,3.28e-3,600E6
CVBC,1
NALL
NRSEL,X,-1E-2,.5E-2
NRSEL,Y,.57,.594
CVSF,ALL,,,3.348e-3,600E6
CVBC,1
NALL
NRSEL,X,-1E-2,.5E-2
NRSEL,Y,.586,.606
CVSF,ALL,,,3.46e-3,600E6
CVBC,1
NALL
NRSEL,X,-1E-2,.5E-2
NRSEL,Y,.594,.614
CVSF,ALL,,,3.64e-3,600E6
CVBC,1
NALL
NRSEL,X,-1E-2,.5E-2
```

```
NRSEL,Y,.606,.622
CVSF,ALL,,,3.76e-3,600E6
CVBC,1
NALL
NRSEL,X,-1E-2,.5E-2
NRSEL,Y,.614,.63
CVSF,ALL,,,3.88e-3,600E6
CVBC,1
NALL
NRSEL,X,-1E-2,.5E-2
NRSEL,Y,.622,.638
CVSF,ALL,,,4e-3,600E6
CVBC,1
NALL
NRSEL,X,-1E-2,.5E-2
NRSEL,Y,.63,.646
CVSF,ALL,,,5.33e-3,600E6
CVBC,1
NALL
NRSEL,X,-1E-2,.5E-2
NRSEL,Y,.638,.654
CVSF,ALL,,,6.66e-3,600E6
CVBC,1
NALL
AFWRIT
FINISH
/EXE
/INPUT,27
FINISH
/EOF
```

APPENDIX F

THIN SLICE STRESS ANALYSIS

```
/prep7
/title, THERMAL STRESS
C***
C***                              "STR"
C***
C*** THIS COMPUTER PROGRAM IS AN INPUT FILE TO "ANSYS" REV. 4.3.
C*** THIS FILE RESUMES THE MESH AND THE THERMAL ANALYSIS FROM
C*** THE ANALYSIS OF FILE CASTSL.  THIS FILE DOES THE STRESS ANALYSIS.
C*** THE OUPUT IS STORED AS STR#.
C***
resume
merge
kan,0                             * stress analysis
et,1,45,,,1                       * Generalized plane strain option
tref,308                          *  reference  temperature
C***
C*** MATERIAL
C***
dens,1,0                          * zero mass (no dynamic analysis)
dens,2,0
alpx,1,15.5e-6                    * alpha for steel in 1/K
ex,1,210e9                        * Young's modulus of steel in Pa
nuxy,1,.3                         * thermal expansion coeff. of steel
alpx,2,15.2e-6                    * alpha for copper in /K
ex,2,1.1e8                        * Young's modulus of copper in Pa
nuxy,2,.36                        * thermal expansion coeff. of copper
C***
C*** BOUNDARY CONDITIONS
C***
```

```
d,1241,ux,0,,,,uy,uz
d,188,ux,0,,,,,uz
afwrite
finish
/exe
/input,27
finish
```

APPENDIX G

PROGRAM TENSIL

```
c-----------------------------------------------------------------------
      program  tensil
c-----------------------------------------------------------------------
c
c            ******************************************
c      *     EDTP = A * exp(-q/T)*(S - m*(Ep**c))**n          *
c            ******************************************
c
c    This computer program is written in FORTRAN77 on a Ridge32.
c     The program integtrates the differential equation, edtp, using
c     a predictor-corrector method.
c
c   s = stress
c    e = young's modulus
c    r = total strain rate (const.)
c    a = parameter
c    m = slope parameter
c     c = parameter controls curvature
c     n = parameter controls stiffness
c    q = Q/R parameter
c   t = time
c    h = time increment
c    runtime = desired time
c    edtp1 = plastic strain rate
c    edte = elastic strain rate
c    edtp = plastic strain rate
c    ds = change in stress
c   sdt = stress rate
c   etot = total strain
c    ep = plastic strain
c    ee = elastic strain
c
```

```
c  Define and read parameters
c
      double precision a,e,r,h,t,s,sdt,ds,edtp1,edte,edtp,etot
      double precision ep,ee,m,c,n,dt,h1,runtime,k

      open(unit=16,file='ten4res',status='unknwon')
 5    print*,' Enter strain rate,temperature(C).(to stop enter zero)'
      read*,r,temp
      if( r .eq. 0d0 .or. temp .eq. 0d0) goto 100
      print*,'Enter the equat.variables: a,m,c,n,q'
      read*, a,m,c,n,q
      print*,'Enter printing interval desired'
      read*,iprint
      s = 0.0d0
      t = 0.0d0
      runtime = .05d0/r
      h = 0.001d0
      h1 = h
      dt = 0.0d0
      edtp1 = 0.0d0
      edte = 0.0d0
      edtp = 0.0d0
      ep = 0.0d0
      ee = 0.0d0
      ds = 0.0d0
      i = 0.0d0
      j = 0.0d0
      if(temp .le. 500) e = 210 - .075*temp
      if(temp .gt. 500 .and. temp .le. 714) e=283.5-.222*temp
      if(temp .gt. 714 .and. temp .le. 1400) e=181-.075*temp
      if(temp .gt. 1400 .and. temp .le. 1500) e=425-.25*temp
c
c  Start of integration
c
      e = e*1d+3
      k=  a*dexp(-q/(temp+273))
```

```
 10   edtp1  =  k*((dabs(s-m*(ep**c)))**(n-1))  *  (s-m*(ep**c))
      edte = r-edtp1
      sdt = e*edte
      ds = h1*sdt
      s = s+ds
      edtp  =  k*((dabs(s-m*(ep**c)))**(n-1))  *  (s-m*(ep**c))
c
c  Check  error
c
      if(abs(edtp-edtp1)  .lt.  5d-3)  then
       ee = ee + edte*h1
       ep = ep + edtp*h1
       etot = ee + ep
c
c  Printing  interval
c
        if((i/iprint)*iprint  .eq.  i  )then
          write(16,20)t,s,etot,ee,ep,j
 20       format(e9.4,2x,e9.3,2x,e9.3,2x,e9.3,2x,e9.3,2x,i4)
        endif
       j =0.0d0
       i =i+ 1
       t = t+h1
      endif
      j=j+1
      if(t .lt. runtime) go to 10
c
      write(16,*)
      write(16,*)
      goto5
 100  print*,'job  is  done'
      close(unit=16,status='keep')
      stop
      end
```

APPENDIX H

PROGRAM SIMPLEX

```
c-----------------------------------------------------------------------
      program  simplex
c-----------------------------------------------------------------------
c
c  This computer program is written in FORTRAN77 on a Ridge32.
c  The main program is taken from Himmeblau (see reference).
c  The program searches for a minimum of a function by changing
c  parameters. The search is based on method proposed by Nelder
c  and Mead. The function to be optimized is the error between
c  the integrated curves of a differential equation and the experimental
c  data. The program is followed by three subroutines. The second subroutine
c  integrates the differential equation, edtp,. The third subroutine
c  reads data from another file.
c
c       nx is the number of independent variables.
c       STEP is the initial step size.
c       X(I) is the array of initial guesses.
c
      dimension  x1(50,50),x(50),  sum(50)
      common  x,x1,nx,step,k1,sum,in
c
      open(unit=20,file='simpout',status='unknown')
      call  ioinit(.false.,.false.,.true.,'',.false.)
  1   format  (i5,f10.5)
100   read*,nx,step
      if (nx)  998,999,998
998   read *, (x(i), i=1,nx)
      write(20,*)nx,step,(x(i),i=1,nx)
  2   format  (10f10.5)
      close(unit=20,status='keep')
      alfa=1.0
```

```
      beta=0.5
      gama=2.0
      difer= 0.
      xnx = nx
      in = 1
      call  sumr
      open(unit=20,file='simpout',status='unknown')
      write(20,102)sum(1),(x(i),  i=1,nx)
      write(20,1002)step
      write(20,103)
103   format(4x,14hfunction  value,15x,3hx1=,20x,3hx2=,20x,3hx3=,20x,
     +  3hx4=,16x,12hfunc.  change)
102   format(1h1,12x,23hfunction  starting  value,f10.5,
     +  5x,10(e11.4,2x))
1002  format(12x,f6.2)
      close(unit=20,status='keep')
      k1 = nx + 1
      k2 = nx + 2
      k3 = nx + 3
      k4 = nx + 4
      call  start
25    do 3 i =1,k1
         do 4 j =1,nx
4        x(j) = x1(i,j)
         in = i
         call  sumr
3     continue
c  select largest value of sum(i) in simplex
28    sumh = sum (1)
      index = 1
      do 7 i = 2,k1
         if (sum(i).le.sumh) go to 7
         sumh = sum (i)
         index = i
7     continue
c  select minimum value of sum(i) in simplex
```

```
      suml = sum(1)
      kount = 1
      do 8 i = 2,k1
         if (suml .le. sum(i)) go to 8
         suml = sum(i)
         kount = i
 8    continue
c  find centroid of points with i different than index
      do 9 j =1,nx
         sum2 = 0.
         do 10 i =1,k1
10       sum2 = sum2 + x1(i,j)
         x1(k2,j) = 1./xnx*(sum2 - x1(index,j))
c  find reflection of high point through centroid
         x1(k3,j) = (1. + alfa) *x1(k2,j) - alfa*x1(index,j)
 9    x(j) = x1(k3,j)
      in = k3
      call sumr
      if(sum(k3) .lt. suml) go to 11
c  select second largest value in simplex
      if (index .eq. 1) go to 38
      sums = sum(1)
      go to 39
38    sums = sum(2)
39    do 12 i = 1,k1
         if ((index - i) .eq. 0) go to 12
         if (sum(i) .le. sums) go to 12
         sums = sum(i)
12    continue
      if (sum(k3) .gt. sums) go to 13
      go to 14
c  form expansion of new minimum if reflection has produced one minimum
11    do 15 j = 1,nx
         x1(k4,j) = (1 - gama)*x1(k2,j) + gama*x1(k3,j)
15    x(j) =x1(k4,j)
      in = k4
```

```
      call  sumr
      if (sum(k4) .lt. suml) go to 16
      go to 14
 13   if (sum(k3) .gt. sumh) go to 17
      do 18 j=1,nx
 18   x1(index,j) = x1(k3,j)
 17   do 19 j=1,nx
        x1(k4,j) =beta*x1(index,j) +(1. - beta) * x1(k2,j)
 19   x(j) = x1(k4,j)
      in = k4
      call  sumr
      if(sumh .gt. sum(k4)) go to 16
c     reduce simplex by half if reflection happens to produce a larger
c     value than the maximum
      do 20 j = 1,nx
      do 20 i = 1,k1
 20   x1(i,j) = 0.5*(x1(i,j) + x1(kount,j))
      do 29 i = 1,k1
        do 30 j = 1,nx
 30     x(j) = x1(i,j)
        in = i
        call  sumr
 29   continue
      go to 26
 16   do 21 j = 1,nx
        x1(index,j) = x1(k4,j)
 21   x(j) = x1(index,j)
      in = index
      call  sumr
      go to 26
 14   do 22 j = 1,nx
      x1(index,j) = x1(k3,j)
 22   x(j) = x1(index,j)
      in = index
      call  sumr
 26   do 23 j = 1,nx
```

```
 23     x(j) = x1(k2,j)
        in = k2
        call  sumr
        difer = 0.
        do 24 i=1,k1
 24     difer = difer + (sum(i) - sum(k2))**2
        difer  =  1./xnx*sqrt(difer)
        open(unit=20,file='simpout',status='unknown')
        write(20,101)suml,(x1(kount,j),  j=  1,nx),difer
101     format(2(2x,e16.6),3(7x,e16.6),12x,e16.6)
        close(unit=20,status='keep')
        if (difer .ge. 0.0000001) go to 28
        go to 100
999     continue
        stop
        end
c-----------------------------------------------------------------------
        subroutine  start
c-----------------------------------------------------------------------
        dimension  a(50,50),  x1(50,50),  x(50),  sum(50)
        common  x,x1,nx,step,k1,sum,in
        vn = nx
        step1  =  step/(vn*sqrt(2.))*(sqrt(vn  +  1.)  +  vn-  1.)
        step2  =  step/(vn*sqrt(2.))*(sqrt(vn  +  1.)  -  1.)

  1     a(1,j) = 0.
        do 2 i= 2,k1
        do 2 j = 1,nx
           a(i,j)=  step2
           l = i-1
           a(i,l)  =  step1
  2     continue
        do 3 i = 1,k1
        do 3 j = 1,nx
  3     x1(i,j)  =  x(j)+  a(i,j)
        return
```

```
      end
c-----------------------------------------------------------------------
      subroutine  sumr
c-----------------------------------------------------------------------
c
c            ************************************************
c     *    EDTP = A * exp(-q/T)*(S - m*(Ep**c))**n                  *
c            ************************************************
c
c  s = stress
c   e = young's modulus
c   r = total strain rate (const.)
c  a = coeff.
c  m = slope
c   c = power controls curvature
c   n = power controls stiffness
c  t = time
c   runtime = total time
c   h = time increment
c   edtp1 = plastic strain rate
c   edte = elastic strain rate
c   edtp = plastic strain rate
c   ds = change in stress
c   sdt = stress rate
c   etot = total strain
c   ep = plastic strain
c   ee = elastic strain
c   w = strain data
c   ws = stress data
c   er = error
c
      real  a,e,r(7),h,h1,t,s,sdt,ds,edtp1,edte,edtp,etot,const
      real  ep,ee,m,c,n,nn,w(6),ws,runtime,temp(2),q,er,tempc
      integer  l,ll

      common  x,x1,nx,step,k1,sum,in
```

```
      dimension  x1(50,50),  x(50),  sum(50)
c
      er = 0.0
      temp(1)=1223
      temp(2)=1373
c
      do 200 ll =1,2
        if  (temp(ll)  .eq.  1223)  then
          r(1) = 2.3e-2
          r(2) = 8.3e-3
          r(3) = 2.4e-3
          r(4) = 5.6e-4
          r(5) = 1.5e-4
          r(6) = 2.9e-5
          r(7) = 7.2e-6
        else
          r(1) = 2.3e-2
          r(2) = 8.3e-3
          r(3) = 2.9e-3
          r(4) = 5.4e-4
          r(5) = 1.4e-4
          r(6) = 2.9e-5
          r(7) = 5.6e-6
        endif
        do 150 l = 1,7
          w(1) = 0.001
          w(2) = 0.002
          w(3) = 0.005
          w(4) = 0.01
          w(5) = 0.02
          w(6) = 0.05
          k = 1
          s = 0.0e0
          nn = x(1)*10
          a = (x(2)*10)*(10**nn)
          m = (x(3)*1000) -  (x(4)*temp(ll))
```

```
      c = x(5)
      n = x(6)*10
      q = x(7)*1e5
      t = 0.0e0
      runtime = .025d0/r(l)
      h = 0.001e0
      h1 = h
      edtp1= 0.0e0
      edte = 0.0e0
      edtp = 0.0e0
      ep = 0.0e0
      ee = 0.0e0
      ds = 0.0e0
      i = 0.0e0
      j = 0.0e0
      tempc = temp(ll) - 273
      if(tempc .le. 500) e=210 - .075*tempc
      if(tempc .gt. 500 .and. tempc .le. 714)e=283.5-.222*tempc
      if(tempc .gt. 714 .and. tempc .le. 1400)e=181-.075*tempc
      if(tempc .gt. 1400 .and. tempc .le. 1500)e=425-.25*tempc
c
      e = e*1d+3
      const= a*exp(-q/temp(ll))
10    edtp1=const*(s-(m*1e+0)*(dabs(ep))**c)**n
      edte = r(l)-edtp1
      sdt = e*edte
      ds = h1*sdt
      s = s+ds
      edtp =const*(s-(m*1e+0)*(dabs(ep))**c)**n
c
      if(abs(edtp-edtp1) .lt. 5e-3) then
         ee = ee + edte * h1
         ep = ep + edtp * h1
         etot = ee + ep
c        print*,t,etot,s,w(k)
         j =0.0e0
```

```
                i =i+ 1
                t = t+h1
                if( abs( etot - w(k) ) .lt. 1e-4 ) then
c                 print*,temp(ll),r(l),w(k)
                  call   findata(temp(ll),r(l),w(k),ws)
                  er = er + abs(s - ws)
                  k =k + 1
                endif
              endif
              j=j+1
              if((t .lt. runtime).and.(k.le.6) ) go to 10
c
 150        continue
 200      continue
c
          sum(in) = er
          return
          end
c-------------------------------------------------------------------------------
          subroutine   findata(temp,r,w,ws)
c-------------------------------------------------------------------------------
c
          real  temp,r,w,ws,x,y,z
c
          open(unit=24,file='wraydata1',status='old')
          rewind(unit=24)
 10       read(24,*)x,y,z,ws
          if (x .eq. temp .and. y .eq. r .and. z .eq. w) then
             close  (unit=24,status='keep')
             return
             else
             goto 10
          endif
          return
          end
```